This is to certify that the
dissertation entitled

**SYNTHESIS OF NOVEL BIODEGRADABLE COPOLYMERS: POST-POLYMERIZATION MODIFICATION OF POLY(L-LACTIDE-CO-DIALLYLGLYCOLIDE)**

presented by

Christopher Paul Radano

has been accepted towards fulfillment
of the requirements for the

Ph.D. degree in Chemistry

Major Professor's Signature

8/1/03

Date

# SYNTHESIS OF NOVEL BIODEGRADABLE COPOLYMERS: POST-POLYMERIZATION MODIFICATION OF POLY(L-LACTIDE-CO-DIALLYLGLYCOLIDE)

By

Christopher Paul Radano

A DISSERTATION

Submitted to
Michigan State University
In partial fulfillment of the requirement
for the degree of

DOCTOR OF PHILOSOPHY

Department of Chemistry

2003

ABSTRACT

DESIGN OF NOVEL BIODEGRADABLE COPOLYMERS: POST-POLYMERIZATION MODIFICATION OF POLY(L-LACTIDE-CO-DIALLYLGLYCOLIDE)

By

Christopher Paul Radano

Poly(lactic acid) (PLA) represents a class of biodegradable polymers, which are used extensively in biomaterials such as dissolvable sutures, surgical implants, matrices for drug delivery, and scaffolds for tissue engineering. In order to improve the biocompatibility of these materials, research groups have designed copolymers of PLA with the goal of introducing unique functionality and enhancing cell adhesion properties. Our group has also made progress in this area of research. However, the approach of our research is different, in that we are employing a post-polymerization modification of a common biodegradable polymer based on PLA. Using diallylglycolide as a comonomer, we have synthesized a single biodegradable copolymer, which is able to undergo functional group transformations through existing methods commonly used in organic chemistry.

We have demonstrated that olefin cross metathesis and hydroboration/oxidation transformations are both successful methods of functionalizing PLA. However, the most successful method of functionalizing PLA was readily achieved via DCC coupling of various bioactive substrates with our functional copolymer. After synthesizing a series of copolymers containing bioactive substrates we prepared thin films of the polymers and examined their ability to support tissue growth, specifically osteoblast growth and

differentiation. The synthesis and characterization of these copolymers as well as the initial results of physiological experiments using our biodegradable copolymers are reported.

ACKNOWLEDGMENTS

I would like to acknowledge my advisor Mitch Smith for his guidance during my graduate career. I value tremendously the training he has imparted to me, teaching me to carefully think and effectively execute scientific research. I would also like to thank him for his time and patience, as I had the opportunity to work on a very unique project for someone who entered as an inorganic chemist. Secondly, I would like to thank Greg Baker for his guidance, and for his time answering many of my questions. I would like to thank my committee members, Aaron Odom and Ned Jackson, for helpful discussions and suggestions. I would also like to thank Professor Michael Mackay and his students for their time and use of their equipment, as well as Professor Laura McCabe for her discussions, and her students for carrying out the physiological studies on the polymer surfaces. Also, I would like to thank former group members Dean, Carl, and Baixin for their training, Jian-Yang Cho his friendship during the toughest five years of my life, and colleagues Kin, Dan, and Jim for their friendship and profitable scientific discussions. I would also like to thank Mei for her very helpful scientific insight and Abbas for his diligent efforts in "taking over the family business." I would also like to collectively thank the MSU faculty and staff for catering to my needs for five years. Finally and most importantly, I would like to thank my family and my extended family for their prayers, support, and wisdom for me during my graduate career.

"..For by him all things were created: things in heaven and on earth, visible and invisible, whether thrones or powers or rulers or authorities; all things were created by him and for him. He is before all things, and in him all things hold together.."

TABLE OF CONTENTS

# LIST OF ABBREVIATIONS

| | |
|---|---|
| ADMET | Acyclic Diene Metathesis Polymerization |
| BBA | 4-*tert*-Butylbenzylalcohol |
| br | broad |
| BrdU | Bromodeoxyuridine |
| CM | Cross Metathesis |
| δ | ppm |
| d | Doublet |
| DAG | 3,6-Diallyl-2,5-dioxan-1,4-dione (Diallylglycolide) |
| DCC | Dicyclohexylcarbodiimide |
| dd | Doublet of Doublets |
| ΔH | Heat of Fusion (crystallinity) |
| DMAP | N,N-Dimethyl-4-aminopyridine |
| DMSO | Dimethylsulfoxide |
| DSC | Differential Scanning Calorimetry |
| ECM | Extracellular matrix |
| EI | Electron Impact |
| $Et_2O$ | Diethyl Ether |
| EtOAc | Ethyl Acetate |
| EtOH | Ethanol |
| GC/MS | Gas Chromatography/Mass Spectrometry |
| GPC | Gel Permeation Chromatography |
| HAp | Hydroxyapatite |
| HPA | 2-Hydroxypent-4-enoic acid |
| Hz | hertz |
| J | Coupling Constant |
| LA | Lactide |
| LLA | L-lactide |
| LRMS | Low resolution mass spectrometry |
| m | multiplet |
| MHz | Megahertz |

| | |
|---|---|
| $M_n$ | Number average molecular weight |
| $M_w$ | Weight average molecular weight |
| NMR | Nuclear magnetic resonance |
| PCL | Poly(ε-caprolactone) |
| PDAG | Poly(diallylglycolide) |
| PDI | Polydispersiy index ($M_w/M_n$) |
| PDLLA | Racemic poly(lactide) |
| PDLLA-*co*-DAG | Poly(D,L-lactide-*co*-diallylglycolide) |
| PEG | Poly(ethylene glycol) |
| PGA | Poly(glycolide) |
| PHB | Poly(hydroxybutyrate) |
| PLA | Poly(lactide) |
| PLGA | Poly(lactide-*co*-glycolide) |
| PLLA | Poly(L-lactide) |
| PLLA-*co*-DAG | Poly(L-lactide-*co*-diallylglycolide) |
| PLLA-*g*-AB | Poly(L-lactide-*g*-allylbenzene) |
| PLLA-*g*-ArPr | Poly(L-lactide-*g*-arachidonic acid propyl ester) |
| PLLA-*g*-BocLysPr | Poly(L-lactide-*g*-N,N'-di-Boc-lysine propyl ester) |
| PLLA-*g*-decenal | Poly(L-lactide-*g*-decenal) |
| PLLA-*g*-decenyloxy-NB | Poly(L-lactide-*g*-decenyl-1-oxy-(4-nitrobenzene)) |
| PLLA-*g*-decenyloxy-TBS | Poly(L-lactide-*g*-decenyl-1-oxy-TBS) |
| PLLA-*g*-DPAPr | Poly(L-lactide-*g*-diethylphosphonoacetic acid propyl ester) |
| PLLA-*g*-HP | Poly(L-lactide-*g*-hydroxypropane) |
| PLLA-*g*-LnPr | Poly(L-lactide-*g*-linoleic acid propyl ester) |
| PLLA-*g*-LysTFAPr | Poly(L-lactide-*g*-lysine bis(trifluoroacetate) propyl ester) |
| PLLA-*g*-MyPr | Poly(L-lactide-*g*-myristic acid propyl ester) |
| PLLA-*g*-OlPr | Poly(L-lactide-*g*-oleic acid propyl ester) |
| PLLA-*g*-PAPr | Poly(L-lactide-*g*-phosphonoacetic acid propyl ester) |
| PLLA-*g*-PB | Poly(L-lactide-*g*-2-(2-propenyloxy)benzaldehyde) |
| PLLA-*g*-StPr | Poly(L-lactide-*g*-stearic acid propyl ester) |
| q | quartet |

| | |
|---|---|
| RCM | Ring-Closing Metathesis |
| RGD | Arginine-Glycine-Aspartic Acid |
| ROMP | Ring-Opening Metathesis Polymerization |
| ROP | Ring-Opening Polymerization |
| RT | Room Temperature |
| s | singlet |
| SAM | Self-Assembled Monolayer |
| $Sn(Oct)_2$ | Tin(II)-2-ethylhexanoate |
| t | triplet |
| TBS | *tert*-Butyldimethylsilyl |
| $T_c$ | Crystallization Temperature |
| $T_g$ | Glass Transition Temperature |
| THF | Tetrahydrofuran |
| $T_m$ | Melting Temperature |
| UV-Vis | Ultraviolet-Visible |

LIST OF FIGURES

LIST OF TABLES

Images in this dissertation are presented in color.

CHAPTER ONE

# 1 Materials Used in Biomedical Applications

Material applications in the area of organ replacement represent one of the most significant developments to medicine. In the area of tissue engineering, the primary goal is to design a compatible synthetic environment for cells to proliferate, divide, and differentiate, where the regenerated tissue remains physiologically indistinguishable from tissue formed under natural conditions. In the area of drug delivery, biologically compatible materials are used to support the controlled release of a variety of substrates, thereby inducing the desired physiological effect. The requirements for these applications are met in various biodegradable polymers.

Biodegradable polymers can be categorized into two classes: Natural and Synthetic. Naturally occurring biodegradable polymers include, but are not limited to, polypeptides, dextran, collagen, and chitosan (Figure 1). Many of these natural biopolymers constitute what is known as the extracellular matrix (ECM), which provides the environment from which cells can grow into tissue. Often, this process is predicated on the cells' response to the proteins, polysaccharides, and glycosoaminoglycans which make up the ECM.[1] The most common synthetic biodegradable polymers are poly(glycolide) (PGA), poly(D,L-lactide) (DL-PLA or PDLLA), poly(L-lactide) (L-PLA or PLLA), poly(lactide-*co*-glycolide) (PLGA), poly(hydroxybutyrate) (PHB), and poly(ε-caprolactone) (PCL) (Figure 2).

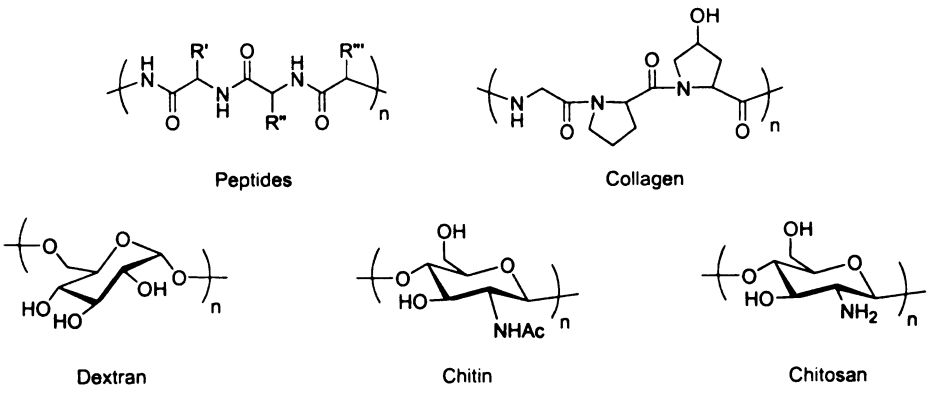


**Figure 1.** Natural biodegradable polymers.

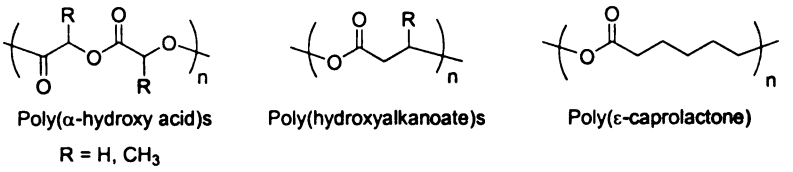


**Figure 2.** Synthetic biodegradable polymers.

Synthetic biodegradable polyesters such as PLA have emerged as an important class of materials. Ultimately derived from readily available agricultural sources such as corn and starch, PLA offers an environmentally benign alternative to polymers derived from petrochemical sources.[2-4] As one of a few biodegradable polyesters, PLA breaks down into lactic acid, a naturally occurring by-product in human metabolism. As a result, the biomedical field has benefited from these materials. Materials made from PGA, PLA, PLGA, PHB, and PCL can be used for resorbable sutures,[5] medical implants,[6-8] matrices for drug delivery,[9-12] and in tissue engineering applications,[11,13,14] where PLA polymers and copolymers have been used as biodegradable scaffolds to support tissue growth. Progress in both of these fields must be made through the design of materials that emphasize favorable surface interactions between the material and the targeted biological entity. Patterned surfaces, natural and synthetic biodegradable

polymers, and the modifications thereof constitute a significant portion of the advancements made in biomaterial science implemented to optimize surface-cell interactions in the areas of tissue engineering and drug delivery.

The uses of natural biodegradable polymers are limited primarily by their poor enzymatic degradation profiles as well as their poor mechanical properties.[15] Conversely, because of their favorable degradation rates and flexibility in their mechanical properties, development of synthetic biodegradable polymers is the preferred route used in tissue engineering (Table 1).[16,17]

| Polymer type | Melting point (°C) | Glass trans. temp. (°C) | Degrad. time (months)[a] | Density ($g/cm^3$) | Tensile strength (MPa) | Elongation (%) | Modulus (GPa) |
|---|---|---|---|---|---|---|---|
| PLGA | Amorph. | 45-55 | Adjustable | 1.30 | 41.4-55.2 | 3-10 | 1.4-2.8 |
| DL-PLA | Amorph. | 55-60 | 12-16 | 1.25 | 27.6-41.4 | 3-10 | 1.4-2.8 |
| L-PLA | 173-178 | 60-65 | >24 | 1.24 | 55.2-82.7 | 5-10 | 2.8-4.2 |
| PGA | 225-230 | 35-40 | 6-12 | 1.53 | >68.9 | 15-20 | >6.9 |
| PCL | 58-63 | -65 | >24 | 1.11 | 20.7-34.5 | 300-500 | 0.21-0.34 |

**Table 1.** Properties of biodegradable polymers.[18-21] [a] Time to complete mass loss. Time also depends on part geometry.

## 1.1 Engineering Surfaces for Cell Growth

Surface chemistry plays an integral role in tissue engineering and drug delivery, since the surface interaction of cells with any material, natural or unnatural, dictates the biological response in either tissue engineering or drug delivery processes. The development of materials addressing this important feature focuses on overcoming the key challenge of uncontrolled adsorption of cells onto surfaces of materials rendering them useless, characterized by the nonspecific reactivity with the desired biological entity.[1] The high reactivity and specificity with which biological processes operate, such as enzymatic pathways and growth cycles, is quite remarkable. Man-made biomaterials that would be able to mimic the reactivity and specificity seen in Nature would be highly

desirable. Since surface chemistry is of paramount importance, engineering materials with specific surface properties has been an active area of research.

Surface modification using self-assembled monolayers (SAMs) has proved to be a promising approach toward the design of new biomaterials. SAMs based primarily on alkanethiolates attached to gold have been the starting materials for the modification of many surfaces. Whitesides and Mrksich both have developed alkanethiolate SAMs that present different groups such as oligomeric ethylene glycol units,[22,23] carbohydrates,[24,25] peptides,[26,27] and hydrophobic ligands.[28] All of these surfaces show some influence in regulating protein adsorption. For example, the hydrophilicity of carbohydrates and ethylene glycol units attached to the termini of the hydrophobic SAMs help reduce cell adhesion to the surface. However, the uniqueness between these two hydrophilic terminal groups was further observed by Luk and Mrksich as they showed that patterned hydroxyl-terminated SAMs are able to direct adhesion of 3T3 fibroblasts on the surface of the material. Patterns using ethylene glycol terminated SAMs began to fade away after nine days, whereas mannitol-terminated SAMs retained the pattern integrity for over twenty-five days.[24] This work highlights the potential benefits of SAMs in controlling cell adhesion and the use of well-defined patterns to regulate material-cell interactions.

Surface patterning is used primarily to invoke a geometrical constraint for cells on the surface of the material in a way to influence the biology of the system. The types of materials that have been patterned range from alkanethiolate SAMs,[29] proteins,[30,31] saccharides,[32,33] and even minerals such as apatite. A resist patterned $CaO\text{-}SiO_2$ modified glass substrate was exposed to an ionic solution containing simulated body fluid. The ions in the simulated body fluid induced apatite formation, and after removal of the resist

by dissolution in an organic solvent, the apatite appeared as well-defined patterns on the glass surface. Moreover, an array of shapes and even alphanumeric characters with lines as narrow as 2 μm were patterned.[34] The size and scale of the pattern depends on the desired purpose of the pattern. Surfaces can be patterned over a wide range of dimensions (Table 2).

| Substrate | *Pattern Size* | Research Topic |
|---|---|---|
| Alkanethiolate SAM | *2 x 4 $nm^2$* | Study of organization and self-assembly of ligands[35] |
| Alkanethiolate SAM | *2-10 μm* | Measuring cell adhesion strength on patterns coated with cell integrins.[36] |
| Polystyrenes | *2-100 μm* | Cell growth on patterned polystyrene using specific patterns.[37] |
| PLA/PEG | *12-70 μm* | Patterning a biodegradable polymer containing a biotinylated surface group.[38,39] |
| Poly(acrylic acid)/PEG-coated Alkanethiolate SAM | *50-100 μm* | Regulating cell growth on poly(acrylic acid)/PEG-modified SAMs.[40] |

**Table 2.** Patterning sizes typically used to control cell adhesions in materials.

The result of patterning substrates, in essence, affects the shape of the cells by controlling adhesion. This interaction has dynamic effects on the conformation of the cell and consequently influences the cell's physiological function.[41-43] Recognizing this, Whitesides and Ingber have studied the effects of cell geometry on its physiological function. Cells were seeded onto micro-patterned surfaces of different sizes (5-50 μm), and the micron-sized surfaces were coated with adhesive proteins. Through control of cell adhesion and consequently the size of the cell, they studied the effect of cell

geometry with respect to apoptosis (cell death), differentiation, and growth (Figure 3). In their experiments, endothelial cells died (apoptosis) when their surface area was $\leq 500\mu m^2$, and cell growth occurred when the surface area was $\geq 1500\ \mu m^2$. When the cell surface area was approximately 1000 $\mu m^2$, both growth and apoptosis cycles were stopped and differentiation started.

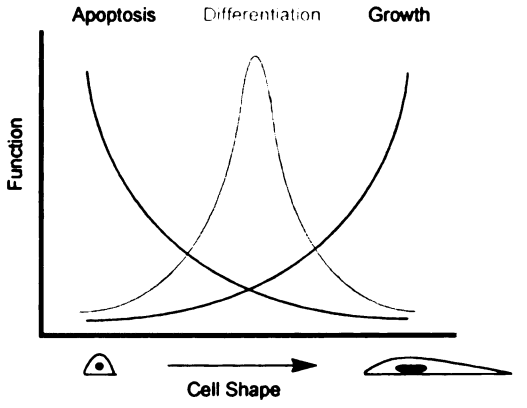


**Figure 3.** Correlation of the physiological function of cells with respect to cell shape.

## 1.2 Biodegradable Polymers as Scaffolding Materials

### 1.2.1 Three-Dimensional Scaffolds

Intricate designs and structures of synthetic biodegradable polymers such as PGA, PLA, and PLGA as scaffolding materials have been studied extensively.[15-17,44,45] The use of highly porous scaffolding materials as templates for cell growth is desirable because of the high surface area for cellular attachment as well as the mechanical strength of the material. The design of porous three-dimensional scaffolds can be achieved by different methods (Figure 4).

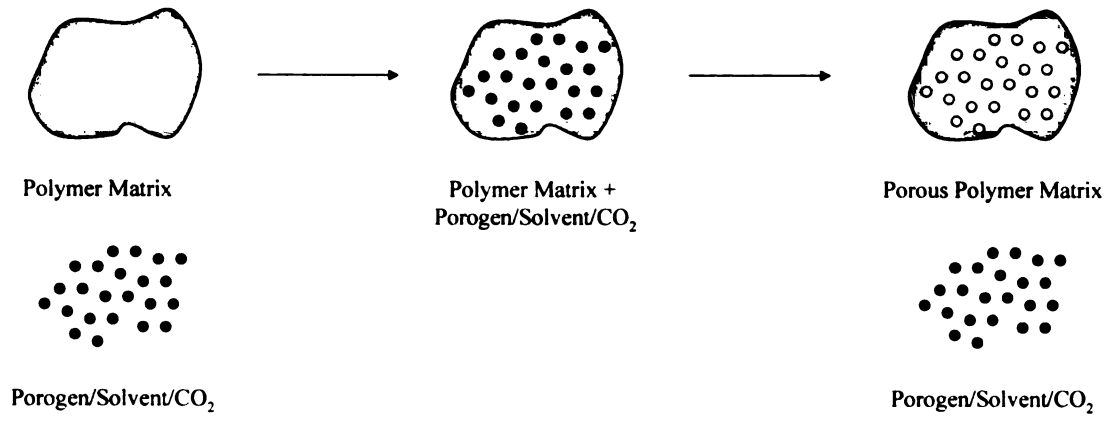


**Figure 4.** Illustration of the common methods used to synthesize three-dimensional scaffolds.

Porogen leaching is a common method used to create pores within the PLA matrix. In this technique, a suspension of a water-soluble "porogen" such as a salt (salt leaching) is mixed with the polymer. Once the solvent is removed, the water-soluble particulates can be washed away leaving a porous, three-dimensional scaffold. Using this technique, pore size can be easily controlled by the choice of the particulate used.

Mooney and coworkers have used gases such as carbon dioxide as a foaming agent in the design of PLLA and PLGA porous materials.[46,47] Carbon dioxide gas diffuses into the material creating a polymer/gas solution. As the pressure of carbon dioxide is decreased, macropores form within the matrix. The pressure, gas type, and diffusivity all determine pore size of the material. Park and Yoon also created foams by combining porogen leaching and gas forming techniques. PGA/PLA copolymers containing ammonium bicarbonate salts as a porogenous gas forming agent were immersed into an aqueous citric acid solution to generate carbon dioxide *in situ*, generating scaffolds containing pore sizes varying from 200-500 μm.[48,49]

A phase separation technique can also be used, where instead of mixing a solid porogen additive, solvent molecules of a polymer solution can act as the additive.

Removal of the solvent by freeze-drying can result in a variety of polymer foams. Depending on whether there are liquid-liquid or solid-liquid phase separations between polymer and solvent during cooling, the overall infrastructure of the material can change. Ma and coworkers have used this technique to synthesize highly porous nanofibrous structures of PLLA and PLGA for tissue scaffolding.[50,51]

Although high surface area and highly porous materials can be prepared, the limitation is that no specific reactive sites or functionality is presented. Porous scaffolds possessing framework functional sites would be beneficial. Nonetheless, porogen leaching still remains a popular method for the design of three-dimensional porous scaffolds.

Increased surface area can also be found in fibrous meshes of synthetic polymers. These meshes can be woven in three-dimensional patterns or designs, perhaps most commonly as sutures. Meshes of PLA, PGA, and PLGA have all been used to as materials to aid the regeneration of many forms of human tissue.[52-56] This method emphasizes the improved mechanical strength of PGA while utilizing the more biocompatible surface properties of the PLLA or PLGA coating. Langer and Mooney designed a bonding technique by spraying an atomized solution of PLLA or PLGA onto PGA woven fibers.[57] In spite of the increase strength of the material, the strength is still dependent on the efficiency of the connection between the PLLA and PGA layers. Moreover, the lack of functionality still remains a limitation to such materials.

### 1.2.2 Hybridization of Synthetic Polymers With Natural Polymers

Although use of some biodegradable scaffolds has shown much promise in tissue growth applications, with control over their degradation properties and cell-scaffold

interactions, they are deficient since they lack functionality, and possess an overall hydrophobic character. Hybrid materials based on PLA, PGA and a natural biologically functional polymer, such as collagen, provide a material that possesses increased biocompatibility and mechanical strength over just the PLA or collagen alone (Figure 5). For example, PLLA-coated collagen fibers showed a 200% increase in tensile strength and modulus over the PLLA alone.[58] The inverse are also made, such as PLLA sponges coated with collagen.[59] In fact, collagen coated-PLLA sponges interact more with mouse fibroblast L929 cells than did the PLLA sponges alone.[15]

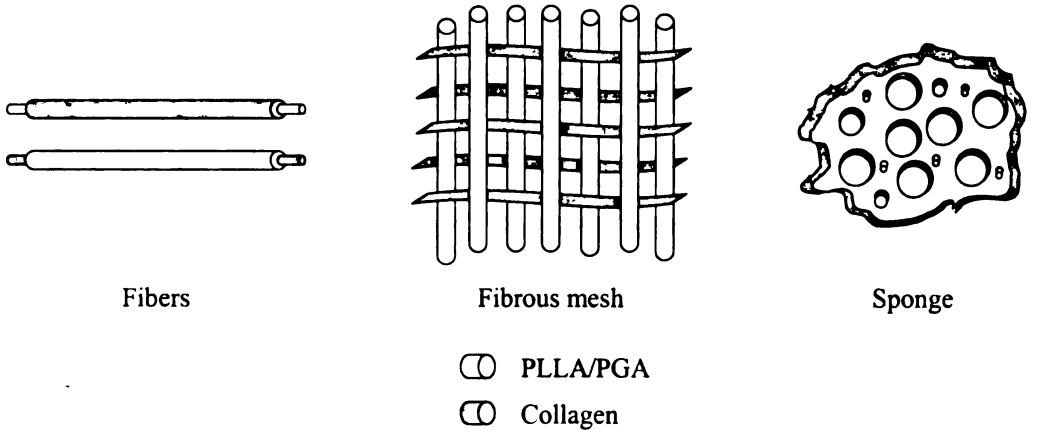


**Figure 5.** Different three-dimensional structures of PLLA-collagen hybrids.

### 1.2.3 Substrate Encapsulation

A similar form of hybridization can be achieved using more specialized substrates which possess a more specified type of reactivity. The biocompatibility of a polymer can be improved by the blending or encapsulation of proteins,[60-62] growth factors,[63-66] or minerals,[50,51,67,68] directly with PLA or PGA (Figure 6). These methods all show improved activity in tissue regeneration when compared to PLA and PGA polymers and copolymers alone.

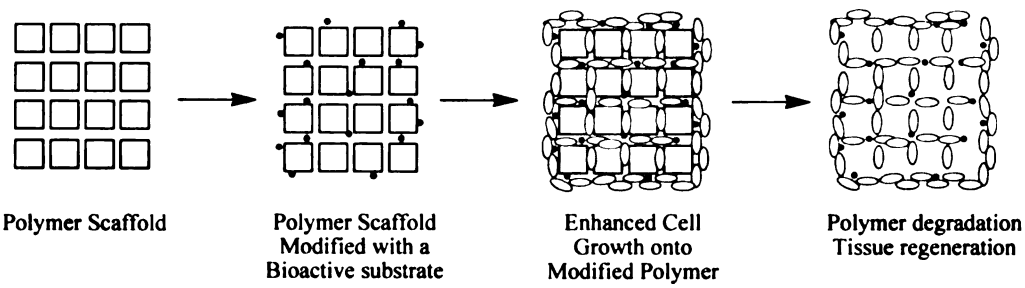


**Figure 6.** Tissue regeneration through the templation of bioactive substrates.

Growth factors such as bone morphogenic proteins (BMPs), for example, are used precisely for this purpose. The growth factors used in combination with a defined scaffold create a hybrid material which carries out a specific physiological role. For example, Hollinger and Winn had reported that using a porous collagen-coated PLA scaffold embedded with BMP-2 growth factors, produced more bone than the PLA-collagen scaffold without the BMP-2.[69] Peter and Mikos synthesized microspheres of PLGA/PEG (95/5) containing transforming growth factor-β1 (TGF-β1), which [70] subsequently improved both proliferation and differentiation. Mooney et al. and Patrick independently prepared functional porous PLGA scaffolds using a gas foaming process containing embedded vascular endothelial growth factor (VEGF). The materials ultimately led to increased proliferation of human umbilical vein endothelial cells.[71,72] Ma has capitalized on the high porosity of a three-dimensional scaffold and doped hydroxyapatite in order to enhance osteoblast growth.[50] While not part of the framework of the biomaterial itself, the growth factors and minerals offer a way to influence cell proliferation and differentiation.

## 1.3 Biodegradable Polymers as Drug Delivery Matrices

Biodegradable polymers in drug delivery are largely based on PLA, PLGA or PCL copolymers. Many approaches have been taken to obtain the optimal drug delivery device. The use of biodegradable polymers is effective because the by-products are safely eliminated *in vivo*. In drug delivery, a polymeric system can deliver a pharmaceutical agent, *via* a controlled or systematic release (Figure 7).[73]

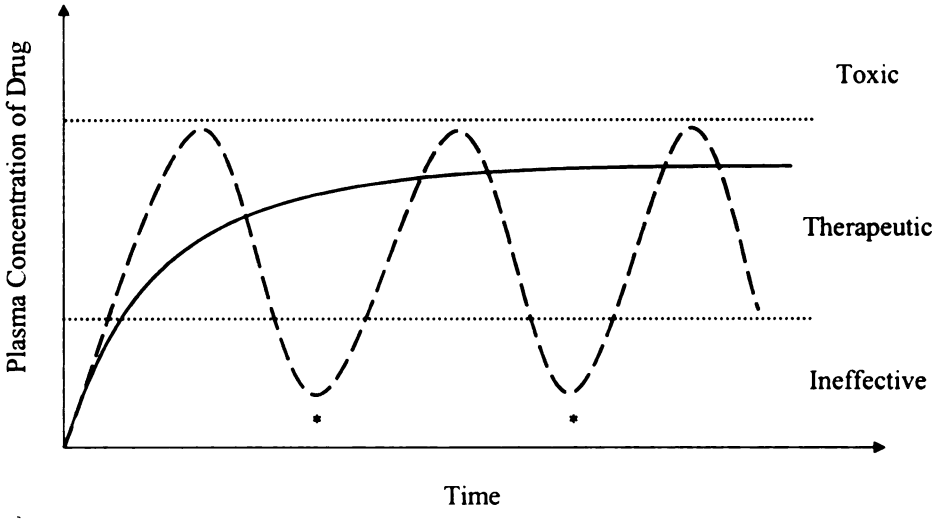


**Figure 7.** Plasma concentration of a drug as a function of time. (—) Prolonged delivery system. (—) Traditional delivery system with repetitive administration (*).

The therapeutic agent can be delivered as the polymeric system undergoes slow degradation, *via* diffusion of the agent through the matrix.[74,75] Polymeric drug delivery systems can be derived from natural polymers such as polysaccharides,[76] chitosan,[77] collagen[76] or synthetic polymers which include PGA, PLA, PLGA, or PCL.[78-82] Typically, microspheres of these polymers are prepared using an oil-in water evaporation technique (Figure 8).[73]

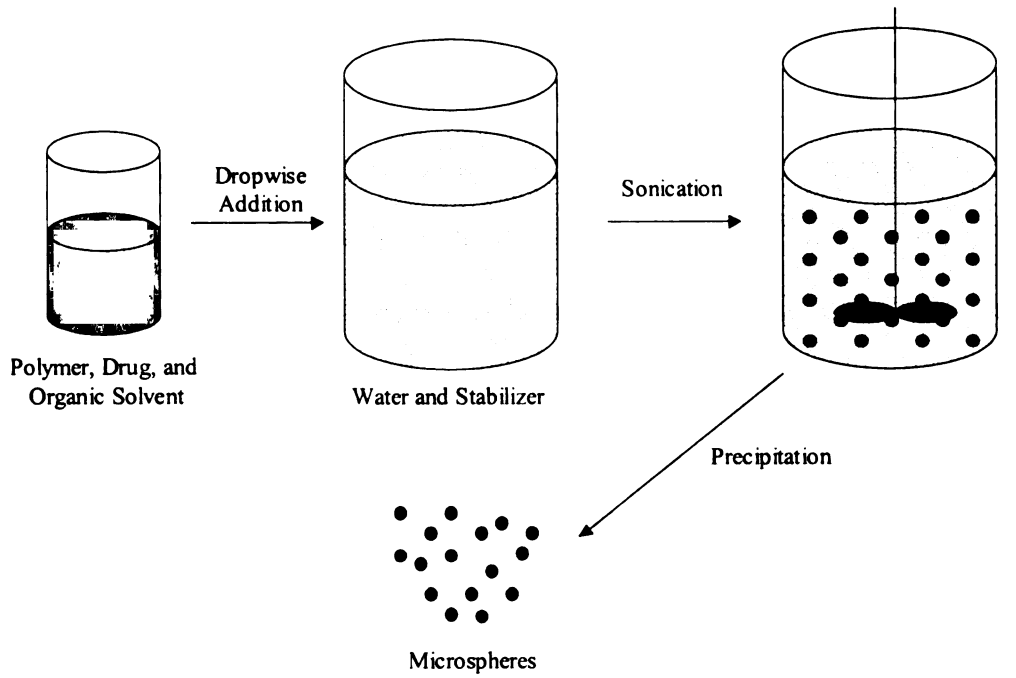


**Figure 8.** Schematic illustration of microsphere preparation by the oil-in-water solvent evaporation technique.

Copolymers which combine natural and synthetic polymers are also very common as matrices. Li and coworkers have prepared comb-like copolymers containing a dextran backbone with PGA and PLA oligomeric side chains.[83] These copolymers are good drug delivery matrices for the continuous release of fluorescein isothiocyanate labeled dextran and bovine serum albumin (BSA), with accelerated degradation not seen in the pure PGA or PLA. Since polyesters like PGA and PLA are very hydrophobic, hydrophilic domains are generally incorporated in some way. Copolymers and blends of PLA and polyethylene glycol (PEG) are also commonly used to deliver proteins and drugs.[84-87] For example, Yeh has prepared microspheres from blends of PLGA, PEG and insulin. Stable microspheres (3-8 μm in diameter) provided a steady release of insulin over the course of 28 days.[88] PLA-chitosan blends[89-91] and PLA-peptide blends[92] are some of the other

polymeric systems which have been prepared as microspheres for the delivery of proteins and drugs.

Incorporating hydrophobicity in polymeric matrices can also improve drug delivery processes by promoting surface erosion as opposed to internal degradation. Hydrophobic regions maintain the integrity of the matrix by protecting the interior from the aqueous media while the hydrophilic regions interact with the aqueous media to promote surface erosion. In order to address this issue, Langer prepared polyanhydrides using a melt polycondensation technique under reduced pressure (Figure 9).[93-95]

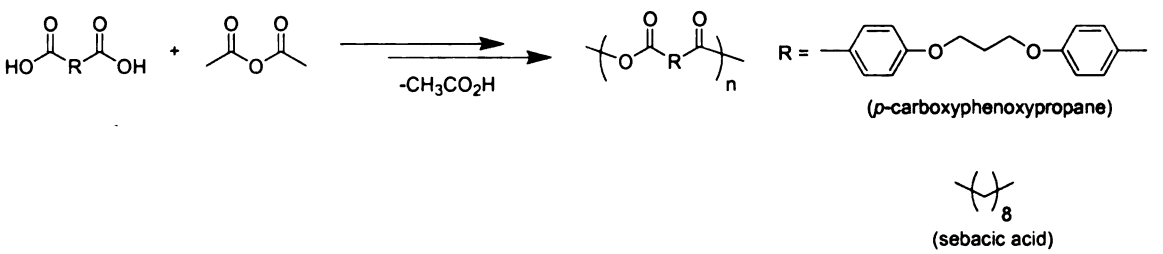


**Figure 9.** Synthetic route to poly(anhydrides) via polycondensation.

Polyanhydrides have become attractive drug delivery matrices because of the variability in their properties. For example, aliphatic polyanhydrides can degrade within days to weeks, while aromatic polyanhydrides may take several months to years.[96] This interesting feature can be exploited to design materials to fit the desired degradation profile. Polyanhydrides derived from *p*-carboxyphenoxypropane and sebacic acid have generated the most pharmaceutical interest.[94,97,98] However, has been introduced by Domb and coworkers introduced other functionality by incorporating fatty acids and other hydrophobic groups through end group modification and copolymerizations with polyanhydrides.[99-103]

These fatty acid based polyanhydrides have been used as carriers for anesthetics and chemo-therapeutic agents,[98,104] while the FDA approved poly(*p*-carboxyphenoxypropane-co-sebacate) has been used as an implant to deliver drugs for brain cancer treatments.[105] A PLA-coated hybrid polyanhydride sheet loaded with heparin resulted in the controlled local delivery of heparin in laboratory rats over the course of 20 days, as opposed to 4 days for the uncoated heparin loaded polyanhydride sheet.[106]

Natural and synthetic biodegradable polymers have numerous advantages as both tissue engineering scaffolds and drug delivery matrices. Often, copolymers or hybridizations of these two classes of polymers are used in complementary fashion. Simple adaptations of biodegradable polyesters such as PLA and PGA with different forms of functionality have been explored.

## 1.4 Modification of Poly(Lactic Acid)

Due to their biocompatibility, PLA, PGA, and PLGA, are the most common materials from which biodegradable tissue scaffolds are made.[107-110] However, a significant drawback to using the materials of PLA and PGA in tissue engineering is the lack of control in cell adhesion, where the hydrophobic polymer (e.g. PLA) will adhere too strongly to cells and cell adhesion proteins, thereby decreasing its bioactivity.[111,112] This exposes a core problem for researchers who use biodegradable polymers such as PLA in the areas of tissue engineering and drug delivery. While the biocompatibility and biodegradability of these polymers may be adequate enough to actually grow tissue or release drugs, the specificity with which cells bind is minimal. The current solution to this problem is to design functionalized copolymers to counteract the lack of specific

functionality in the PLA or PGA polymers or copolymers. Since the only site available for chemical modification on poly(α-hydroxy acids) are the endgroups, the synthesis of block and graft copolymers, random copolymers using functional monomers, and coupling between a polymer and bioactive substrate must be pursued.

### 1.4.1 Endgroup Modification of Biodegradable polymers

#### 1.4.1.1 Polymer Macroinitiation

Both diblock[113-115]and triblock[86,116-118] copolymers of PLA/PGA and poly(ethylene glycol) (PEG) have been prepared in order to create biomaterials with both hydrophobic and hydrophilic domains (Figure 10).

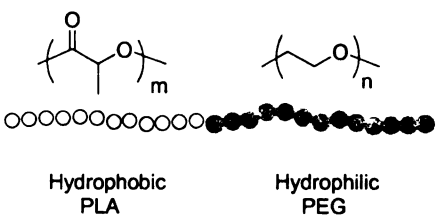


**Figure 10.** Block copolymer of poly(lactic acid) and poly(ethylene glycol).

The PEG segments in the copolymers serve as a means to better control the protein and cell adhesion while maintaining the biocompatibility of the material.[112] The synthesis of these block copolymers is achieved by polymerizing lactide using the hydroxylated chain end of the PEG unit as a macroinitiator (Figure 11).

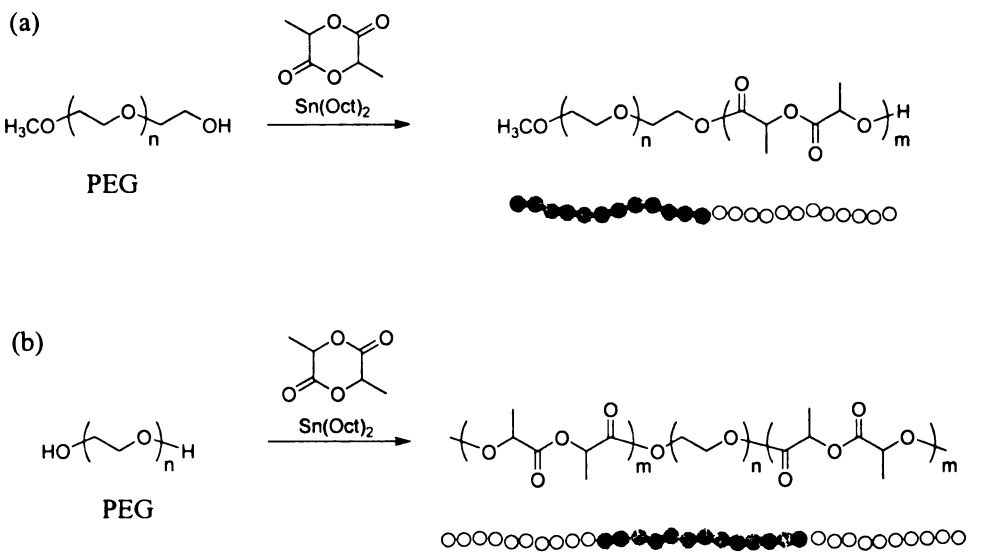


**Figure 11.** Block copolymers of poly(lactide) and poly(ethylene glycol) synthesized by PEG macroinitiation. *(a)* -AB- block copolymer *(b)* -ABA- block copolymer.

Recently, Mikos has shown the use of a block copolymer, PLA-*b*-PEG, as a tissue scaffold for the differentiation of bone marrow cells. The copolymer was synthesized through the ring-opening polymerization of D,L-lactide with tin(II)octanoate as the catalyst and poly(ethylene glycol)-monomethyl ether as the macroinitiator. The PEG domain serves to regulate cell adhesion of adsorbed serum proteins (e.g. fibronectin), thus resulting in differences in cell shape and increased osteoblast differentiation as compared to PLA, PLGA and tissue culture polystyrene dishes.[111,115] This result emphasizes that controlled adhesion of serum proteins to the biomaterial affects the shape and conformation of the cell, thereby influencing differentiation. The hydrophilicity of the PEG domains can also be used as a way to synthesize hydrogels.[112] These hydrogels are copolymers of PLA and PEG which are then photochemically cross-linked through reactive endgroups.[119,120] These gels are stronger materials than linear block copolymers, providing a porous material that does not dissolve, but swells in aqueous systems.

Terminal hydroxyl groups of poly(hydroxybutyrate) (PHB),[121] poly(dimethylsiloxane),[122] and poly(e-caprolactone),[123] poly(vinylalcohols),[124] and poly(saccharides)[125] can also be used as macroinitiators to prepare block copolymers and graft copolymers of lactide. These copolymers offer applications in both tissue scaffolds and as drug delivery matrices.

### 1.4.1.2 Functional Group Initiation

The hydroxyl groups of more specified substrates can be used as coinitiators with tin(II)-octanoate to prepare polymers with specific endgroups (Figure 12).

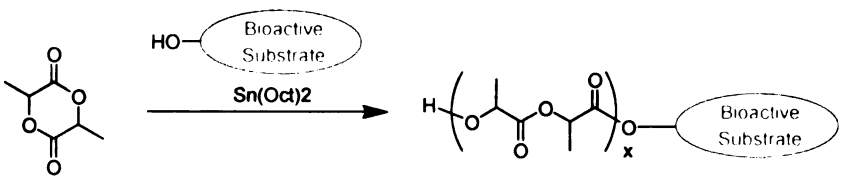


**Figure 12.** Endgroup modification of poly(lactic acid) using a functional coinitiator.

Stupp and coworkers incorporated a cholesterol endgroup in PLA simply by using cholesterol itself as the initiator in the polymerization of lactide.[126] The cholesterol endgroup takes advantage of the cholesterol-cell membrane interaction in fibroblasts. The cholesterol-functionalized PLA affected the overall shape fibroblasts and improved their adhesion compared to the PLA control.[127] To further demonstrate the utility of endgroup modification, Gardella and coworkers functioalized the endgroups of PLA with fluorinated alkyl chains through both post-polymerization coupling reactions between flouroalkyl chains and the PLA as well as the use of a fluorinated alcohol as a coinitiator.[128] The fluorinated segments can be used to regulate the surface adhesion properties of the material. Groups with multiple functionality containing groups such as

primary amines, diols, and carboxylic acids are incompatible with the catalyst, thus limiting their use in functional endgroup initiation.

#### 1.4.1.3 Coupling Functional Endgroups

It is also possible to use standard coupling chemistry to link functional endgroups to biodegradable polymers. Utilizing a DCC coupling procedure, galactosyl derivatives have been successfully coupled to carboxylic acid endgroups of PLA to prepare microspheres suitable for drug delivery applications.[129] Langer has also used DCC coupling to link polylysine directly with PLA.[130] Coupling chemistry offers a mild way to introduce diverse functionality, however the only modification site on PLA is the endgroup, which means that the incorporated functionality is limited to coupling at this site.

#### 1.4.1.4 Backbone Modification of Poly(Lactic Acid)

##### 1.4.1.4.1 Amino Acid-Based Copolymers

In order to expand the applications of these biomaterials, two different methods have been developed to modify the structure of PLA using amino acid chemistry. The first is the copolymerization of lactide with a morpholinedione-based comonomer containing amino acid moieties.[131-133] For example, Langer and coworkers synthesized a functional comonomer bearing a protected lysine.[132] Copolymerization of the protected comonomer with L-lactide followed by the deprotection of the copolymer resulted in low loadings (1%-5%) of lysine-functionalized copolymer. The lysine is incorporated into the backbone of the polymer, and sites for adhesion are distributed along the polymer chain, where further chemical modification can be achieved (Figure 13). Chemical

attachment of amino acids is interesting in that it can serve as a model for more specific binding of proteins.

The second approach to modifying biodegradable copolymers with amino acids is through direct coupling of the polymer with amino acid groups.[130,134] One specific type of functionality that is important in the area of cell biology and cell adhesion is found in RGD (arginine-glycine-aspartic acid) containing peptide sequences.

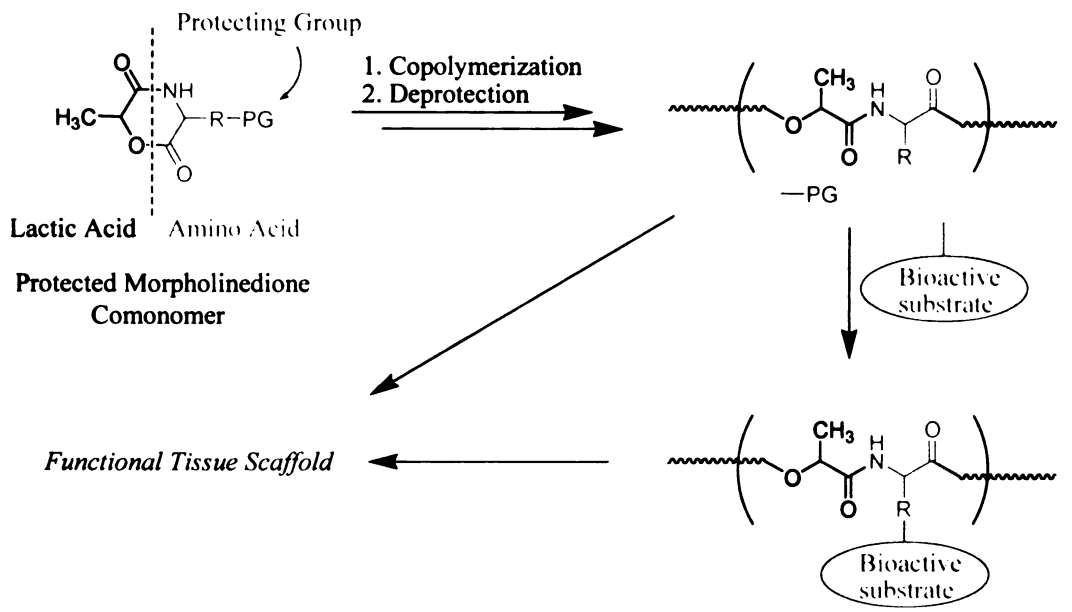


**Figure 13.** Copolymerization and modification of poly(lactic acid) using an amino acid based functional comonomer.

RGD is a specific sequence of amino acids which shows activity in binding to integrins within a cell's membrane, thereby affecting the conformation of the cell, and ultimately its function (Figure 14).[135-137] While using a peptidic functional comonomer that incorporates the whole RGD sequence is not practical, modifiying the backbone of the polymer using coupling chemistry is the preferred direction that research groups have taken. In fact, Langer and coworkers have also synthesized a biodegradable copolymer

containing the RGD sequence,[138] which involved the transformation of their previously synthesized PLA-*co*-lysine copolymer.[132] In this study, the side chain amino groups (-$NH_2$) from lysine incorporation react with carbonyldiimidazole, which is followed by coupling of the 5-unit RGD-containing peptide. Other research groups have also performed such RGD modifications on acrylate-based polymers and ethylene glycol based polymers using an RGD coupling procedure.[139-143]

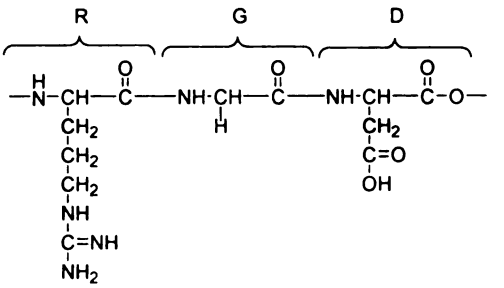


**Figure 14.** RGD amino acid sequence – Arginine-Glycine-Aspartic Acid.

The physiological effect of this modification was seen in the significantly increased surface area of bovine aortic endothelial cells (BAECs) on the RGD modified PLA-*co*-lysine compared to the surface area of BAECs on pure PLA, pure PLA-*co*-lysine, and control RGD-peptide sequences.[138] The coupling procedures of amino acids to existing biodegradable copolymers are an alternative way to incorporate amino acid functionality compared to the design of a protected comonomer.

This work also provides a model for the modification of biodegradable polymers with other large groups such as pharmaceutical agents, growth factors, and other proteins. From a biodegradation standpoint, the lactic acid and amino acid products upon degradation can be processed *in vivo*. Applications of these copolymers in tissue engineering enhance biocompatibility through cell-peptide interactions as well as the cell-

polymer interactions. The latter interface can be altered by the direct coupling of specific substrates.

#### 1.4.1.4.2 Non-Peptidic-Based Copolymers

Although the functionalization of biodegradable polymers has been established as a viable strategy in the design of amino acid/peptide-modified biomaterials, this approach is not limited to amino acids. The synthesis of other functional comonomers and copolymers has also been shown. Gonsalves has synthesized a biodegradable copolymer containing pendant phosphonate groups.[144] The phosphonate groups are incorporated to help induce the nucleation and growth of hydroxyapatite, $Ca_{10},(PO_4)_6(OH)_2$, an essential mineral in the regeneration of tissue responsible for bone formation. Gross and coworkers have demonstrated the incorporation of carbohydrate functionality through the copolymerization of a protected cyclic carbonate with L-lactide.[145] Deprotection results in the random copolymer, PLA-*co*-pentafuranose, with pendant sugars along the backbone. The hydroxyl groups of the pendent sugar are now accessible for further reactivity. Carbohydrates have found their niche as biologically compatible functional groups in part due to their biodegradability, where the degradation rates are much faster in carbohydrate-modified copolymers than in PLA and PGA polymers.[129]

Specific drawbacks to the design of specialized comonomers are (1) addressing the differences in physiological function requires the constant synthesis of new monomers which reflect the function, and (2) functional monomers must be compatible to the conditions of the polymerization. The majority of biodegradable copolymers fall under one of these two categories. The design of a chemically inert monomer possessing sites which could be modified *after* the polymerization would enable us to incorporate

diverse functionality in the framework of the polymer, and prevent a complicated monomer and copolymer synthesis. Once the functional copolymer is prepared, routine organic methodology can provide an avenue for synthesizing a broad range of materials. By employing a combinatorial approach to polymer synthesis, our aim is to develop a biodegradable polymer system based on a ***single copolymer*** by which we can introduce hydrophilicity, hydrophobicity, pendant reactive sites, and macroinitiators for different polymer architectures, all through simple and efficient reactions common to synthetic organic chemists. Post-polymerization modification offers us the possibility of using a functional monomer whose synthesis and copolymerization with lactide can be achieved through the same simple protocol as lactide itself.

CHAPTER TWO

## 2 Modification of Poly(Lactic Acid)

Biodegradable polymers have found their niche as important materials with wide applicability in the biomedical field. Medical devices made from synthetic biodegradable polymers such as PGA, PLA, PLGA, PHB, and PCL have become standard in the medical community.[5-7] In tissue engineering applications, scaffolds made from these synthetic polymers, have been improved by designing unique three-dimensional structures. Despite this improvement, the scaffold itself remains a hydrophobic material, possessing neither control over cell adhesion nor any biospecific functionality. Copolymerizations[131-133] of biodegradable polymers with biologically relevant materials, have helped improve control over cell adhesion, but these materials do not possess any functionality other than a single reactive endgroup. Hybridizations[60-66] may offer more specificity, however, a new material must be made for each new application, and opportunities for multiple functionalization within a given matrix are not available. Our approach towards improving current methods of functionality is to design a single copolymer which possesses sites for modification to introduce functionality by more than one way. Starting with a single biodegradable copolymer, the functional side chain can be modified in a number of different ways through a multitude of organic transformations. This would allow the modification of the biodegradable polymer and subsequent function to be differentiated through established organic methodology. Moreover, at biologically relevant loadings of functionality, the physical properties of the polymer can be maintained. Post-polymerization modification is our method to access a

library of copolymers by simple covalent attachment of the desired functional group to the polymer chain. This would allow us to work from a single copolymer.

## 2.1 Monomer Synthesis

The functional comonomer, 3,6-diallylglycolide (DAG), was synthesized by the acid catalyzed condensation of the allyl substituted α-hydroxy acid, 2-hydroxypent-4-enoic acid. This acid catalyzed condensation is the industrial process by which L-lactide, the monomer precursor of PLA is synthesized, and is the general approach to a variety of alkyl substituted glycolides.[146] Using a different approach, Emrick and coworkers have synthesized α-allyl(δ-valerolactone) *via* allylation of δ-valerolactone.[147] However, in our case, the α-hydroxy acid was readily prepared from the bismuth-zinc mediated allylation of glyoxylic acid monohydrate using allyl bromide as the allyl source. The acid was obtained in excellent yield and could be used directly in the next step or recrystallized from ether and hexanes give a pure crystalline material. The acid-catalyzed condensation of the allyl-substituted α-hydroxy acid was carried out in toluene for 3 days with the water from condensation being removed using a Dean-Stark trap. The crude reaction mixture contained both oligomers and the monomer. An isomer mixture of 3,6-diallylglycolide, was isolated as a colorless oil by distillation of the reaction mixture under reduced pressure using zinc oxide, ZnO, as a transesterification catalyst (Figure 15).

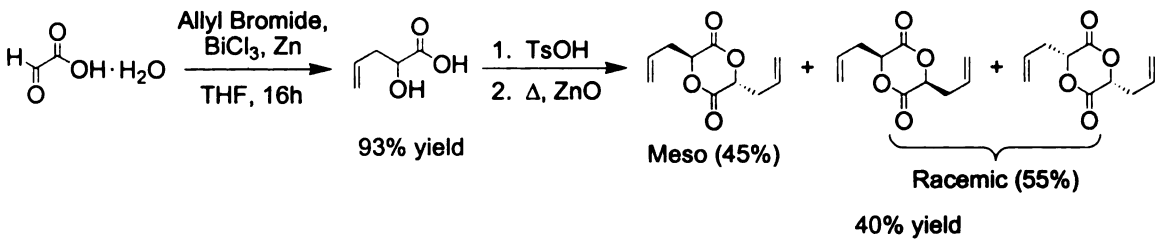


**Figure 15.** Synthetic route to 2-hydroxypent-4-enoic acid and 3,6-diallylglycolide.

The monomer contains a near statistical mixture of RR, RS, and SS stereoisomers which can be distinguished by NMR spectroscopy (Figure 16). This is seen mostly clearly by the observation of the methine region of the proton NMR spectrum. These protons both are observed as doublets of doublets.

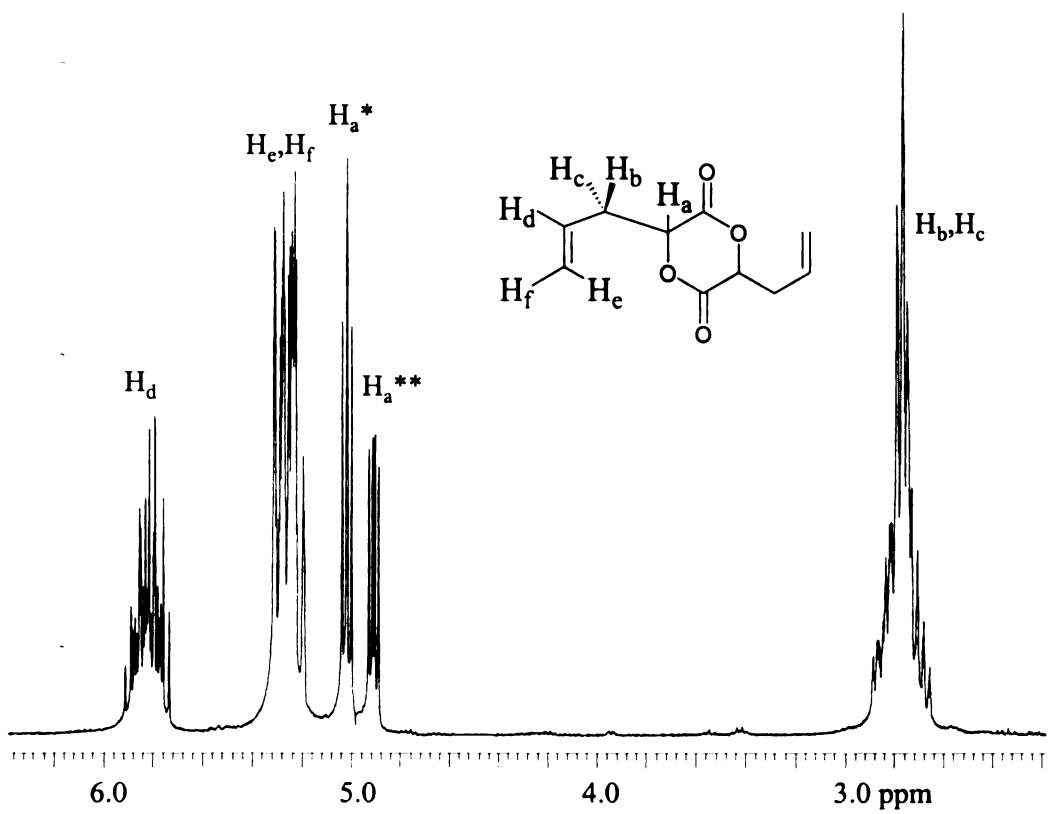


**Figure 16.** $^1$H NMR (300 MHz, $CDCl_3$) spectrum of 3,6-diallylglycolide enriched in the R,S isomer. $H_a$* denotes the R,S isomer. $H_a$** denotes the R,R and S,S isomers.

## 2.2 Polymer Synthesis

The statistical mixture of the monomers was polymerized in solution to give the homopolymer, poly(diallylglycolide), PDAG. The polymerization of 3,6-diallyglycolide in toluene at 80°C for 3 days using tin(II)-2-ethylhexanoate as the initiator gave PDAG as a tacky solid with a number average molecular weight ($M_n$) of 24,100 and a glass transition temperature ($T_g$) of -10°C. Given the allyl side chain of the homopolymer, the low $T_g$ of PDAG is consistent with results obtained by Yin and Baker for alkyl-substituted polyglycolides.[146] The melt polymerization of 3,6-diallylglycolide can also be performed, however, at high temperatures side reactions lead to poor control over the molecular weight and molecular weight distribution. The resultant polymers, whether prepared by solution or the melt polymerization are discolored and their physical texture is tacky making it very difficult to handle. The $^1$H NMR spectrum shows three sets of broad peaks with complicated multiplicities (Figure 17), and a quantitative $^{13}$C NMR spectrum shows multiple resonances for the carbonyl, indicative of a mixture of stereochemistry throughout the polymer. The physical consistency of PDAG and the difficulty with which it is handled, render the use of the low $T_g$ polymer impractical. Greater control over the glass transition, melting point, and other properties can be achieved by copolymerizing DAG with a monomer such as *rac*-lactide or L-lactide. Moreover, the benefit of a copolymer incorporating DAG as the minor component in a copolymer is to maintain similar properties to the homopolymer of the major component, with the added benefit of functional sites for modification.

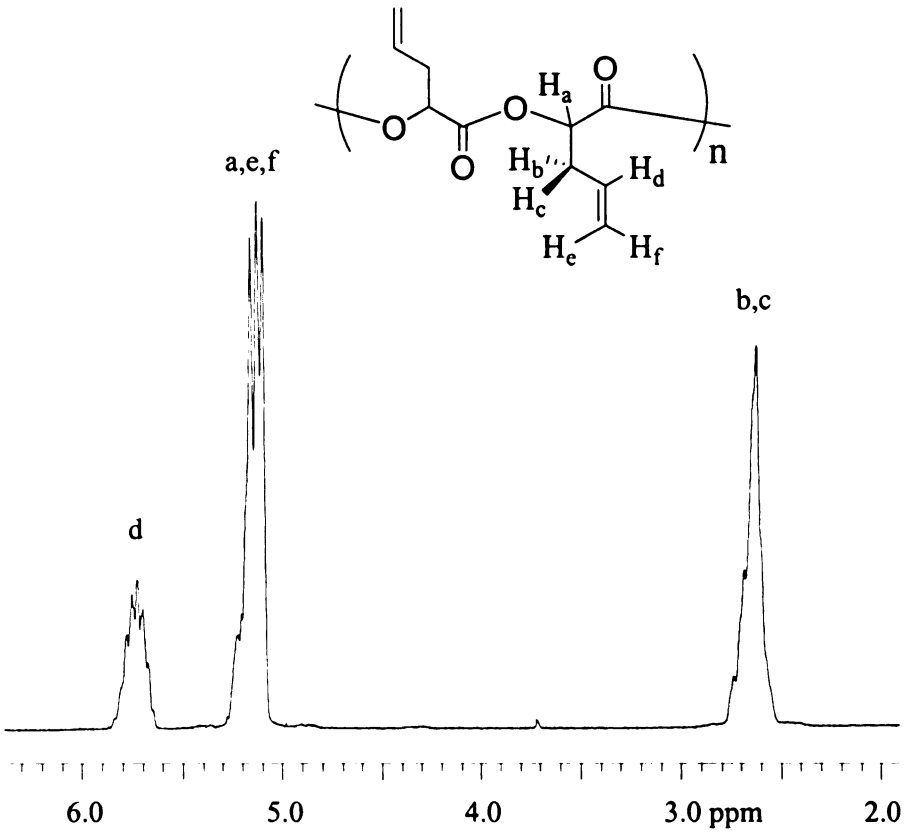


**Figure 17.** $^1$H NMR (300 MHz, $CDCl_3$) spectrum of poly(diallylglycolide) (PDAG).

## 2.3 Copolymer Synthesis and Characterization

Melt polymerizations of mixtures of L-lactide with 3,6-diallylglycolide in the desired ratio using tin(II)-2-ethylhexanoate and 4-*tert*-butylbenzyl alcohol (BBA) as coinitiators affords the copolymer poly(L-lactide-*co*-diallylglycolide), PLLA-*co*-AG. The reaction is carried out at 145°C for approximately 15-20 minutes. Since the ROP of lactide and glycolides is considered a living polymerization, the molecular weights of the polymers can be controlled by the monomer-initiator ratio (M/I).[148,149] Copolymers containing up to 15% of the allyl comonomer were synthesized using *rac*-lactide (Table 3) and 32% using L-lactide (Table 4) as the lactide sources. In both cases, the amounts of allyl in the monomer feed ratio compares well to the allyl content in the copolymer.

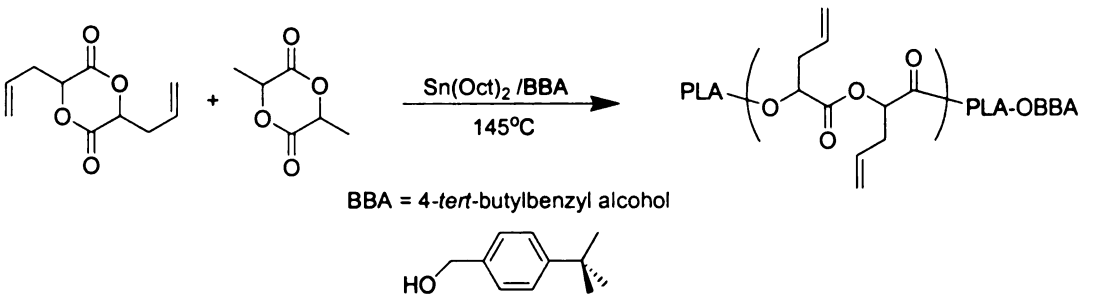


| *Monomer Feed Ratio (LA:DAG)* | *Copolymer Composition*[a] *(LA:DAG)* | $M_n$ /gmol$^{-1}$ (PDI)[b,c] | *Weight Fraction of Allylgycolide* | $T_g$ / °C |
|---|---|---|---|---|
| 100 : 0 | 100 : 0 | 32,000 (1.67) | 0.00 | 50.1 |
| 96 : 4 | 96 : 4 | 30,400 (1.27) | 0.06 | 42.3 |
| 92 : 8 | 91 : 9 | 21,600 (1.27) | 0.12 | 40.9 |
| 89 : 11 | 86 : 14 | 23,800 (1.35) | 0.18 | 35.1 |
| 85 : 15 | 81 : 19 | 16,200 (1.36) | 0.24 | 31.9 |
| 0 : 100[e] | 0 : 100 | 24,100 (1.22) | 1.00 | -10.0 |

**Table 3.** Copolymerization of *rac*-Lactide and 3,6-diallylglycolide ([M]/[I] = 300). [a] Molar composition of DAG determined by integration of the methylene resonance of the allyl repeat unit compared to the methine resonance of the lactide repeat unit. [b] Molecular weight determined by GPC. [c] PDI = Polydispersity index ($M_w/M_n$). [d] Molecular weight determined by intergration of 4-*tert*-butylbenzyl endgroup resonance compared to methine resonances of the lactide and allylglycolide sub-units. [e]Poly(diallylglycolide) prepared by solution polymerization in toluene at 80°C for 72 hours using $Sn(Oct)_2$ as the catalyst.

| *Monomer Feed Ratio (LLA:DAG)* | *Copolymer Composition[a] (LLA:DAG)* | *$M_n$ /gmol$^{-1}$ (PDI)[b,c]* | *$T_m$ / °C* | *$\Delta H$ / Jg$^{-1}$* |
|---|---|---|---|---|
| 100 : 0 | 100 : 0 | 17,000 (1.16) | 175 | 44.1 |
| 95 : 5 | 96 : 4 | 17,900 (1.24) | 158 | 28.2 |
| 90 : 10 | 92 : 8 | 18,800 (1.29) | 141 | 15.5 |
| 85 : 15 | 89 : 11 | 14,100 (1.32) | 131 | 4.4 |
| 50 : 50 | 68 : 32 | 12,800 (1.18) | - | - |
| 0 : 100 | 0 : 100 | 24,100 (1.22) | - | - |

**Table 4.** Copolymerization of L-Lactide and 3,6-diallylglycolide ([M]/[I] = 200). [a] Molar composition of DAG determined by integration of the methylene resonances of the allyl repeat unit compared to the methine of the lactide repeat unit. [b] Molecular weight determined by GPC. [c] Polydispersity index ($M_w/M_n$). [d] Poly(diallylglycolide) prepared by solution polymerization in toluene at 80°C for 72 hours using $Sn(Oct)_2$ as the catalyst.

The copolymers were characterized by $^1$H NMR spectroscopy and clearly show the presence of the allyl subunits in the copolymer (Figure 18). At 5.7-5.8 ppm, the resonance for the internal proton of the olefin is observed as a broad multiplet, while the resonances for the terminal olefin *and* the methine protons are buried underneath the large methine resonance of the PLA backbone. Also, the methylene resonances of the pendant allyl group are observed between 2.6-2.7 ppm. At low enough monomer to initiator ratios, the molecular weights of the polymers can be measured by integrating the *tert*-butyl resonance of the BBA endgroup as the reference. However, at higher monomer to initiators ratios, integration of the *tert*-butyl resonance was unreliable. Since molecular weights of our copolymers determined by the integration of the BBA resonance gave inconsistent results, the molecular weights of our polymers were determined using gel permeation chromatography (GPC).

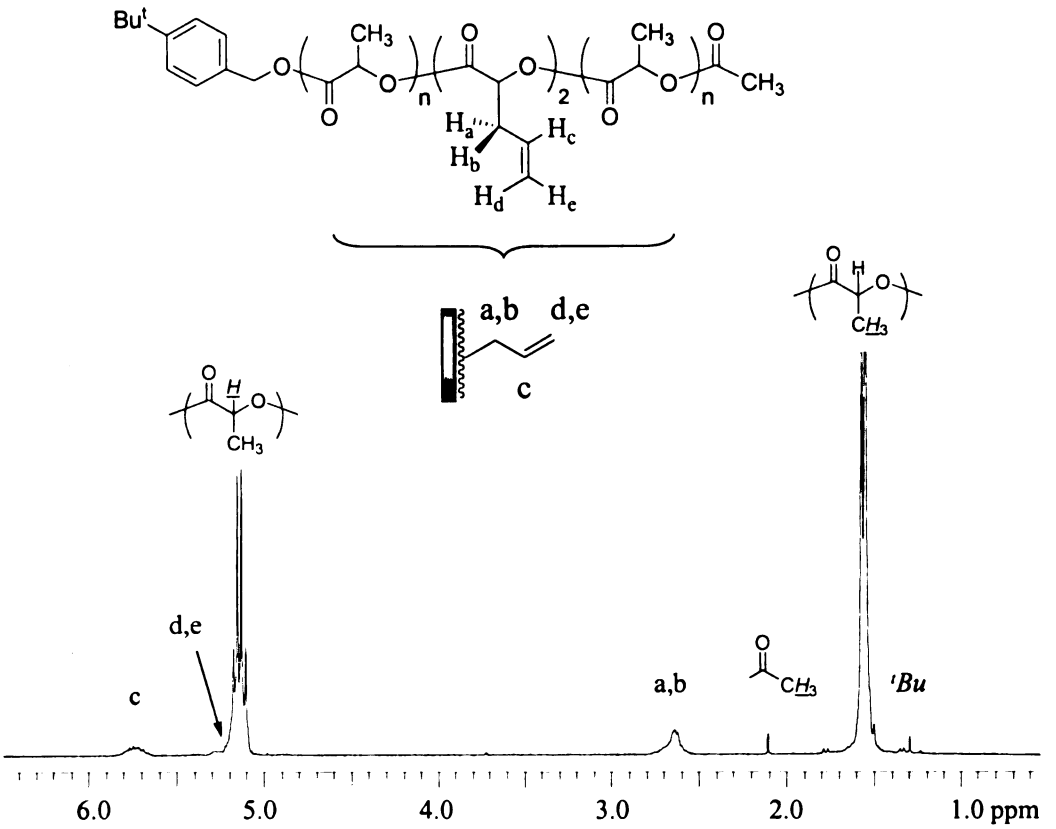


**Figure 18.** $^1$H NMR (300 MHz, $CDCl_3$) spectrum of poly(L-lactide-*co*-allylglycolide).

The copolymers based on *rac*-lactide were amorphous polymers with varying glass transition temperatures, while the copolymers based on L-lactide showed some crystallinity up to at least 11% comonomer incorporation. Both sets of copolymers based on *rac*-lactide and L-lactide were characterized by differential scanning calorimetry (DSC), and can be seen in Table 3 and Table 4, respectively. In the case of poly(*rac*-lactide-co-diallylglycolide), (PDLLA-*co*-AG), an increase in the allyl content in the copolymer results in a decrease in the observed $T_g$. This decrease behaves linearly according to the Fox equation[146,150,151] (Figure 19):

$$\frac{1}{T_g} = \frac{w_A}{T_{gA}} + \frac{w_B}{T_{gB}}$$

**Figure 19.** Fox equation describing the glass transition temperature of a random copolymer. $w$ = weight fraction, and $T_gA$ and $T_gB$ are the glass transiton temperatures for the pure homopolymers.

The glass transition of the pure PDLLA was measured at 50.1°C and the pure PDAG was measured at -10°C. Analysis of the copolymer $T_g$s with respect to the allyl weight fraction reveals a nice fit according to Fox's model (Figure 20).

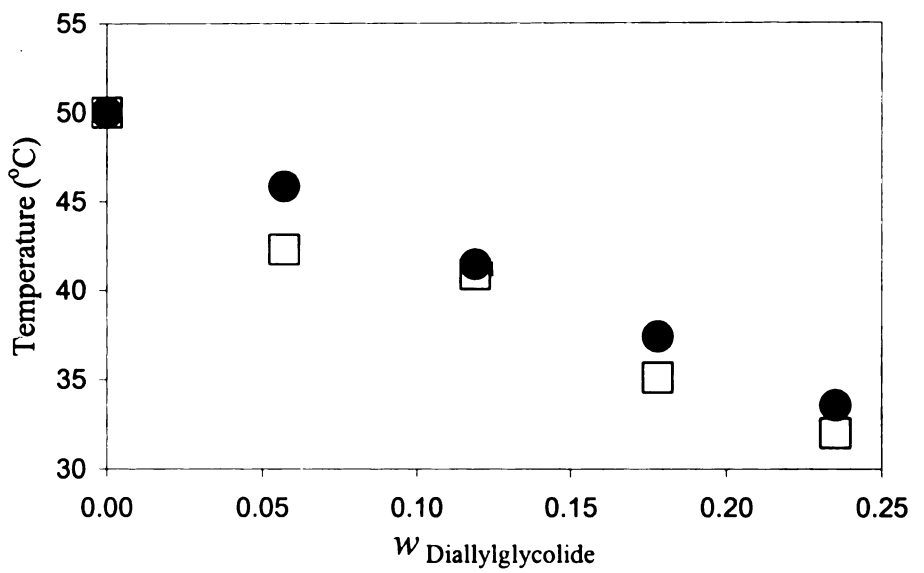


**Figure 20.** Glass transition temperature of poly(*rac*-lactide-*co*-diallylglycolide) with respect to the weight fraction, *w*, of diallylglycolide. (□) Experimental $T_g$s of PDLLA-*co*-AG copolymers. (●) Theoretical $T_g$s predicted by the Fox equation.

In the case of poly(L-lactide-*co*-allylglycolide) (PLLA-*co*-AG), DSC reveals that the melting temperature, $T_m$, and the crystallinity, $\Delta H$, decrease as the allyl content in the copolymer increases. When the mole fraction of DAG exceeds 0.11, the crystallinity disappears and the polymer becomes amorphous. In a similar fashion to the PDLLA-*co*-

AG copolymers, $T_m$ and $\Delta H$ for the PLLA-*co*-AG copolymers are related linearly (Figure 21). This result is not uncommon to copolymers where the addition of a comonomer decreases the crystallinity compared to the homopolymer.[152] Both sets of data are consistent with a random copolymerization as opposed to a block copolymer.

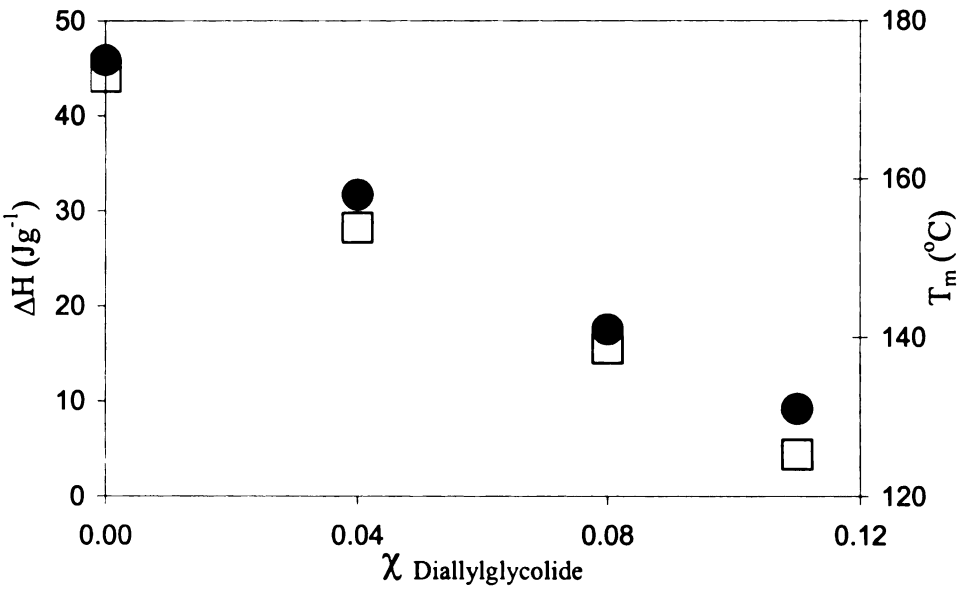


**Figure 21.** (□) Crystallinity ($\Delta H$) of poly(L-lactide-*co*-allylglycolide) with respect to the mole fraction, $\chi$, of diallylglycolide. (●) Melting point, $T_m$, of poly(L-lactide-*co*-allylglycolide) with respect to the mole fraction, $\chi$, of diallylglycolide.

Spectroscopic and thermal characterizations suggest the presence of a random copolymer. Pendant olefins located randomly along the backbone are now ready to undergo functional group transformation.

## 2.4 Post-Polymerization Modification

### 2.4.1 Olefin Cross Metathesis

#### 2.4.1.1 General

Carbon-carbon bond formation *via* ruthenium-catalyzed olefin metathesis has become standard procedure for the synthetic organic chemist in the design of simple and complex organic molecules, such as key intermediates in the synthesis of natural products[153,154] and for polymer synthesis.[155-158] The use of versatile, air-stable ruthenium carbene catalysts developed by the Grubbs[159-161] research group has made olefin metathesis a common synthetic technique. Since the discovery of Grubbs' first generation carbene catalyst, $Cl_2(PCy_3)_2Ru(=CHPh)$ (Figure 22a), a new, more active second generation catalyst, $Cl_2(PCy_3)(IMes)Ru(=CHPh)$, was developed by Grubbs, in which one of the tricyclohexylphosphine ligands is replaced by a less labile N-heterocyclic carbene ligand. (Figure 22b).

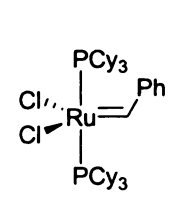


Cy = cyclohexyl

*(a)*

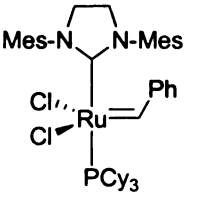


Mes = 2,4,6-trimethylbenzene

*(b)*

**Figure 22.** *(a)* Grubbs' first generation ruthenium carbene olefin metathesis catalyst. *(b)* Grubbs' second generation ruthenium carbene olefin metathesis catalyst.

Compared to ring-closing (RCM) metathesis, ring-opening metathesis polymerization (ROMP), and acyclic diene metathesis (ADMET), olefin cross metathesis (CM) has not been applied nearly as often. The reaction offers a unique method of carbon-carbon bond

formation, yet the lack of selectivity with which CM operates makes widespread applications impractical (Figure 23). Therefore, until general conditions for highly selective CM have been discovered, it will remain a reluctantly approached technique.

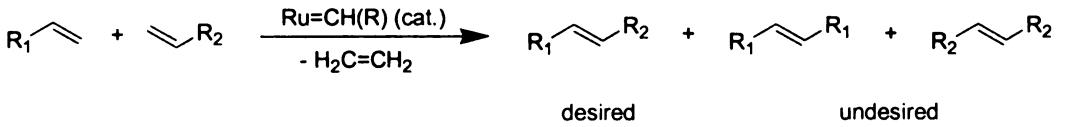


**Figure 23.** General scheme for ruthenium-catalyzed olefin cross metathesis.

Achieving selectivity for olefin cross metathesis must be found in choosing in the appropriate substrate. Selectivities may be improved by adjusting the cross metathesis conditions to decrease a substrate's reactivity *via* its inherent electronic or steric properties.[162,163] Interesting applications of cross metathesis used in biologically relevant systems include the CM of allyl-modified amino acids[164] and natural products.[165,166] In spite of the limitations, there are examples of CM that provide useful avenues to highly desirable compounds. An exquisite example of cross metathesis is found in the "dimerization" of the immunosuppresant FK506, which is used as a chemical inducer of dimerization.[167] Like its small molecule analogues, CM on polymer substrates is not utilized nearly as much as RCM or ROMP. However, the benefits of performing CM on polymer substrates are useful when it comes to purification of the products, since the products can be much more easily separated from the small molecule by-products.

Blechert and coworkers have demonstrated the use of allyldimethylsilylphenyl-functionalized polystyrene as a template for the synthesis of organic substrates by ruthenium-catalyzed cross metathesis (Figure 24).[168] After the cross metathesis product is synthesized, the silyl group is subjected to electrophilic cleavage of the olefinic substrate, resulting in the formation of a new C-C bond. Breed has also demonstrated CM on

polymers by reacting a hydrophilic triethyleneglycol allyl ether side chain bound to a polystyrene resin with simple olefins.[169]

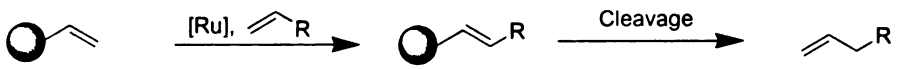


**Figure 24.** Schematic of polymer-bound ruthenium-catalyzed cross metathesis (CM), followed by cleavage from the polymer support.

### 2.4.1.2 Synthesis and Characterization

In preparing the allyl-functionalized copolymer, PLLA-*co*-AG, we designed a biodegradable copolymer able to participate in olefin cross metathesis. In order to test its metathesis reactivity and demonstrate a proof of concept, we chose a group of olefin substrates to perform cross metathesis with PLLA-*co*-AG: 9-decenyl-1-oxy-(4-nitrobenzene), allylbenzene, 2-(2-propenyloxy)benzaldehyde, 9-decene-1-oxy-(*tert*-butyldimethylsilane), and 9-decen-1-al (Figure 25).

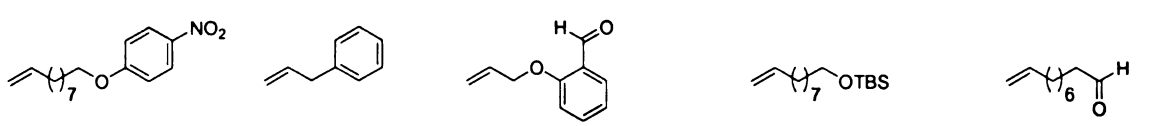


9-Decen-1-oxy-(4-nitrobenzene) | Allylbenzene | 2-(2-propenyloxy) benzaldehyde | 9-Decen-1-oxy-(*tert*-butyldimethylsilane) | 9-Decene-1-al

**Figure 25.** Substrates used for polymer-bound olefin cross metathesis to PLLA-*co*-AG.

Quantification of the metathesis conversion of the PLLA-*co*-AG copolymer was carried by $^1$H NMR and UV-Vis spectroscopy. For all substrates, $^1$H NMR analysis was performed by comparing the integration of the resonances between newly formed functionalized copolymer and the unreacted copolymer. In order to demonstrate the validity of quantitative analysis using UV-Visible spectroscopy, we chose an olefin substrate possessing considerable reactivity and a UV-Vis-active chromophore. The

olefin cross metathesis between PLLA-*co*-AG and 9-decenyl-1-oxy-(4-nitrobenzene) was carried out at room temperature in dichloromethane for 24 hours using Grubbs' 1st generation ruthenium carbene catalyst (Figure 26).

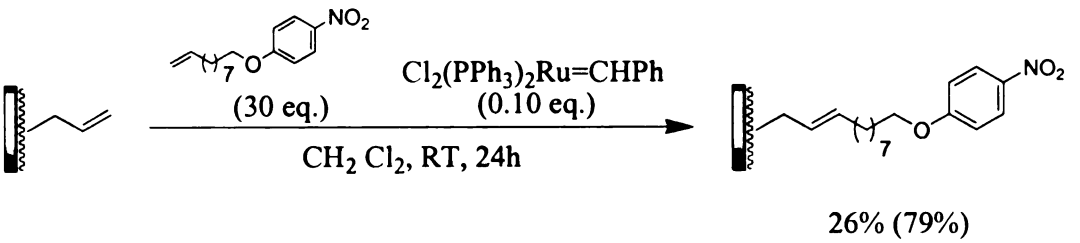


**Figure 26.** Polymer-bound olefin cross metathesis between PLLA-*co*-AG and 9-decenyl-1-oxy-(4-nitrobenzene). Conversion of allylglycolide sub-units (isolated yield).

Purification of poly(L-lactide-*g*-9-decenyl-1-oxy-(4-nitrobenzene) (PLLA-*g*-Decenyloxy-NB) required dissolving the polymer in dichloromethane and passing it through a plug of silica gel. The unreacted olefin and cross metathesis by-products passed through the column while the polymer remained bound to the silica gel. The polymer was then extracted from the silica gel using dichloromethane and ethyl acetate and was precipitated from hexanes. Once the polymer was filtered it was dissolved in dichloromethane a second time and reprecipitated from methanol. A second precipitation the addition of hexanesequential precipitation from hexanes followed by methanol. The isolated yield of the polymer was 79% and the $M_n$ increased from 10,500 to 13,300 gmol$^{-1}$ ($M_w/M_n$ = 1.40). The molecular weights provide no evidence for degradation, but the polymer was discolored, indicating that trace amounts of ruthenium still may be present.

After work up of the polymer, $^1$H NMR clearly shows the incorporation of the decenyloxy nitrobenzene olefin substrate onto the copolymer (Figure 27). Integration of the olefinic regions around 5.2-6.0 ppm and the substrate methylene resonance at 4.0 ppm, with respect to the functionalized and unfunctionalized copolymer methylene

resonances between 2.5-2.7 ppm, revealed the conversion of the pendant allyl groups of the PLLA-*co*-AG copolymer.

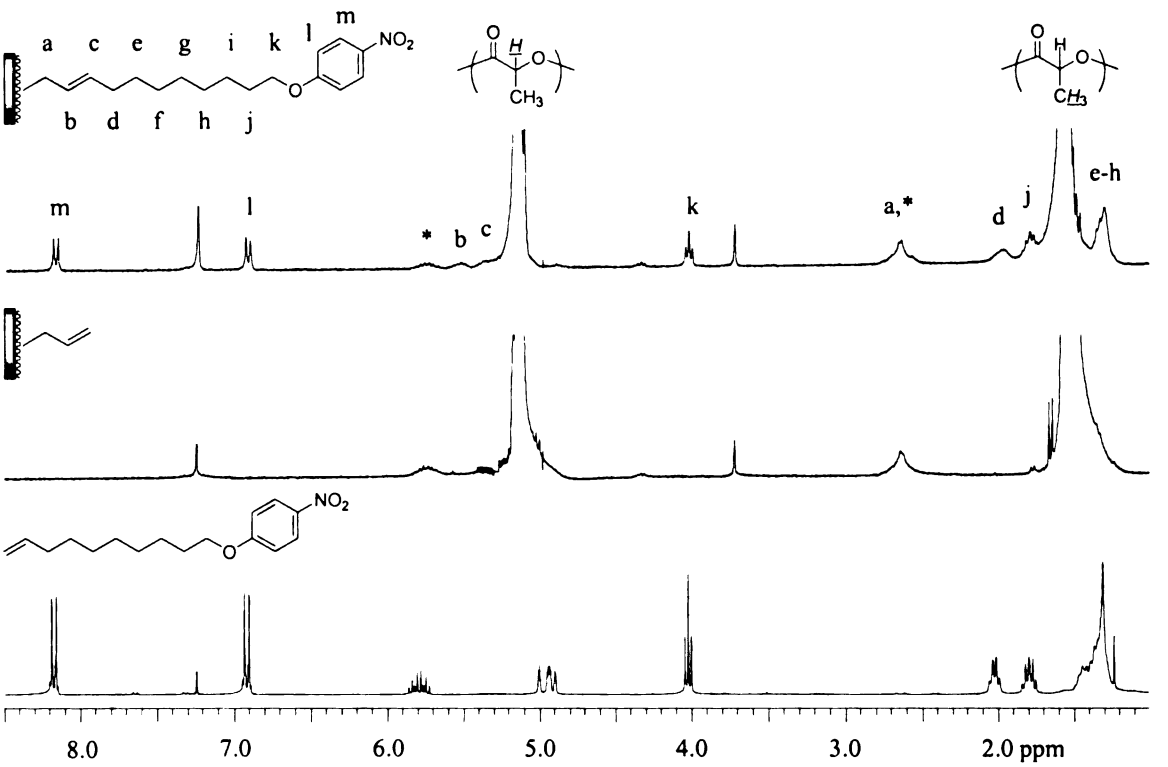


**Figure 27.** $^1$H NMR (300 MHz, $CDCl_3$) spectrum of polymer-bound cross metathesis between PLLA-*co*-AG and 9-decenyl-1-oxy-(4-nitrobenzene). (*) Unreacted PLLA-*co*-AG.

Using GPC, we were also able to measure the olefin metathesis conversion quantitatively using ultraviolet-visible spectroscopy. Since GPC is a chromatographic separation technique, we measured the absorbance of the polymer using the UV-Visible detector and correlated it to the concentration of the sample using 9-decenyl-1-oxy-(4-nitrobenzene) as the calibration standard. From these data we can determine the percent conversion of the olefins that underwent metathesis. The prerequisite for reliable UV-Vis quantification is that the side chain chromophore has a strong absorption at a wavelength where the polymer backbone is transparent. In our case, $\lambda_{max}$ is 232 nm for PLLA-*co*-

AG, while the $\lambda_{max}$ is 307 nm for the 9-decenyl-1-oxy-(4-nitrobenzene) (Figure 28). Thus, we were able to quantify the amount of conversion using UV-Visible spectroscopy. NMR and UV-Vis analytical methods give consistent results for the conversion of 26.3 and 29.4%, repectively.

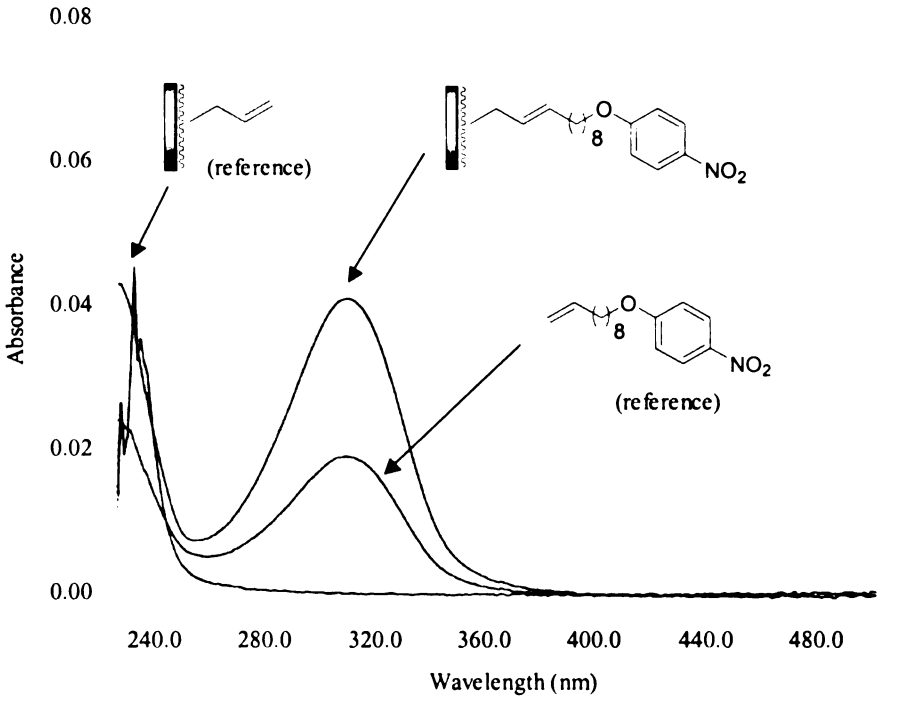


**Figure 28.** UV-Vis spectrum of polymer-bound olefin cross metathesis between PLLA-*co*-AG and 9-decenyl-1-oxy-(4-nitrobenzene).

The order of the addition of reactants turns out to be quite important. Routinely, the polymer is dissolved in dichloromethane with approximately five equivalents of the olefin substrate. Grubbs' second generation ruthenium catalyst is then added to the stirred solution and a syringe pump slowly delivers additional substrate at a rate of 0.1 mL/min. If the ruthenium catalyst is added in the absence of the five equivalents of olefin substrate, the solution becomes viscous and ultimately forms a gel after ten minutes, presumably as a result of cross-linking the pendant allyl groups. Interestingly,

this rapid gellation was not observed with Grubbs' first generation catalyst. Degradation of the polymer to its alkyl esters was carried out by refluxing the polymer in ethanol and excess of $Sn(Oct)_2$ for 48 hours (Figure 29). Both alkyl ester products were observed by gas chromatography in the case of the linear copolymer. In the case of the cross-linked gel, the dihydroxy-diethyl ester degradation product that arises from allyl metathesis was observed and the absence of the allylhydroxy ethyl ester indicated the full consumption of the terminal olefin sub-units.

***Linear Copolymer:***

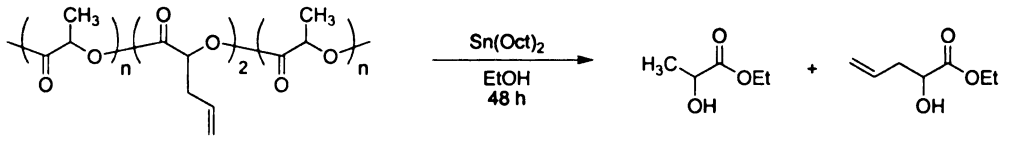


***Cross-linked Copolymer:***

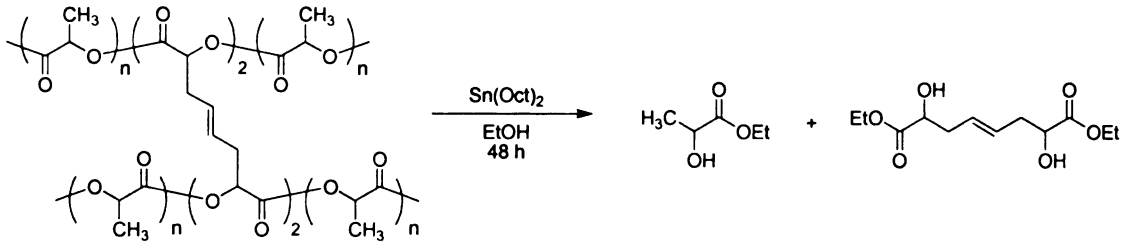


**Figure 29.** Degradation of linear copolymer PLLA-*co*-AG and cross-linked copolymer PLLA-*co*-AG copolymer.

The mechanism of cross-linking is similar to the mechanism of ADMET, where diene monomers undergo metathesis to combine as in a step growth mechanism.[158] Without the presence of a monomeric olefin to participate in cross metathesis reactions, intermolecular metathesis of the side chains on the polymer is a likely occurrence. Poché observed a similar cross-linking phenomenon when he reacted polypeptides containing olefin side chains with Grubbs' first generation ruthenium catalyst.[170] Therefore, for

cross metathesis reactions, five equivalents of olefin substrate were added prior to the catalyst in order to favor cross metathesis instead of cross-linking.

Because of the proximity of the terminal olefins in the diallylglycolide sub-unit, we did not rule out the possibility of ring-closing metathesis along the polymer chain (Figure 30). In our model of ring-closing metathesis between adjacent allyl sub-units, the eight-membered ring-closed product was not observed by GC/MS. While five-, six-, and seven-member rings are thermodynamically stable, an eight-member ring is less stable, and consequently, not as easily formed by ring-closing metathesis.[171] Macrocycle formation (> 8-membered rings) is also possible, but alone, would not account for the gel formation. Therefore, it is likely that intermolecular metathesis between polymer chains is primarily responsible for the gel formation.

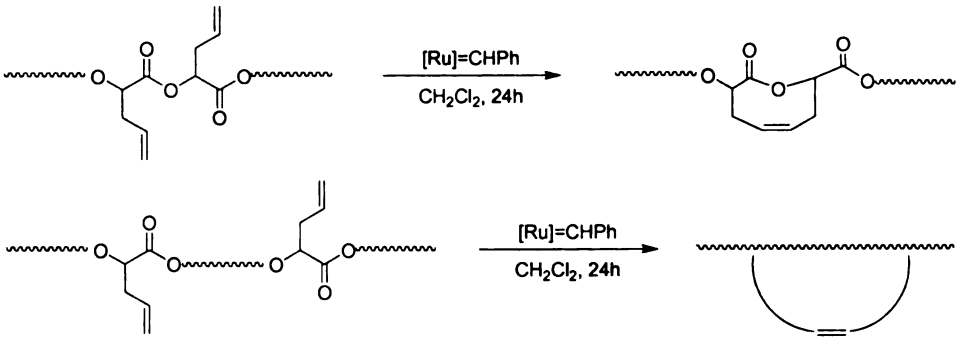


*(a)*

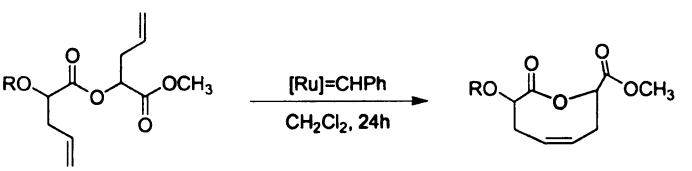


R = H, tetrahydropyran Not Observed

*(b)*

**Figure 30.** (*a*) Possible polymer ring-closing metathesis reactions. (*b*) Ring-closing metathesis of the methyl ester of the ring-opened diallylglycolide performed under polymer-bound cross metathesis conditions.

The catalyst loading is an important variable in metal-catalyzed olefin metathesis. High catalyst loadings require more extensive purification steps to remove the metal. This is even more important when the metathesis reaction involves a biodegradable material. The effect of catalyst loading on the conversion of the polymer-bound olefins to products was investigated (Figure 31). Conversion increases with catalyst loading, but conversions exceeding 50% require impractically high catalyst loadings.

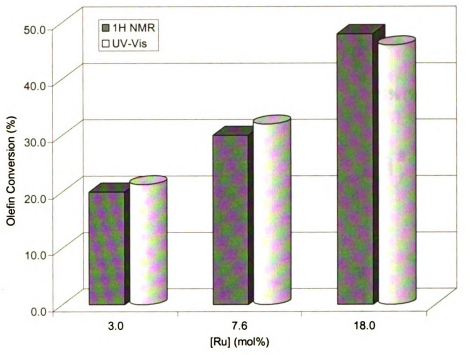


**Figure 31.** Percentage of olefin conversion of 9-decenyl-1-oxy-(4-nitrobenzene) with respect to Grubbs 1st generation catalyst loading.

Although Grubbs' catalysts are known to be functional group tolerant, we wanted to evaluate polymer reactivity with a substrate possessing no functionality. Allylbenzene is a simple aromatic molecule, where the ring is essentially nonfunctional. Furthermore, allylbenzene metathesis products can be characterized spectroscopically. The metathesis was carried out by the slow addition of the olefin in dichloromethane solution of the polymer using 10% ruthenium catalyst relative to the amount of allyl sub-units in the copolymer. After 24 hours, the polymer underwent successful cross metathesis as determined by $^{1}$H NMR (Figure 32).

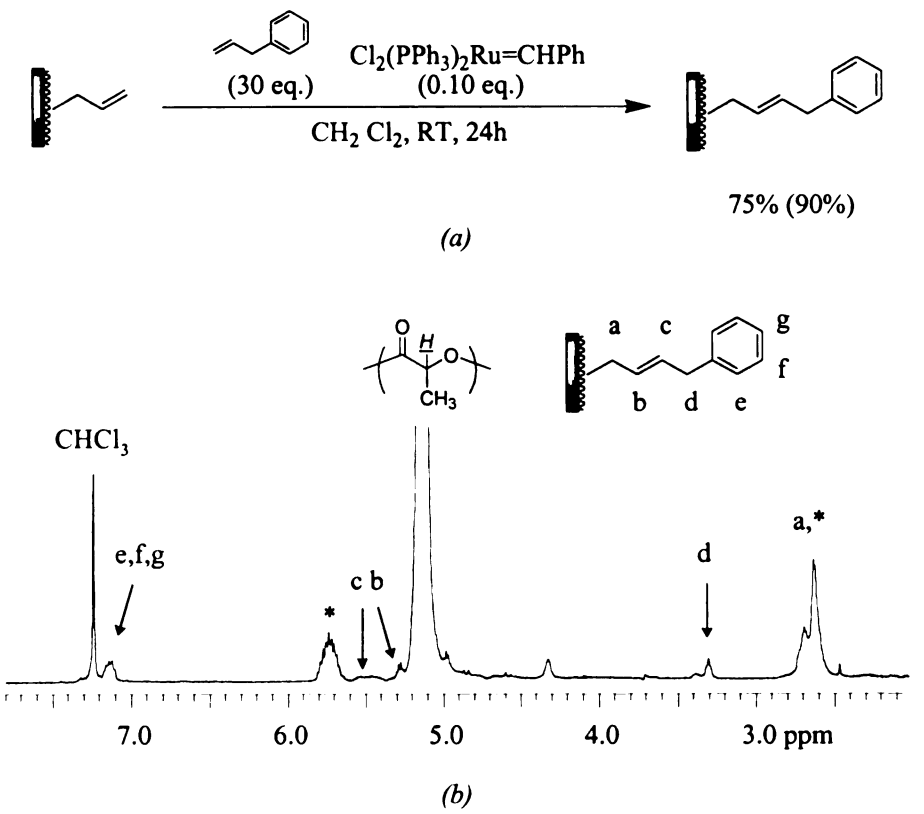


**Figure 32.** *(a)* Polymer-bound cross metathesis between PLLA-*co*-AG and allylbenzene. Conversion of allylglycolide sub units (isolated yield). *(b)* $^1$H NMR (500 MHz, $CDCl_3$) spectrum of polymer-bound cross metathesis between PLLA-*co*-AG and allylbenzene. (*) Unreacted PLLA-*co*-AG.

Polymer purification was carried out by a simple washing of the polymer with hexanes, followed by precipitation from methanol. This procedure washes away the self-metathesis by-product of allylbenzene, 1,4-diphenyl-2-butene. After multiple precipitations, residual ruthenium was likely responsible for the discoloration of the material. After determining the reactivity of the allylbenzene, we looked for a substrate which could be covalently attached and further modified by exploiting some form of secondary reactivity. We chose the allyl ether of salicylaldehyde, 2-(2-propenyloxy)benzaldehyde. Once the aldehyde was linked to the polymer, we could

envision the use of Schiff-base chemistry to link a broad range of molecules to the polymer.

While the metathesis of allylbenzene proceeded well with good percent conversion and in excellent yield, the 2-(2-propenyloxy)benzaldehyde conversions and yields were significantly lower. Spectroscopically, we are able to observe the 2-(2-propenyloxy) benzaldehydic $^1$H NMR resonances, however, there is a substantial amount of unreacted polymer and substrate (Figure 33).

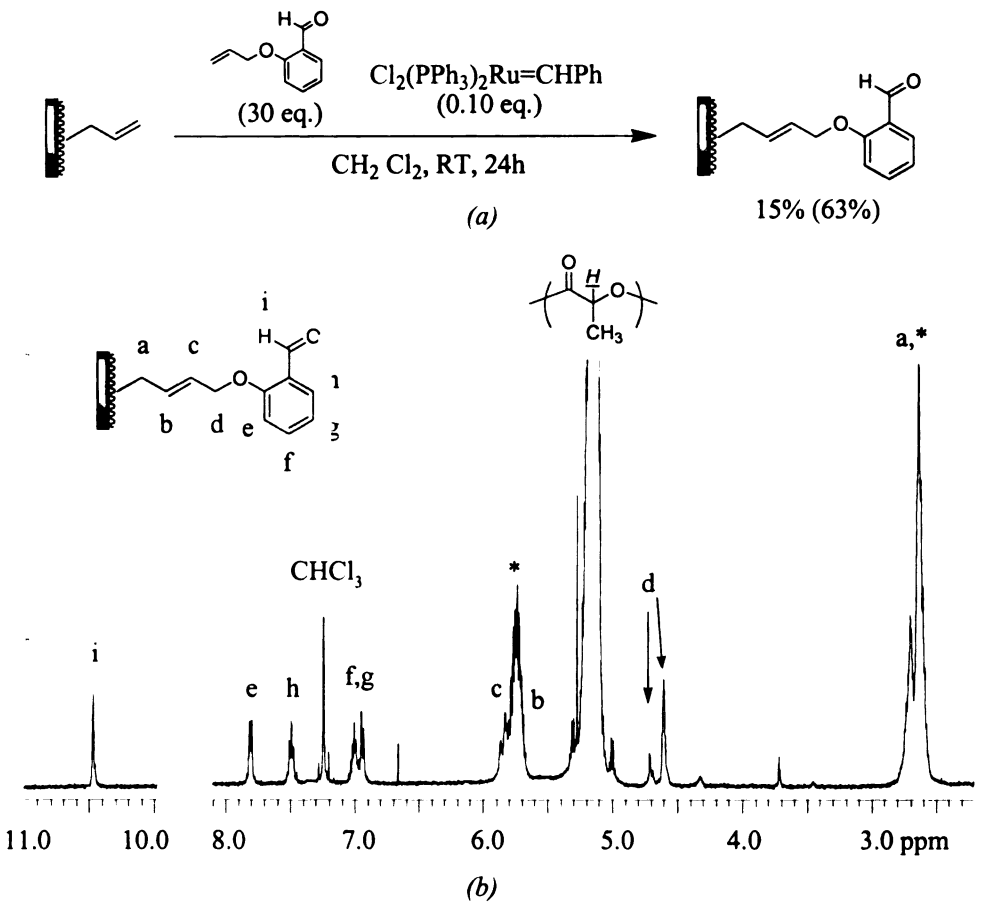


**Figure 33.** *(a)* Polymer-bound cross metathesis between PLLA-*co*-AG and 2-(2-propenyloxy)benzaldehyde. Conversion of allylglycolide sub-units (isolated yield). *(b)* $^1$H NMR (500 MHz, $CDCl_3$) spectrum of polymer-bound cross metathesis between PLLA-*co*-AG and 2-(2-propenyloxy)benzaldehyde. (*) Unreacted PLLA-*co*-AG.

In order to assess the reactivity of the 2-(2-propenyloxy)benzaldehyde, the self-metathesis reaction was carried out under similar conditions to the polymer-bound cross metathesis reactions. The result showed only 15% consumption of the olefin after 14 hours. Thus, the slow self-metathesis rate for 2-(2-propenyloxy)benzaldehyde explains the low yield by cross metathesis products on the polymer. We speculate that the lower reactivity may be chelation of the carbonyl oxygen of the aldehyde to the active ruthenium catalyst during metathesis. This is consistent with literature assertions that stable ruthenium-carbonyl chelates during metathesis can adversely affect activity.[172]

In order to make a substrate more accessible to the polymer, and thus more reactive, we have incorporated a ten-carbon alkyl chain as a spacer between the olefin and the desired functionality of the substrate. Substrates possessing the 9-decenyl spacer such as the 9-decenyloxy-*tert*-butyldimethylsilane and 9-decenal have improved conversions compared to the benzaldehyde case and similar conversions compared allylbenzene. However, a more detailed purification procedure must be used. The 9-decenyloxy-*t*-butyldimethylsilane modified copolymer (PLLA-*g*-decenyloxy-TBS) and 9-decenal modified copolymer (PLLA-*g*-decenal) required precipitation from dichloromethane into hexanes followed by a second precipitation from dichloromethane into methanol in order to remove the by-products. The dimerized alkyl chain in both cases is insoluble in methanol, and co-precipitated when only methanol was used. Once the purification was complete, the $^{1}$H NMR spectrum of PLLA-*g*-decenyloxy-TBS showed the presence of the TBS groups as well as the other characteristic resonances for the alkyl chain spacer (Figure 34). The percent conversion of the allyl groups was determined by the integration of the TBS groups with respect to the methylene

resonances of the copolymer at 2.5-2.7 ppm, which represent both metathesized and unmetathesized allyl groups along the copolymer.

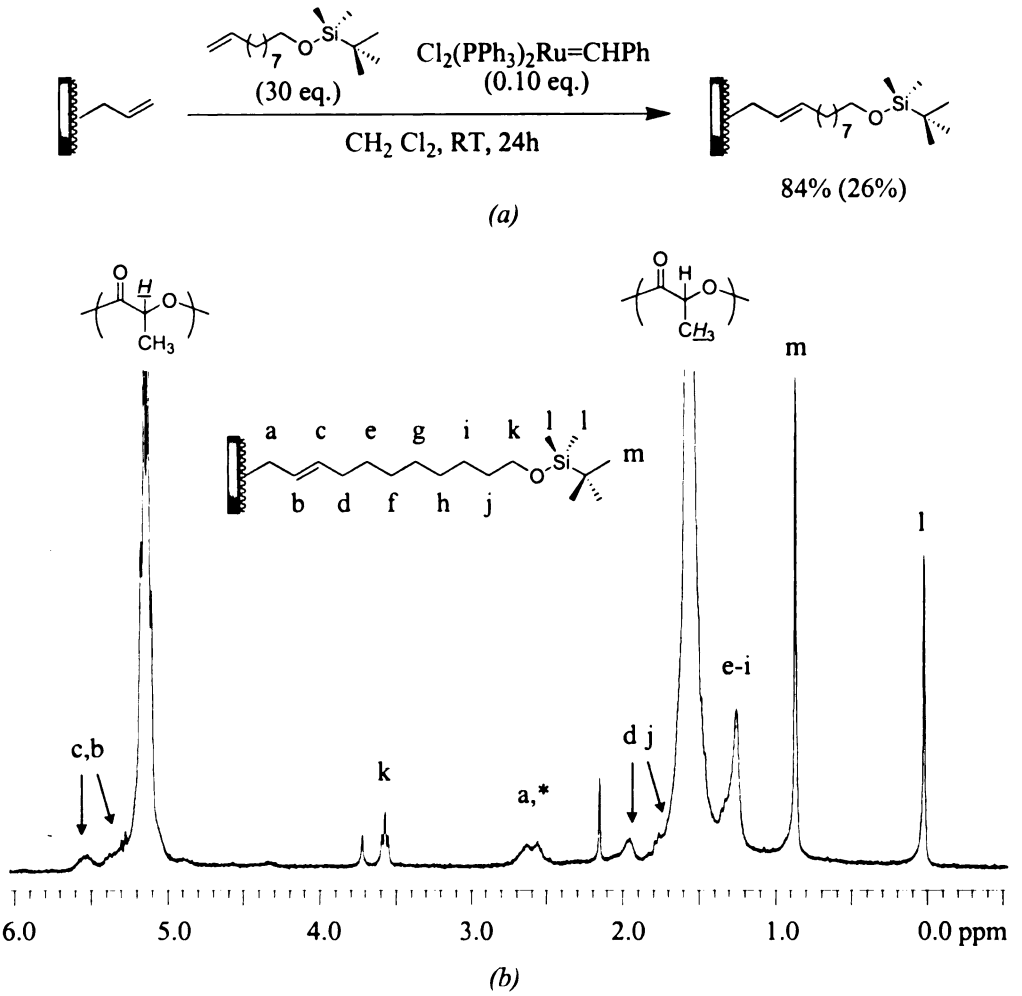


**Figure 34.** *(a)* Polymer-bound cross metathesis between PLLA-*co*-AG and 9-decenyl-1-oxy-*tert*-butyldimethylsilyl ether. Conversion of allylglycolide sub units (isolated yield). *(b)* $^1$H NMR (300 MHz, $CDCl_3$) spectrum of polymer-bound cross metathesis between PLLA-co-AG and 9-decenyl-1-oxy-*t*-butyldimethylsilyl ether. (*) Unreacted PLLA-*co*-AG.

Similar to PLLA-g-decenyloxy-TBS, the $^1$H NMR spectrum of PLLA-*g*-decenal showed the resonances of the alkyl chain spacer as well as the characteristic aldehyde proton resonance at 9.74 ppm (Figure 35). Conversion of allyl groups was determined by

comparison of the methylene adjacent to the carbonyl at 2.39 ppm with respect to the metathesized and unmetathesized methylene resonances of the copolymer at 2.5-2.9 ppm.

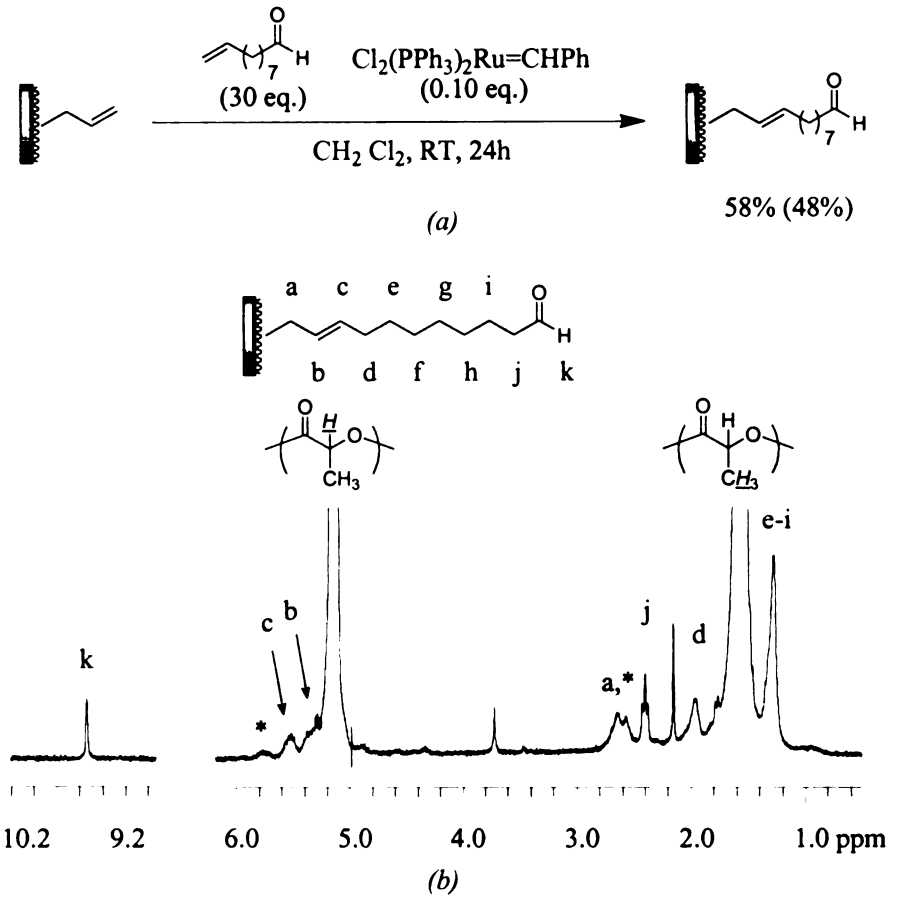


**Figure 35.** *(a)* Polymer-bound cross metathesis between PLLA-*co*-AG and 9-decenal. Conversion of allylglycolide sub units (isolated yield). *(b)* $^1$H NMR spectrum of polymer-bound cross metathesis between PLLA-co-AG and 9-decenal. (*) Unreacted PLLA-*co*-AG.

Ruthenium-catalyzed olefin cross metathesis of the biodegradable copolymer PLLA-*co*-AG with specific olefinic substrates has been successfully demonstrated. $^1$H NMR and UV-Vis spectroscopic techniques have been shown to quantitatively determine the conversion of the pendent olefins on the polymer. From a synthetic standpoint, we have observed that the workup protocol varied from substrate to substrate. Furthermore, we also see substrate dependence in the reactivity of different olefins. This is consistent

with what is known in the literature regarding the electronic and steric effects of olefin metathesis.[162,163] However, as a method for modifying biodegradable materials, even low conversions using a bioactive substrate could be extremely valuable in tissue engineering applications. Moreover, orthogonal functionalization strategies would further enhance the utility of olefin cross metathesis for modifying DAG copolymers.

### 2.4.2 Hydroboration-Oxidation

#### 2.4.2.1 General

In hopes of expanding our current method of post-polymerization modification, we wanted to pursue an alternative means of functionalization which will allow us to screen a broader range of biologically relevant substrates. While olefin metathesis can be useful if the appropriate reactive substrate is used, not every substrate is metathesis active. In certain cases, an appropriate bioactive ligand might first require chemical modification before the polymer-bound olefin cross metathesis is applied (e.g. synthesizing the alkenyl ether or ester of the ligand). Therefore, modification of the terminal olefin through functional group transformation would allow us to explore other types of coupling chemistry. Alcohols are a particularly useful functional group for tethering substrates through reactions such as esterification or etherification, as well as carbonate and carbamate linkages. The best known transformation for converting olefins to alcohols is hydroboration followed by oxidation.

The first example of hydroboration was reported by H.C. Brown who discovered the groundbreaking reaction for converting terminal olefins to alcohols.[173-176] In his pioneering work, he used diborane ($B_2H_6$) to synthesize organoboranes from terminal olefins followed by treatment of the organoborane with sodium hydroxide and aqueous

hydrogen peroxide to afford the primary alcohol. Hydroboration-oxidation has been one of the most utilized methods to synthesize primary alcohols from olefins.

Similar to small molecule cases, polymer-bound hydroborations have also been performed, mostly on polyolefins to generate block and graft copolymers.[177-180] However, the hydroboration reaction in the context of biodegradable polymers such as poly(α-hydroxy acids) has not been exploited. The primary benefit of performing hydroboration-oxidation on biodegradable polymers would be to incorporate hydroxyl graft sites for polymer modification. The chemistry of primary alcohols is plentiful, and incorporating a hydroxyl site along the polymer backbone would position us to modify our copolymer in a number of different ways using traditional synthetic organic chemistry. However, preparing a hydroxyl monomer is impractical, as it will react adversely under our polymerization conditions, namely with the $Sn(Oct)_2$ catalyst. Since a hydroxyl group such as an alcohol is required to initiate polymerization with $Sn(Oct)_2$ as the catalyst, polymerizing a monomer containing a hydroxyl would prevent the formation of high molecular weight polymer. Yang and coworkers have circumvented this by synthesizing a glycolide monomer bearing a benzyl-protected vinyl alcohol.[181] After polymerization and deprotection, both homopolymer and copolymer with lactide yielded the polyglycolide containing pendant hydroxyl groups.[182] Gross has also incorporated hydroxyl graft points by copolymerizing a carbohydrate-modified cyclic carbonate monomer with lactide.[145] Subsequent deprotection of the benzyl groups yields PLLA-*co*-pentofuranose. Jerome and coworkers synthesized a silyl-protected γ-hydroxy-ε-caprolactone which they copolymerized with ε-caprolactone in order to use the free hydroxyl groups as macroinitiators for lactide grafts.[183] Each of these approaches

achieves the goal of incorporating hydroxyl functionalization, however at the expense of synthesizing a specialized monomer.

Utilizing a post-polymerization modification of our allyl-functionalized copolymer PLLA-*co*-DAG, we report an efficient way to incorporate hydroxyl functionality along our copolymer by avoiding the synthesis a complex monomer, and the subsequent protection and deprotection schemes before and after polymerization. Simple hydroboration of PLLA-*co*-DAG and further oxidation to the terminal alcohol has enabled us to incorporate hydroxyl groups as grafting sites for additional modification.

### 2.4.2.2 Synthesis and Characterization

The hydroxylated copolymer of PLLA-*co*-DAG was synthesized by the hydroboration of the copolymer followed by oxidation using aqueous sodium acetate and hydrogen peroxide (Figure 36).

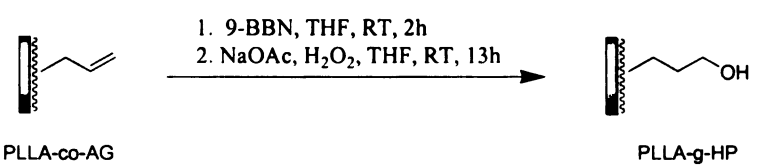


**Figure 36.** Synthetic route to poly(lactide-*g*-hydroxypropane) *via* hydroboration-oxidation of poly(lactide-*co*-diallylglycolide).

In the first step of the hydroboration, the polymer was stirred at room temperature for 1.5 to 2 hours using 9-borabicyclononane (9-BBN) as the borane source. The progress of this reaction was monitored by the appearance of the trialkylboron resonance centered at 88 ppm in the $^{11}B$ NMR spectrum. Once the hydroboration was determined to be complete, the polymer was treated with a two-fold excess of aqueous base and hydrogen peroxide. In our first attempt to prepare the hydroxylated copolymer, we used

sodium hydroxide. After 12 hours of oxidation, the polymer had degraded and could not be precipitated. This prompted us to select a milder base such as sodium acetate, since the polyester PLLA-*co*-AG is sensitive to harshly basic conditions. The reaction was then stirred at room temperature for 13 hours or until the oxidation was complete. Precipitation of the polymer from methanol two times gave the hydroxylated copolymer poly(lactide-*graft*-hydroxypropane) (PLLA-*g*-HP). Under oxidation conditions using sodium acetate and hydrogen peroxide, GPC analysis confirmed that our copolymer did not degrade, where the molecular weight of the copolymer increased from $M_n$ = 12,800 $gmol^{-1}$ for PLLA-*co*-AG to $M_n$ = 13,800 $gmol^{-1}$ for PLLA-*g*-HP, an increase expected as a result of copolymer fractionation through multiple precipitations. The $^1H$ NMR spectrum of the copolymer shows the disappearance of the allyl resonances and the appearance of the primary alcohol at 3.6 ppm. Also, the alkyl methylene resonances of the hydroxypropane graft are seen between 1.5-2.0 ppm (Figure 37).

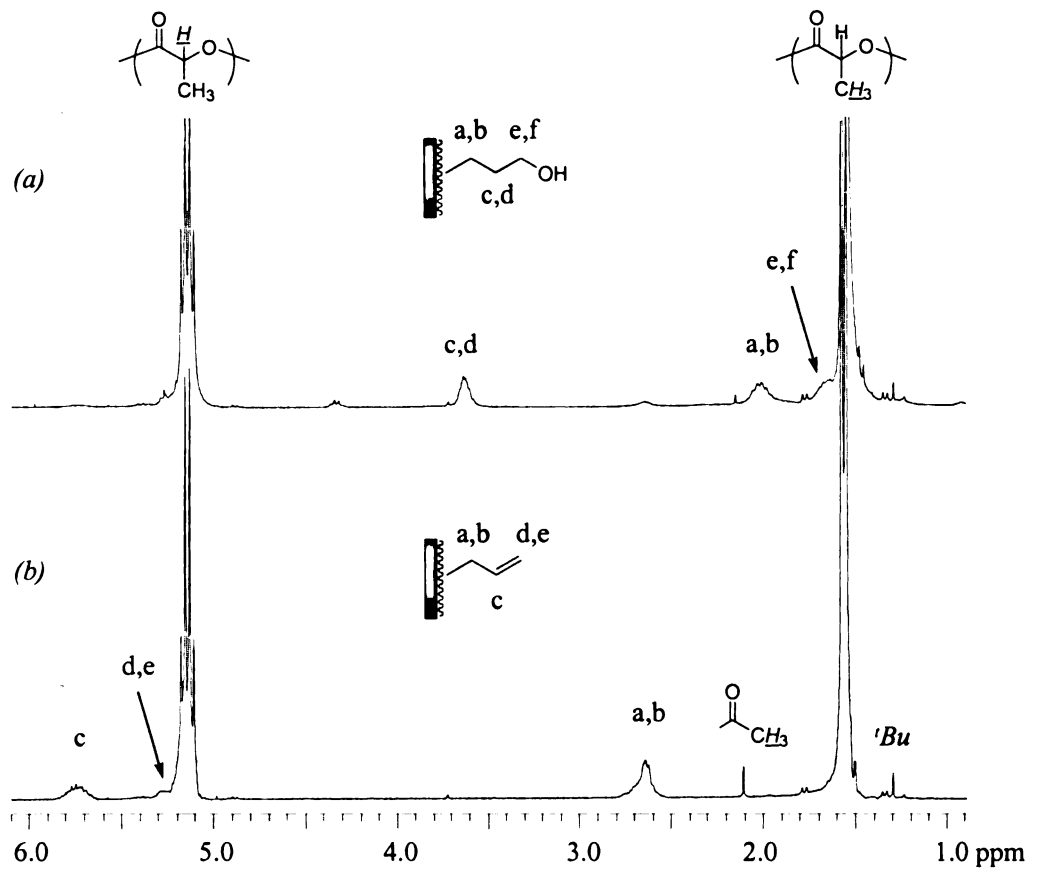


**Figure 37.** $^1$H NMR (300 MHz,$CDCl_3$) spectra of *(a)* PLLA-*g*-HP; poly(lactide-*g*-hydroxypropane) and *(b)* PLLA-*co*-AG; poly(l-lactide-*co*-diallylglycolide).

The advantages of a hydroxylated polymer are two-fold. First, the hydroxylated copolymer can be used directly as a functional biomaterial, to improve biocompatibility through hydrogen bonding, interactions with other bioactive groups, or through substrate binding.[184-186] Second, and perhaps more significant is the ability to support further chemistry, such as macroinitiation or other coupling reactions. Primary alcohols have a wealth of chemistry and this copolymer provides an ideal starting point to directly exploit simple chemistry to create a variety of new materials.

Since initiation of lactide using $Sn(Oct)_2$ requires an alcohol coinitiator, it is possible to consider new polymer architectures using the pendant hydroxyl groups as

macroinitiators in the design of graft and dendrimeric-type copolymers.[187-189] A unique example of this chemistry was carried out by Zheng and coworkers in designing hydrophobic-hydrophilic microspheres of polydivinylbenzene and poly(hydroxyethyl methacrylate) (poly(HEMA)). Hydroboration-oxidation of the pendant olefins and subsequent esterification generated ATRP initiators for the grafting of the hydrophilic acrylate.[190]

Using the hydroxyl sites merely as attachment points for further chemistry has also been accomplished. Gross and coworkers have designed cyclic carbohydrate-modified carbonate monomers, which have been copolymerized with lactide. After the copolymerization of the carbonate monomer with lactide, the deprotection of the pendant sugars are carried out to reveal hydroxyl groups now accessible for further functionalization.[145,191-194]

### 2.4.3 DCC Coupling

#### 2.4.3.1 General

Esters can be synthesized by a number of different methods, many of which require acidic conditions. However, using dicyclohexylcarbodiimide (DCC) coupling, we have used an established route to the efficient synthesis of esters, which are covalently attached to our copolymer (Figure 38). DCC coupling is a well-known synthetic route applied in dendrimer chemistry,[195-197] peptide synthesis,[198,199] block copolymer synthesis,[130] and coupling substrates to polymers.[200,201] An extremely attractive feature of DCC coupling is the ease of purification. Under the reaction conditions of DCC coupling, the insoluble dicyclohexyl urea by-product is simply removed by filtration, facilitating purification.

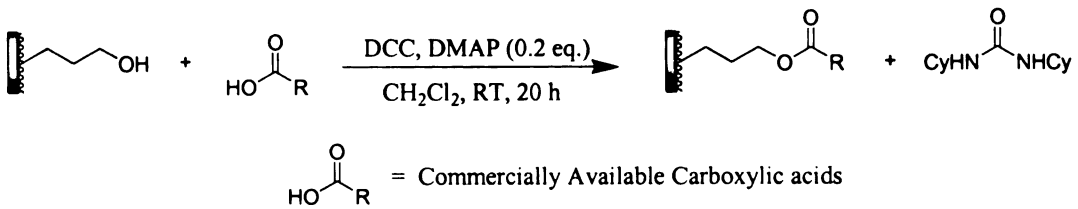


**Figure 38.** General synthetic route to polymer-bound esters using DCC coupling.

The generality of this approach is also appealing. DCC coupling of our copolymer with a variety of carboxylic acids affords a simple way to covalently attach substrates containing a carboxylic acid functional group. An added benefit is the creation of an ester linkage. Since our copolymer is a polyester, the ester linkage adjoining our functional side chain to the polymer is an insignificant perturbation to the polymer itself. Additionally, the esterified functional group may enhance the biocompatibility of our copolymer as a material in tissue regeneration.

### 2.4.3.2 Side-Chain Esterification of Fatty Acids

There are a few classes of biodegradable materials which have utilized fatty acids or long chain alkyl substituents. Such polymers have been used with the incorporated alkyl chain acting as an inherent plasticizer,[103,202,203] a bioactive substrate amenable for drug delivery applications,[100,101,204] or as a cross-linking agent.[205-207] These classes of materials include medium chain length poly(hydroxyalkanoates) (mcl-PHAs),[208] polyesters based on glycerol and diacid functional groups which incorporate fatty acids, and polyanhydrides functionalized with substituted fatty acids (Figure 39).[100,103,205,206]

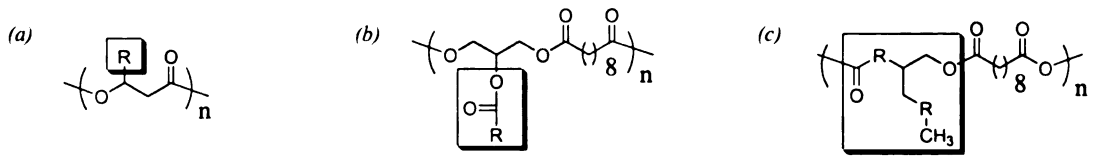


R = Medium length alkyl chain — *Witholt et al.*

R = Fatty acid-based alkyl chain — *Kobayashi et al.*

R = Fatty acid-based alkyl chain — *Domb et al.*

**Figure 39.** Fatty acid-modified polymers. *(a)* medium chain length poly(hydroxyalkanoate). *(b)* biodegradable polyester based on glycerol, sebacic acid, and a fatty acid. *(c)* polyanhydride containing fatty acid moieties.

Using commercially available fatty acids we have demonstrated DCC coupling as a viable method for functionalizing PLLA-*g*-HP (Figure 40). The pendant hydroxyl groups reacted with the fatty acid in the presence of DCC and a catalytic amount of N,N-dimethyaminopyridine (DMAP) to form the ester linkages onto our copolymer. We chose a group of long chain fatty acids, some of which have influence in the biology of bone tissue growth.[209,210]

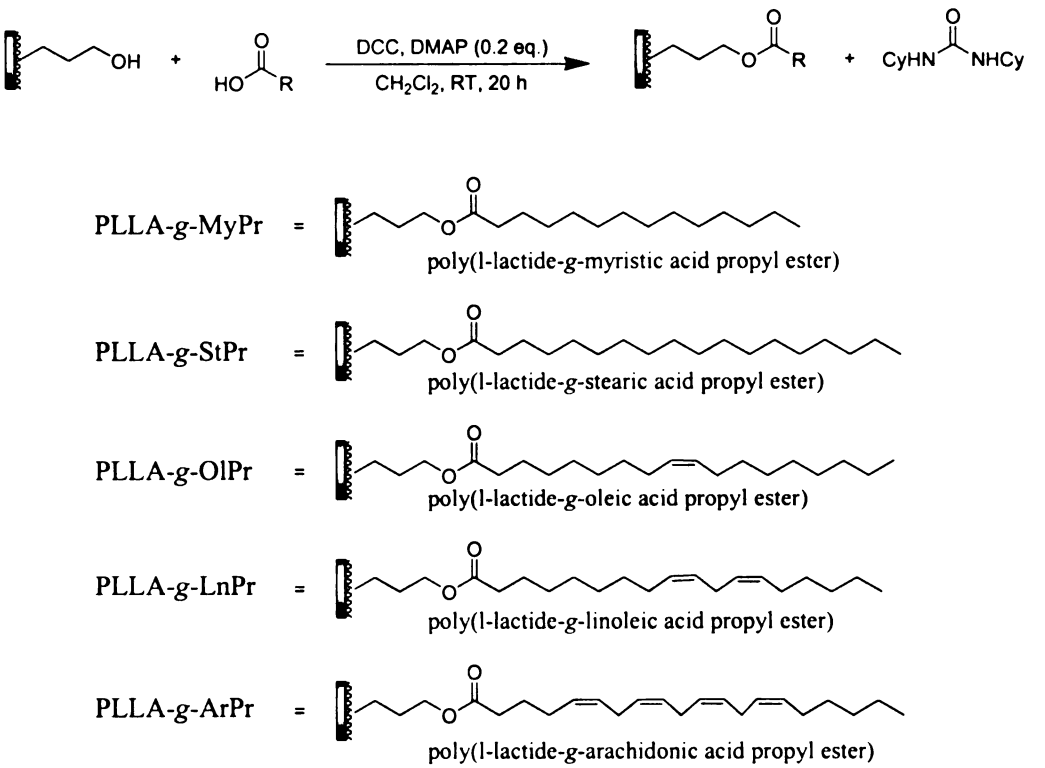


**Figure 40.** Synthetic route to saturated and unsaturated fatty acid-modified PLLA using DCC coupling.

The reactions were carried out in dichloromethane for 20 hours to ensure complete coupling. After the desired reaction time, the insoluble dicylcohexyl urea was removed by filtration, and the polymer was concentrated, and reprecipitated twice from methanol. The reaction conditions provide a simple and efficient method for ester formation without harsh acidic or basic conditions. In spite of reports of polymer degradation using DMAP,[211] we observe good yields, full conversions, and no molecular weight loss for the polymer (Table 5).

| *Fatty Acid (Carbon:Unsaturated)* | $M_n$ / gmol$^{-1}$ (PDI)[a,b] | $T_g$[c] / °C | $T_c$[c] / °C | $T_m$[c] / °C ($\Delta H$/Jg$^{-1}$) | % Yield |
|---|---|---|---|---|---|
| Myristic (14:0) | 16,300 (1.37) | 27 | 86 | 135 (24.3) | 85 |
| Stearic (18:0) | 15,800 (1.37) | 25 | 79 | 131 (29.5) | 87 |
| Oleic (18:1) | 17,700 (1.36) | 23 | 90 | 135 (25.5) | 89 |
| Linoleic (18:2)[d] | 18,300 (1.48) | 21 | 87 | 132 (23.7) | 81 |
| Arachidonic (20:4)[d] | 20,000 (1.63) | 18 | 86 | 132 (26.1) | 80 |
| Linoleic (18:2)[e] | 18,300 (1.48) | 32 | - | - | 81 |
| Arachidonic (20:4)[e] | 19,900 (1.84) | 52 | - | - | 80 |
| PLLA-*g*-HP[f] | 13,500 (1.58) | 54 | 121 | 142 (12.9) | 75 |
| PLLA (6% D)[g] | 17,700 (1.28) | 53 | -[h] | 151 (25.6) | 73 |

**Table 5.** Saturated and unsaturated fatty acid-modified PLLA copolymers containing 6 mol % fatty acid. [a] Molecular weight determined by GPC. [b] PDI = Polydispersity index. [c] Differential scanning calorimetry of 6 mol % fatty acid-modified copolymers. Second heating scan at 10°C/min under helium atmosphere. [d] Functional polymer not exposed to air. [e] Exposed to air until gellation renders the functional polymer insoluble. [f] Hydroxylated copolymer starting material used to couple fatty acids. [g] Independently prepared PLLA containing 6 mol % D units. [h] Sample annealed at crystallization temperature.

$^1$H NMR spectra show the quantitative incorporation of the saturated fatty acids myristic ($C_{14}$) and stearic ($C_{18}$) acid (Figure 41). Spectral analysis of the $C_{18}$ unsaturated acids also reveals complete conversion of the fatty acids to their polymer-bound esters (Figure 42). Additionally, the polyunsaturated arachidonic acid-modified ($C_{20}$) polymer was synthesized and spectroscopically characterized (Figure 43). Proton NMR assignments for all the fatty acid modified polymers were made in order to identify the protons corresponding to the side chain. Some notable features in the NMR are that linoleic acid and arachidonic acid-modified polymers both have bisallylic methylene protons appearing at 2.7-2.8 ppm, which were absent in the saturated fatty acid and oleic acid polymers. Also, the increase in intensity of the olefinic proton region at 5.3-5.5 ppm is a characteristic feature of the covalent attachment of the unsaturated fatty acids.

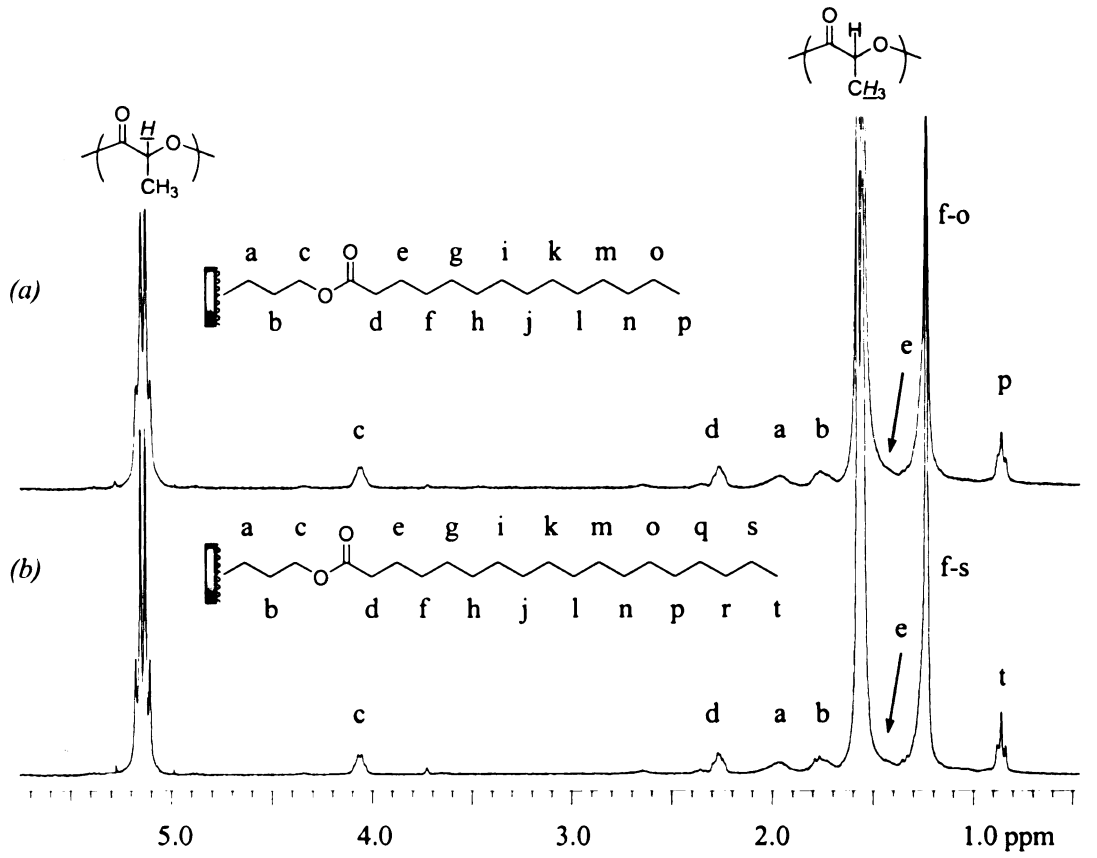


**Figure 41.** $^{1}$H NMR (300 MHz, $CDCl_3$) spectra of *(a)* PLLA-*g*-MyPr; Myristic acid-modified PLLA-*g*-HP and *(b)* PLLA-*g*-StPr; Stearic acid-modified PLLA-*g*-HP.

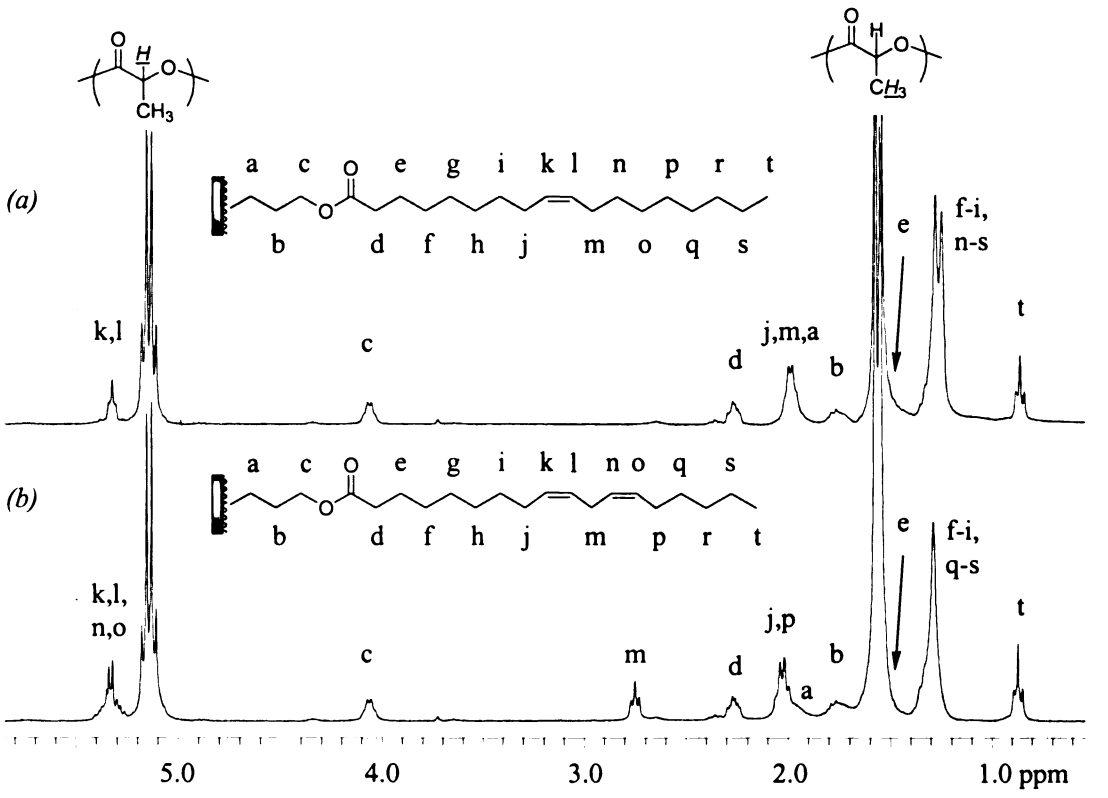


**Figure 42.** $^1$H NMR (300 MHz, $CDCl_3$) spectra of *(a)* PLLA-*g*-OlPr; Oleic acid-modified PLLA-*g*-HP and *(b)* PLLA-*g*-LnPr; Linoleic acid-modified PLLA-*g*-HP.

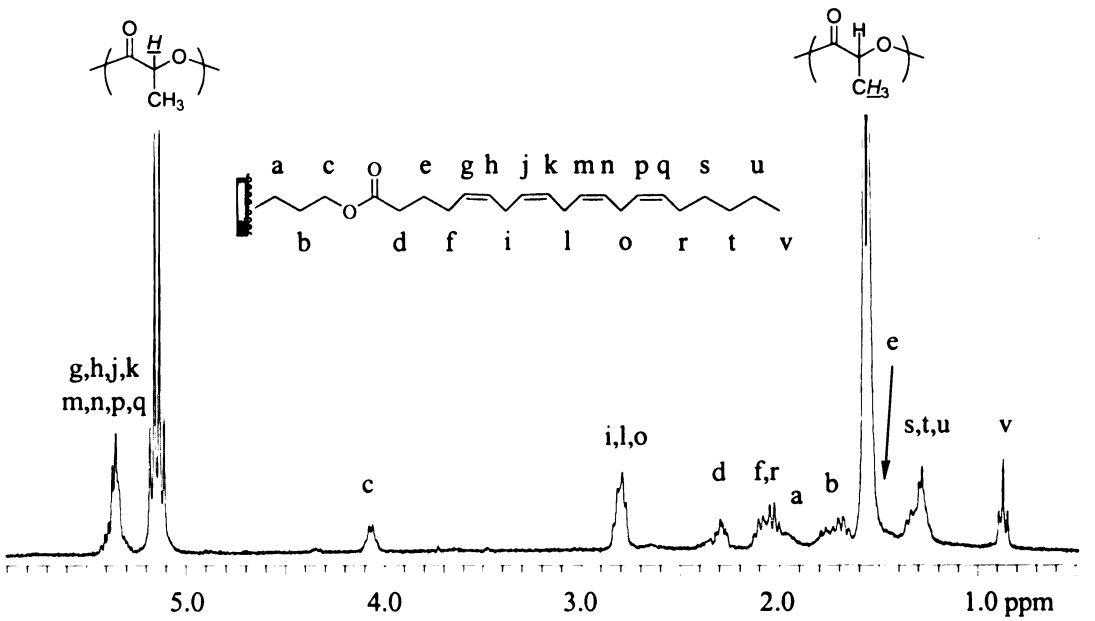


**Figure 43.** $^1$H NMR (300 MHz, $CDCl_3$) spectrum of PLLA-*g*-ArPr; Arachidonic acid-modified PLLA-*g*-HP.

Thermal analysis of the copolymers using DSC showed the $T_g$ of the materials decreased from the original PLLA-*g*-HP (54°C) upon esterification of the fatty acids (Figure 44). The glass transition, crystallization, and melting temperatures of the fatty acid-modified materials are all very similar. The crystallinity seen here is due to the crystallinity of the backbone, since both PLLA-*g*-HP and PLLA-*co*-AG containing 6% allyl units are still crystalline. The two observed melting points are due to α- and β-structures of PLLA, and have been discussed by other groups.[212-214]

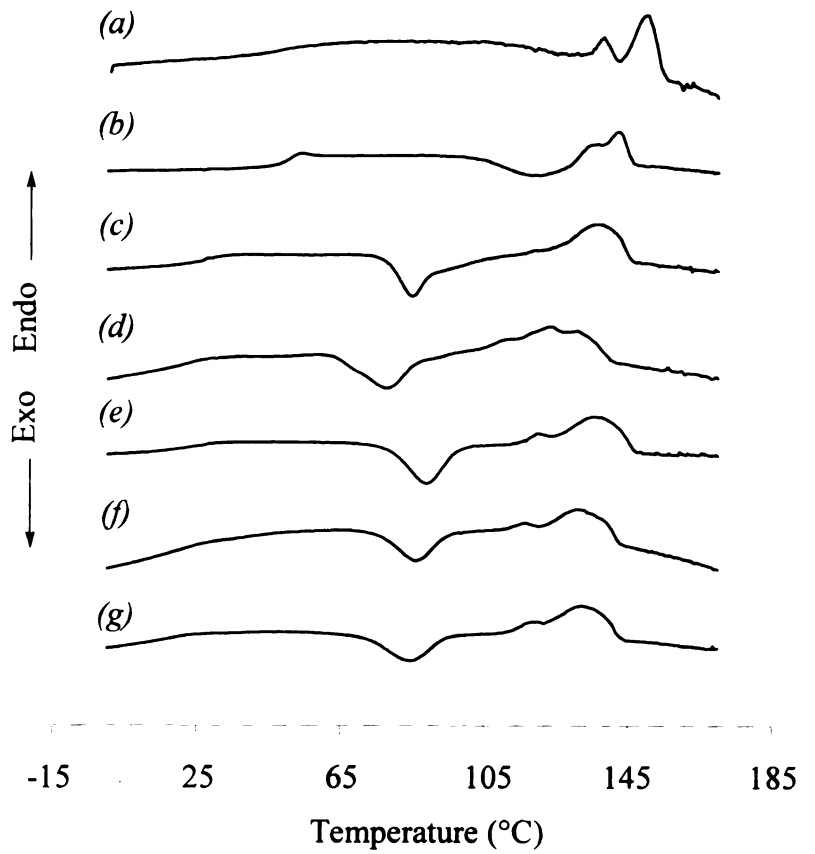


**Figure 44**. Differential scanning calorimetry of 6 mol % fatty acid-modified copolymers. Second heating scan at 10°C/min under helium atmosphere. *(a)* PLLA (6% D-lactide); *(b)* PLLA-*g*-HP; *(c)* PLLA-*g*-MyPr; *(d)* PLLA-*g*-StPr; *(e)* PLLA-*g*-OlPr; *(f)* PLLA-*g*-LnPr; *(g)* PLLA-*g*-ArPr.

A noteworthy feature of the DSC results is the behavior of the linoleic acid and the arachidonic acid-modified copolymers. When left standing for a prolonged period of time in solution in the presence of oxygen, the polymers became viscous and gelled. After longer periods of time, the polymer became completely insoluble in any solvent, providing evidence of oxidative cross-linking. The mechanism of cross-linking occurs *via* oxidatively-induced isomerization of the bisallylic methylene hydrogens to generate a peroxy-radical.[215] The peroxy-radical then acts as the propagating species to facilitate cross-linking between double bonds on adjacent chains (Figure 45). This cross-linking behavior, known as curing, is common in the cross-linking of certain oils,[216] and can also

be thermally induced, as in the case of Kobayashi's glycerol-based biodegradable polyester containing fatty acid side chains.[206] These biodegradable polyesters were thermally cured to give cross-linked, transparent polymeric films showing increased hardness. In his work, only samples containing bisallylic hydrogens underwent cross-linking.

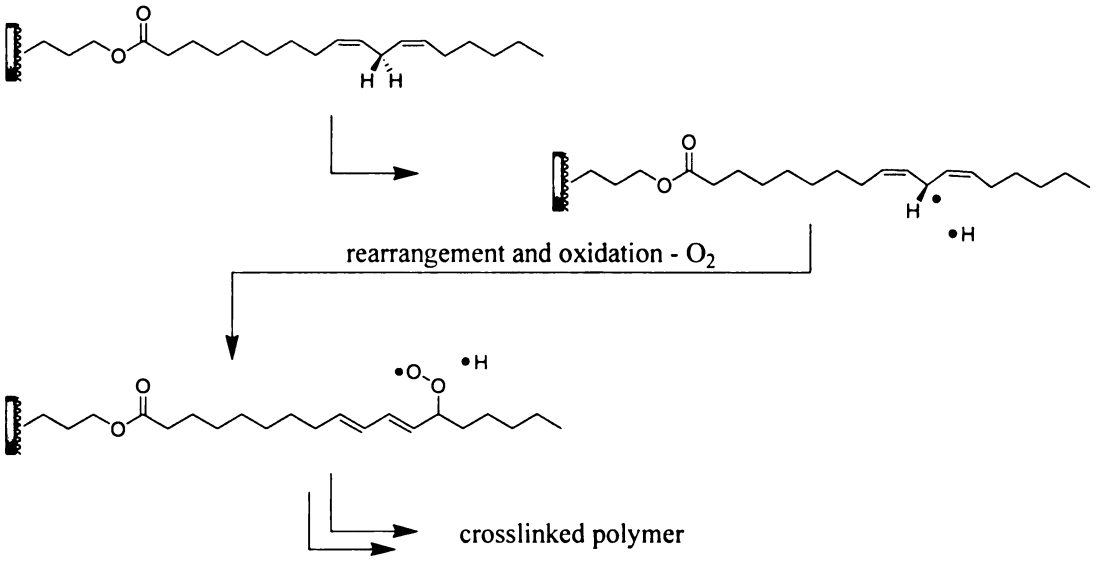


**Figure 45.** Simplified synthetic route to the cross-linking of polyunsaturated fatty acid modified PLLA copolymers. Proposed by Vogl and Blanksby.[216]

For the saturated fatty acid and the oleic derivatives we prepared, there are no labile bisallylic hydrogens, and we observe no cross-linking. This is in agreement with the findings of Kobayashi.[206] Reproducible DSC scans of each copolymer suggests that they are insensitive to oxidative and thermally-induced cross-linking. Consequently, this cross-linking behavior provides a basis for the observed increase in the $T_g$ of the linoleic acid and arachidonic acid-modified copolymers to 32°C and 52°C, respectively. The arachidonic acid containing three bisallylic methylenes should be more susceptible to the cross-linking, which is reflected in the higher $T_g$. Conversely, when the linoleic acid- and

arachidonic acid-modified copolymers are kept from oxygen, there appears to be no cross-linking as indicated by the solubility, *and* the measured $T_g$s of the copolymers are much lower at 21°C and 18°C, respectively (Figure 46).

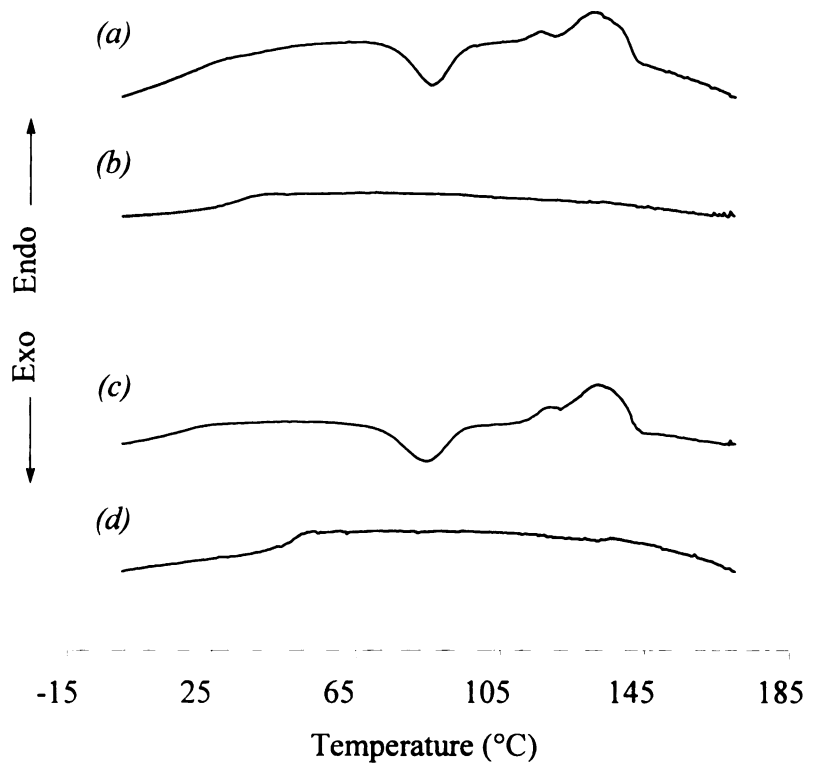


**Figure 46.** Differential scanning calorimetry of 6 mol % fatty acid-modified copolymers. Second heating scan at 10°C/min under helium atmosphere. *(a)* PLLA-*g*-LnPr; linear polymer sample. *(b)* PLLA-*g*-LnPr; cross-linked sample. *(c)* PLLA-*g*-ArPr; linear polymer sample. *(d)* PLLA-*g*-ArPr; cross-linked sample. Linear polymer samples were prepared and stored under a nitrogen atmosphere prior to DSC analysis. Cross-linked polymer samples were exposed to air during workup and allowed to cross-link until the polymer became insoluble.

Increased $M_n$ and PDI values for the linoleic acid and arachidonic acid-modified copolymers may also be reflective of cross-linking between chains. This behavior is an extremely interesting finding, and reveals a potential route to the synthesis of

polyunsaturated fatty acid-modified PLLA copolymers possessing higher $T_g$s, where only small amounts of the coupled unsaturated side chain are required for cross-linking.

#### 2.4.3.3 Side-Chain Esterification of Phosphonic and Amino Acids

##### 2.4.3.3.1 Side Chain Esterification of Phosphonoacetic Acid

The synthesis of biodegradable phosphonated copolymers[217] and biodegradable polymer composites[218-221] have been targeted specifically for their ability to support nucleation and growth of hydroxyapatite (HAp) and other minerals in the biology of osteoblast tissue engineering. Hydroxyapatite, $Ca_{10}(PO_4)_6(OH)_2$, is the mineral deposited by the osteoblast matrix in the formation of bone. Materials that nucleate HAp can help in the proliferation of osteoblasts, which further differentiate into a mineral-depositing, bone-producing matrix. Li and coworkers have designed biodegradable PLLA fibers coated with HAp in order to help nucleate minerals secreted by the differentiated osteoblastic matrix.[218] Gonsalves has designed a synthetic biodegradable copolymer based on poly(ε-caprolactone) which contains pendant vinyl phosphonate groups.[217] Acrylate-based polymers containing pendant phosphonate groups are also used as materials for dental composites.[222,223] Regardless of the nature of the material, the phosphonate groups are chosen for their ability to bind minerals such as calcium. Consequently, the incorporation of phosphonate groups in the copolymer also increases the hydrophilicity of the material. Incorporating hydrophilic moieties within the polymer framework is a strategy employed to help control the cell adhesion properties of a given material. PLLA is a hydrophobic polymer which cannot control cell adhesion. Thus, incorporating pockets of hydrophilicity in the form of phosphonic acid groups to help

regulate cell adhesion as well as help in the templation of minerals which occur during cell differentiation. This material can be used while maintaining the benefits of the biodegradable polymer.

The synthesis of a phosphonic acid-modified copolymer was achieved by the DCC coupling of diethylphosphonoacetic acid to PLLA-*g*-HP in the presence of a catalytic amount of DMAP. After stirring for 20 hours the reaction was filtered and precipitated twice from methanol (Figure 47).

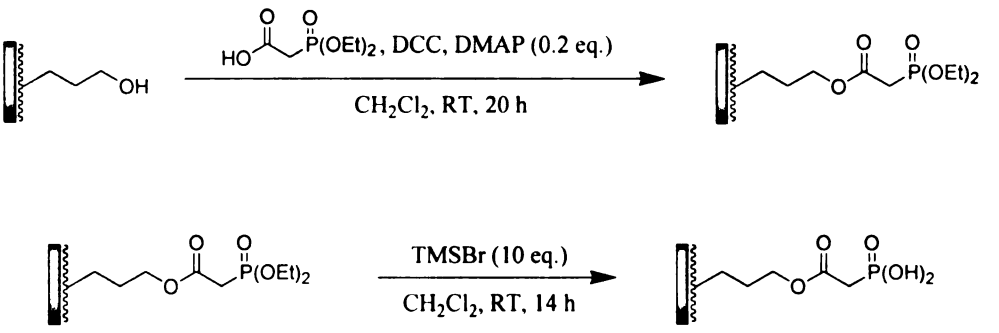


**Figure 47.** Synthetic route to PLLA-g-DAPPr; Poly(lactide-*g*-diethylphosphonoacetic acid, propyl ester) and PLLA-*g*-PAPr; Poly(lactide-*g*-phosphonoacetic acid, propyl ester).

This polymer was characterized by both $^{1}H$ NMR and $^{31}P$ NMR spectroscopy (Figure 48). A distinctive $^{1}H$ NMR resonance for the methylene protons, which are coupled to the adjacent phosphorous, gives rise to a doublet with a $J_{P\text{-}H}$ coupling constant of 22 Hz. The ethyl resonances of the phosphodiester are also clearly seen at 1.2-1.4 and 4.1-4.2 ppm. A single resonance at 20.2 ppm in the $^{31}P$ NMR spectrum is also consistent with the esterification product of diethylphosphonoacetic acid. The spectroscopic data are in agreement with other phosphonated materials containing phosphonates and phosphonodiesters.

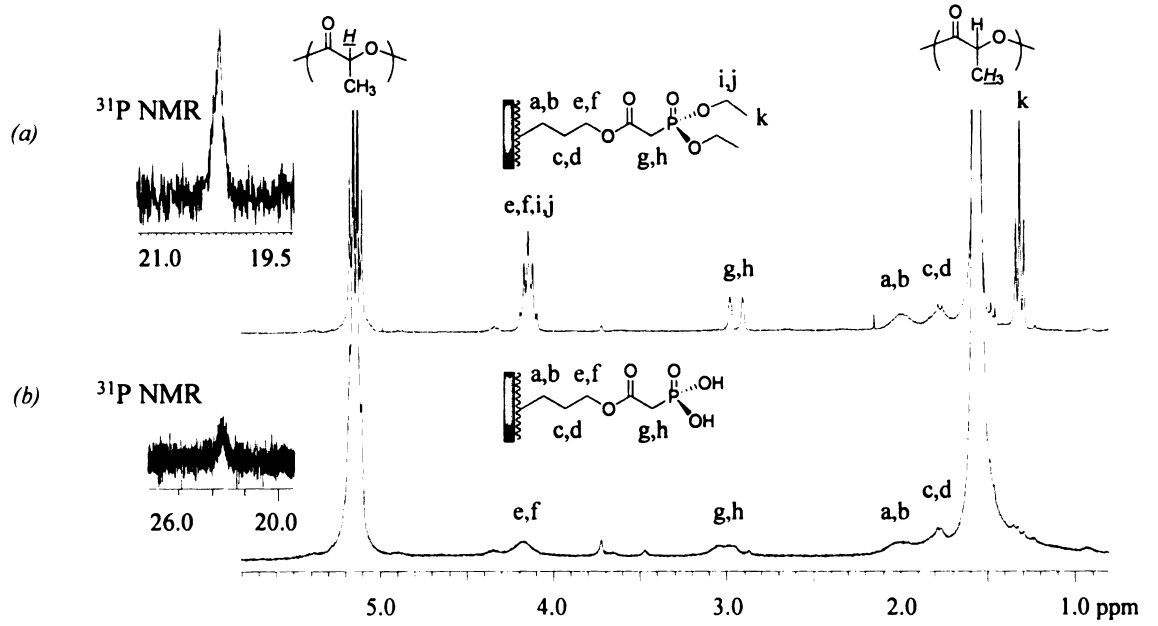


**Figure 48.** $^{1}H$ NMR (300 MHz, $CDCl_3$) and $^{31}P$ NMR (120 MHz, $CDCl_3$) spectra of *(a)* PLLA-*g*-DPAPr; Diethylphosphonoacetic acid-modified PLLA-*g*-HP and *(b)* PLLA-*g*-PAPr; Phosphonoacetic acid-modified PLLA-g-HP.

The deprotection of the phosphodiester copolymer was achieved by simply stirring the copolymer with a ten-fold excess of bromotrimethylsilane. After stirring for 8 hours, the polymer was quenched with methanol and precipitated from dichloromethane into aqueous methanol. The labile silyl groups on the phosphodiester intermediate were cleaved upon aqueous workup to yield pendant phosphonic acid groups covalently attached to the PLLA backbone. The $^{1}H$ NMR shows the disappearance of the ethyl group resonances. Notably, the phosphorous coupling to the methylene protons in the side chain is not as prominent as in the protected phosphoester; however, the coupling is observed when the polymer is characterized in another solvent such as $d_6$-DMSO.

### 2.4.3.3.2 Side Chain Esterification of N,N′-diBoc-Lysine

Amino acids incorporated into biodegradable polymers are important bioactive substrates in tissue engineering applications. They can serve as attachment sites for adhesion peptides,[138,224] growth factors,[65,225,226] and provide a simple model for coupling peptides to biodegradable materials. The known strategy for incorporating amino acids into biodegradable polymers is to synthesize substituted morpholine-2,5-diones as the amino acid-bearing functional comonomer.[227] Copolymerization of the morpholine-2,5-dione with a monomer such as lactide gives a biodegradable copolymer with amino acid groups built into the polymer. Once polymerized, the material can be used directly in biological applications or further modified by additional procedures (Figure 49). Many research groups have taken this approach to incorporate amino acids such as lysine,[132,225] serine,[131,228] aspartic[229-231] and glutamic acid[227,229,232] in polymers.

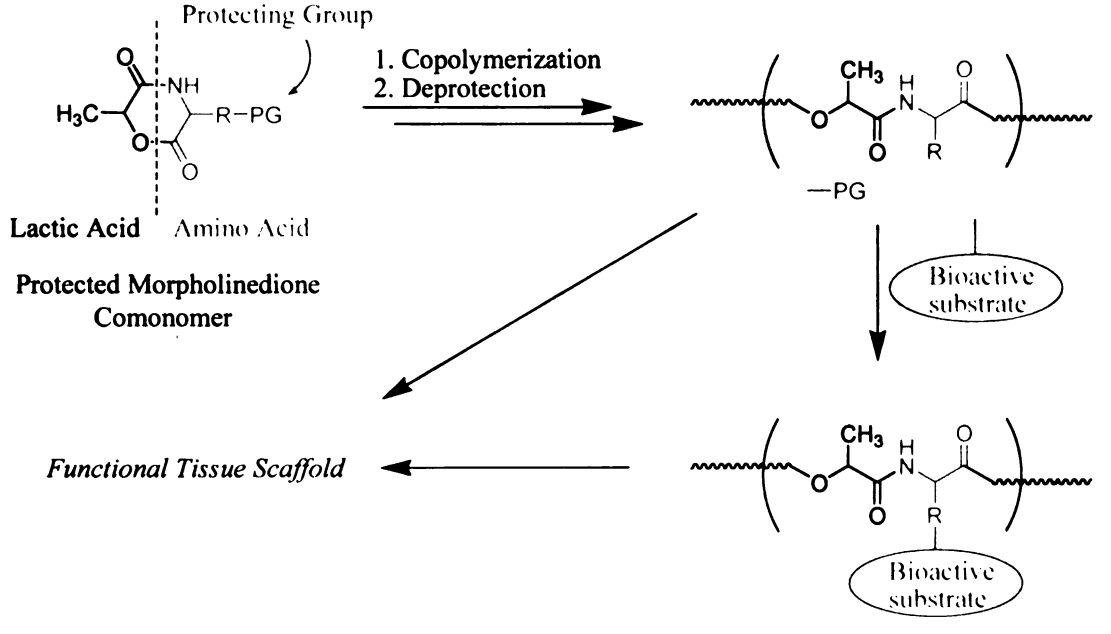


**Figure 49.** Synthetic strategy for designing biodegradable polymers with amino acid functionality.

In an alternative approach, we have employed our DCC coupling chemistry to couple lysine to our biodegradable copolymer. In order for our DCC coupling conditions to work, we used N,N′-diBoc-lysine and carried out the DCC coupling procedure as previously described (Figure 50). The DCC coupling proceeded smoothly, and the polymer was precipitated twice from methanol. The $^{1}H$ NMR spectrum shows the expected peaks from the protected lysine copolymer (Figure 51). In a similar procedure, Langer and Lavik used DCC coupling to modify the endgroup of PLGA, with carboxybenzoyl-protected poly(lysine) resulting in a block copolymer.[130] In our reactions, the BOC protecting groups were removed by reacting the copolymer with an excess of trifluoroacetic acid. The solution was directly poured into water containing an excess of sodium bicarbonate to neutralize the excess acid. This precipitation was done carefully since the evolution of carbon dioxide accompanies the acid-base reaction. The polymer was obtained in nearly quantitative yield and contained the trifluoroacetate ammonium salt of the deprotected lysine. $^{13}C$ NMR of the polymer showed two quartets in the carbon spectrum at 162 ppm ($J_{C\text{-}F}$ = 33 Hz) and 118 ppm ($J_{C\text{-}F}$ = 292 Hz) for the carbonyl and trifluoromethyl carbon respectively. The coupling constants are diagnostic for fluorine coupling with the carbonyl carbon and the trifluoromethyl carbon of the acetate. The mixture was purified by centrifugation to give PLLA-*g*-LysTFAPr in nearly quantitative yield (Figure 51).

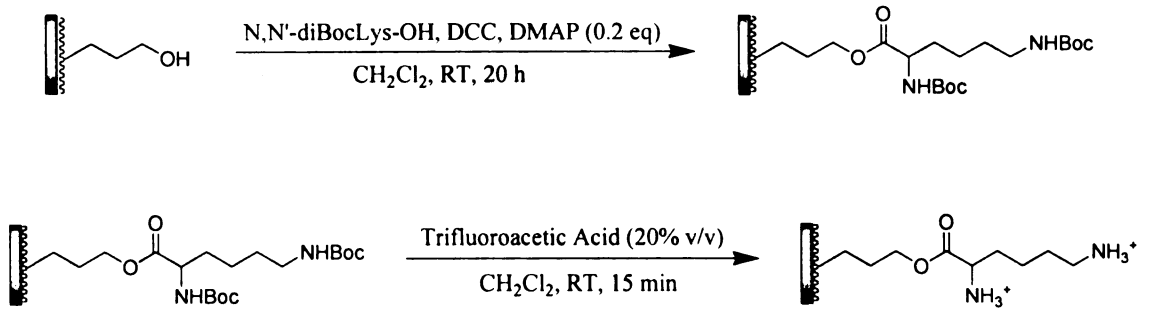


**Figure 50.** Synthetic route to PLLA-*g*-BocLysPr; Poly(lactide-*g*-N,N´-diBoc-lysine propyl ester), and PLLA-*g*-LysTFAPr; Poly(lactide-*g*-lysine bis(trifluoroacetate) propyl ester).

Upon deprotection, the BOC resonance at 1.4 ppm disappeared and the other proton resonances were shifted. The protected lysine-modified copolymer is soluble in typical organic solvents such as dichloromethane, chloroform, and tetrahydrofuran. The solubility of the deprotected form of the copolymer, however, can be dependent on the molar composition of lysine units in the copolymer. We have observed that the lower loading of lysine residues (<5%) increased the solubility in halogenated solvents. However, if the lysine loading is high enough (>5%), the copolymer becomes more insoluble in *d*-chloroform, and NMR characterization must be done in $d_4$-methanol, $d_6$-dimethyl sulfoxide, or $d_8$-thf. This solubility change was also observed by Langer with his copolymers of PLLA-co-lysine, and thus this finding might be expected in our case.[132,233,234] The $^1$H NMR of PLLA-g-LysTFAPr in $d_8$-thf shows the alkyl resonances more clearly (Figure 52). Spectral assignments of the proton resonances were based on two-dimensional COSY NMR experiments.

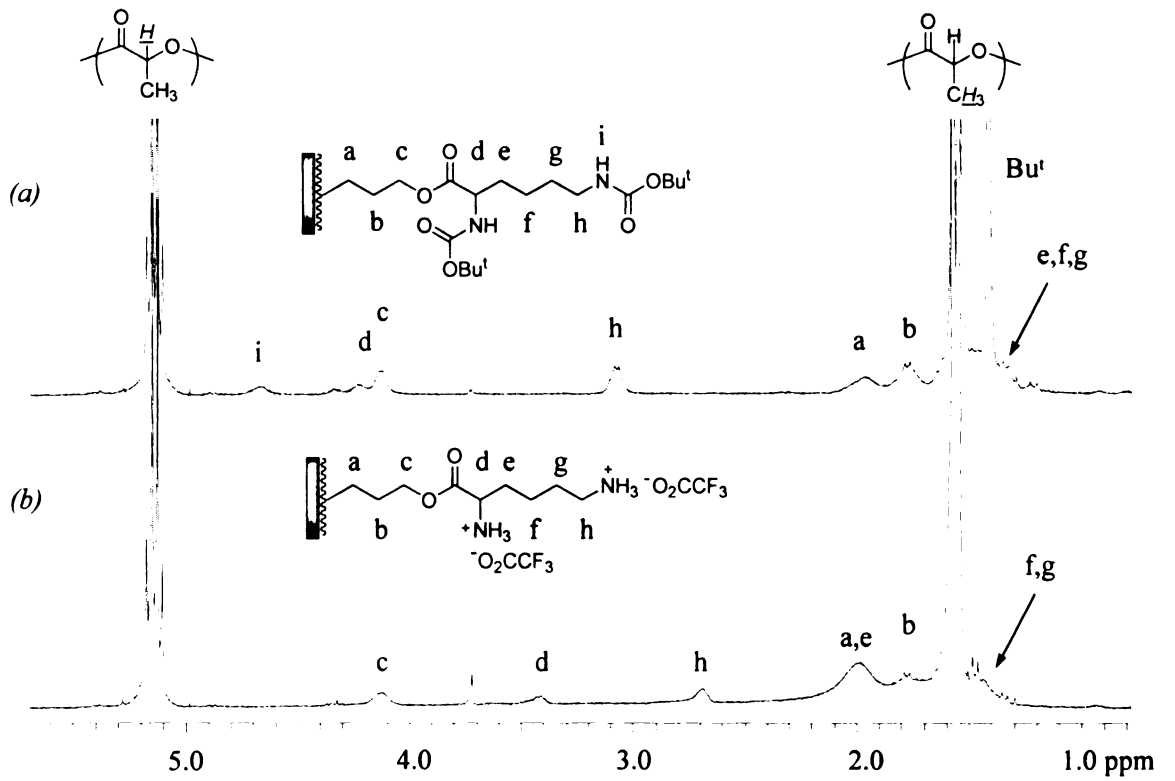


**Figure 51.** $^1$H NMR (300 MHz, $CDCl_3$) spectra of *(a)* PLLA-*g*-BocLysPr; N,N′-diBoc-lysine-esterified PLLA-*g*-HP and *(b)* PLLA-*g*-LysTFAPr; lysine bis(trifluoroacetate)-modified PLLA-*g*-HP.

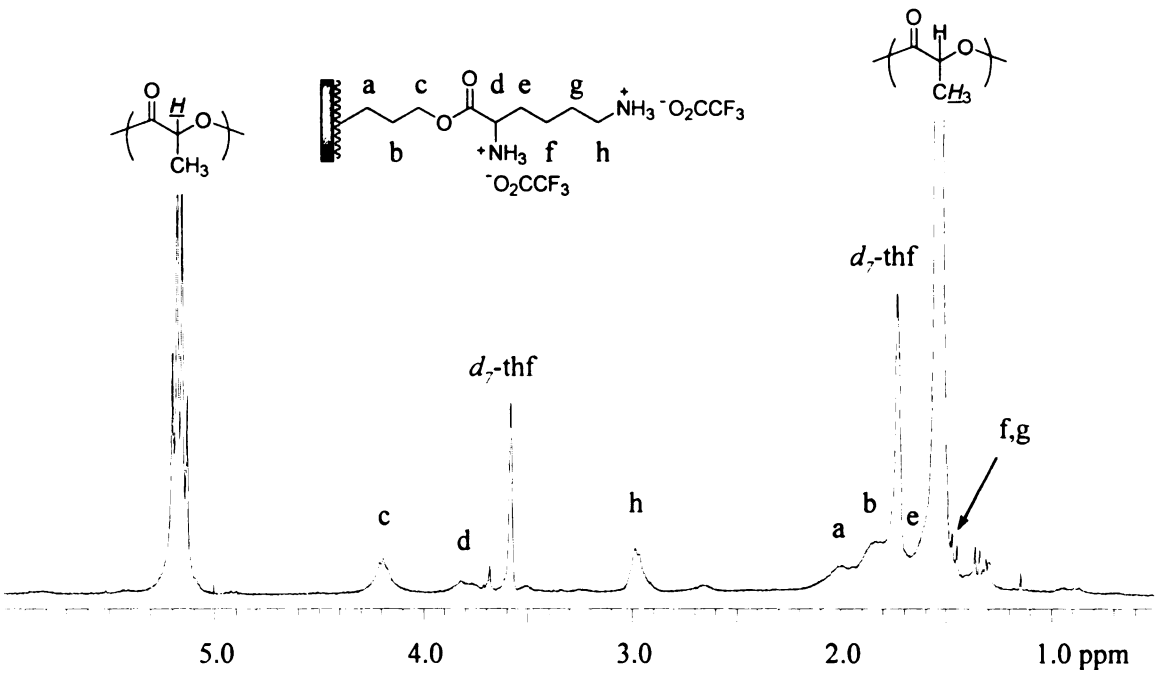


**Figure 52.** $^1$H NMR (300 MHz, $d_8$-thf) spectrum of PLLA-*g*-LysTFAPr; lysine bis(trifluoroacetate)-modified PLLA-*g*-HP.

Table 6 shows the results of molecular weight and thermal analyses of the phosphonic acid and lysine-modified copolymers. In the other copolymers, no apparent decomposition or degradation of the polymer was noted under our DCC coupling or deprotection steps. The DSC profiles for these copolymers change once the phosphonate and the lysine modifications are made. The crystallinity is lost, and a small decrease in the $T_g$ is observed for the protected and deprotected copolymers compared to the PLLA-*g*-HP copolymer.

| *Copolymer* | $M_n$ / $gmol^{-1}$ *(PDI)*[a,b] | $T_g$[c] / °C | *% Yield* |
|---|---|---|---|
| PLLA-*g*-DPAPr | 13,000 (1.45) | 40 | 88 |
| PLLA-*g*-PAPr | 12,000 (1.37) | 57 | 71 |
| PLLA-*g*-BocLysPr | 17,800 (1.42) | 54 | 70 |
| PLLA-*g*-LysTFAPr[d] | -- | 47 | 95 |
| PLLA-*g*-HP[e] | 13,500 (1.58) | 54 | 75 |

**Table 6.** Protected and deprotected phosphonic and amino acid-modified PLLA copolymers containing 6 mol % functional groups. [a] Molecular weight determined by GPC. [b] PDI = Polydispersity index. [c] Differential scanning calorimetry of modified copolymers containing 6 mol % functionality. $T_g$ was obtained after the second heating scan at 10°C/min under helium atmosphere. Molecular weight was not observed by GPC. [d] Independently prepared 6 mol % hydroxypropane-modified copolymer.

Successful preparation of PLLA copolymers containing pendant hydrophobic (fatty acids) and pendant hydrophilic (phosphonic and amino acid) groups was achieved by DCC coupling and deprotection, where necessary, of commercially available and biologically relevant starting materials. Spectroscopic characterization of the copolymers confirm the transformation and covalent attachment of these diverse functional groups. DSC analyses show the influence of the tethered substrates on the $T_g$ of the material compared to its copolymer precursors.

Our goal in creating a simple method of functionalization was achieved by designing a simple comonomer and using simple organic chemistry such as hydroboration and DCC coupling to covalently attach functionally diverse bioactive substrates. The usefulness of this methodology is underscored by the simplicity with which widely biologically-diverse materials can be made. The evaluation of these materials in tissue engineering applications is the next step to determine where our materials best fit into this developing area of research.

CHAPTER THREE

# 3 Cell Biology on Modified Poly(Lactic Acid) Surfaces

## 3.1 Copolymer Thin Films

In order to assess the physiology of our copolymers we prepared thin films to use as surfaces for tissue growth studies. Thin films were prepared by spin-coating the polymer on freshly cleaned polished silicon wafers. Osteoblasts were seeded on the polymer-coated wafers and their proliferation, differentiation, and shape during the culturing process were assessed.

The functional copolymers from which the films were prepared were chosen for their potential interaction with osteoblasts. Osteoblasts are cells that are responsible for the production of bone. The osteoblasts first proliferate (divide) and then reach a critical point where they cease to proliferate and begin to differentiate and secrete the extracellular matrix (ECM). The matrix provides an environment where cells can deposit minerals, which ultimately comprise the material in bone formation. In choosing substrates for our copolymer modification, we were hoping to influence proliferation and differentiation by creating a unique surface over which the cells can spread. The geometric shape of cells has been shown to greatly influence their proliferation and differentiation.[41-43] We have prepared these copolymers with unique functionality with the hypothesis that they will interact with the cells to alter and influence their shape.

To determine whether or not our polymer surfaces possessed any functionality on the surface, we characterized the surfaces of thin films using ellipsometry and contact angle measurements (Table 7). The thicknesses of the films were uniform on a given substrate, but varied slightly between copolymers. All of the films prepared were spin-

coated from a 1% (w/w) solution of the polymer in toluene. The film thicknesses were measured using ellipsometry and had thicknesses generally around 50 nm.

| *Copolymer* | *Loading* [a] | *Thickness / nm* [b] | $\theta_{adv}$ [c] | $\theta_{rec}$ [c] |
|---|---|---|---|---|
| PDLLA | -- | 56 ± 0.5 | 70 ± 2.1 | 51 ± 1.7 |
| PLLA-*g*-HP | 6% | 70 ± 1.5 | 84 ± 2.8 | 50 ± 2.6 |
| LLA-*g*-MyPr | 6% | 47 ± 0.8 | 82 ± 0.9 | 52 ± 2.4 |
| PLLA-*g*-StPr | 6% | 48 ± 1.1 | 85 ± 1.1 | 50 ± 2.7 |
| PLLA-*g*-OlPr | 6% | 47 ± 4.7 | 78 ± 0.7 | 53 ± 1.4 |
| PLLA-*g*-LnPr | 6% | 49 ± 1.1 | 78 ± 1.7 | 52 ± 1.7 |
| PLLA-*g*-ArPr | 6% | 42 ± 3.2 | 82 ± 1.7 | 45 ± 3.2 |
| PLLA-*g*-DPAPr | 6% | 45 ± 0.5 | 75 ± 1.5 | 37 ± 1.2 |
| PLLA-*g*-PAPr[d] | 6% | 96 ± 4.0 | 73 ± 1.1 | 35 ± 1.5 |
| PLLA-*g*-BocLysPr | 6% | 52 ± 0.9 | 79 ± 1.0 | 39 ± 1.9 |
| PLLA-*g*-LysTFAPr[d] | 6% | 68 ± 3.3 | 69 ± 2.4 | 27 ± 0.6 |

**Table 7.** Thin films of copolymers spin-coated on 1-inch diameter silicon wafers from a 1% (w/w) solution in toluene unless otherwise noted. Spin rate: 2500 rpm, spin time: 40 sec. [a] Mole percent loading determined by $^1$H NMR spectroscopy. [b] Determined by ellipsometry. [c] Samples were prepared by heating above the polymer melting point and quenching to room temperature to obtain amorphous samples. Advancing ($\theta_{adv}$) and receding ($\theta_{rec}$) contact angles were measured at a rate of 3 μL/s up to a total volume of 30 μL using Milli-Q grade water. [d] Copolymer were dissolved as a 1% (w/w) solution in tetrahydrofuran.

The wettability of the polymer surface was monitored by recording the advancing and receding contact angles of a droplet of Milli-Q grade water. The polymer samples were all heated 160°C under an atmosphere of nitrogen then immediately placed on a clean surface at room temperature in order to ensure a common sample history. Five separate contact angle measurements were taken on each polymer-coated silicon wafer, with the error set as one standard deviation from the mean. Compared to PLLA-*g*-HP, the change in the advancing and receding contact angles for the esterified fatty acids is

not significant, suggesting that the hydrophobic grafts may not be present near the surface of the film. The contact angle values compare well with side-chain fatty esters of polysaccharides[235] and endgroup fatty esters of polylactides.[236] Conversely, the more polar phosphonate and lysine derivatives result in a notable decrease in the advancing and receding contact angles, suggesting that the polar groups may reside close to the surface of the film. For our lysine derivatives specifically, the advancing and receding contact angles compare well with the PLLA-*co*-lysine polymers synthesized by Langer.[138] The contact angles reflect the wettability of each of the copolymer surfaces and may influence cell shape.

### 3.2 Osteoblast Cell Shape

We have assessed the biocompatibility of our copolymers by seeding osteoblasts on three different surfaces: PLLA, silicon oxide, and phosphonate-modified PLLA (PLLA-*g*-PAPr). In view of the wide applicability of biodegradable polyesters used as biomaterials, our modified PLLA copolymers are more suitable candidates to be used for *in vivo* applications. Therefore, by first assaying the *in vitro* cell growth behavior on the surfaces of modified PLLA copolymers, we hope to obtain information on osteoblast cell growth in the presence of these materials.

MC3T3-E1 osteoblasts were seeded at a concentration of 4400 cells/cm$^2$, cultured for 2 days in α-MEM (minimal essential medium) containing 2 mM β-glycerolphosphate and 25 μg/ml ascorbic acid, after which they were stained and visualized in order to observe their appearance on the silicon oxide wafers, and the phosphonate-modified PLLA. The differences in morphology of these sets of cells show how the osteoblasts spread on each of the surfaces. Cells cultured on the cleaned silicon wafers are more

spread out, while the PLLA-g-PAPr coated wafers are intermediate of the other surfaces, possessing characteristics of both the tissue culture plates and the silicon wafers. Clearly, the silicon wafers and the polymer-coated wafers alter the shape of the osteoblasts, providing positive evidence that the wafers and the polymer are influencing the conformation of the cells and therefore, may be able to influence osteoblast proliferation and differentiation.[42]

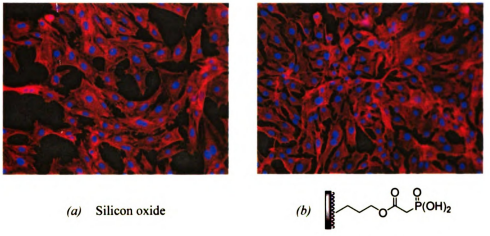


**Figure 53.** Microscope images of osteoblasts cultured for 48 hours on *(a)* silicon oxide and *(b)* 5% phosphonate modified PLLA surfaces.

### 3.3 Osteoblast Proliferation

The quantification of cell proliferation can be carried out by measuring the DNA of a dividing cell. This information is obtained by incorporating a fluorescent-labeled DNA base pair, allowing the cells to divide, and watching the incorporation of the fluorescent label. As the cells continue to replicate, the fluorescent label multiplies and is measured (Figure 54). The fluorescent label used is Bromodeoxyuridine (BrdU).

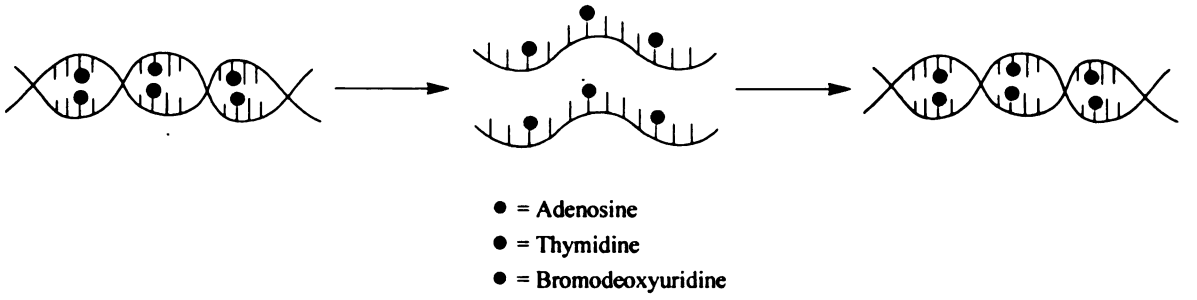


**Figure 54.** Illustration of cell replication incorporating the BrdU fluorescent label.

The cells were cultured for 48 hours and then incubated for 2 hours with BrdU. The BrdU incorporated into the cell nuclei at the S phase of dividing cells. The osteoblasts were then stained with propidium iodide, which was used to stain all cell nuclei. Osteoblast proliferation on unmodified PLLA was poor due to the because of the hydrophobicity of the polyester. However, the results on the other surfaces show that proliferation on the surfaces of silicon oxide and phosphonate-modified PLLA is essentially the same (Figure 55). The cell density viewed in the microscope images is much higher indicating rapid cell division before the BrdU assay at 48 hours. Therefore, while the BrdU assay shows no significant difference in proliferation between silicon oxide and the phosphonate-modified PLLA surface, the phosphonate-modified PLLA surface may have induced a proliferation burst within the first 48 hours.

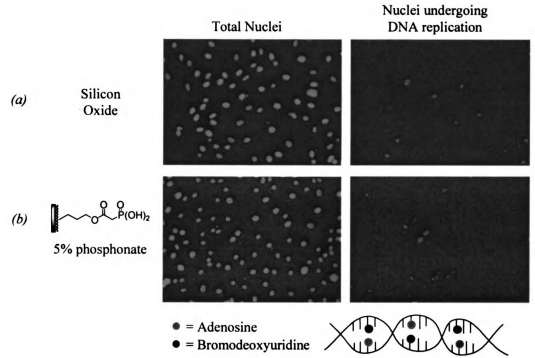


**Figure 55.** Digital photo images of fluorescent BrdU-labeled osteoblasts on *(a)* silicon oxide and *(b)* 5% phosphonate modified PLLA surfaces.

### 3.4 Osteoblast Differentiation

The process through which bone tissue forms begins with the cells' ability to differentiate. As cell proliferation precedes differentiation, longer culture times are required to assess differentiation. As differentiation occurs, the osteoblasts form the matrix for mineralization, and ultimately bone formation. After 14 days, RNA analysis quantifies levels of expressed genes alkaline phosphatase, osteocalcin, and transcription factor runx2 relative the internal control gene cyclophilin. The genes serve as markers to quantitate osteoblast differentiation (Figure 56).

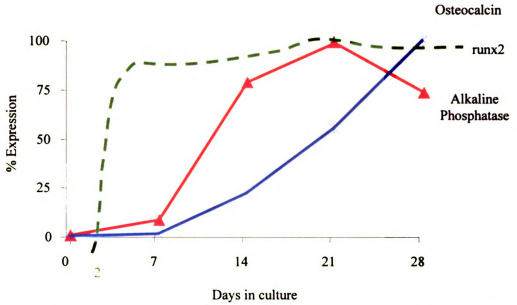


**Figure 56.** Gene expression levels of osteocalcin, runx2, and alkaline phosphatase as a function of osteoblast culture time.

After 14 days, the RNA of the cells was sampled and monitored for runx2 levels. Comparing the four surfaces, the phosphonate-modified copolymers showed a marked increase in differentiation over the unmodified PLLA, while it also exceeds differentiation on the silicon oxide (Figure 57).

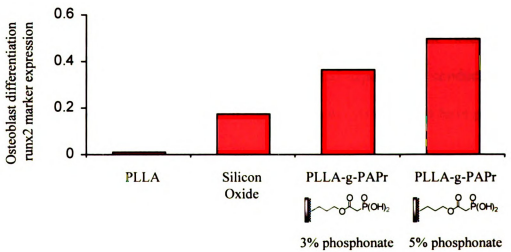


**Figure 57.** Surface comparison of osteoblast differentiation on different surfaces.

The increase in the observed differentiation from 3 mol % to 5 mol % phosphonate suggests that under identical conditions for all of the surfaces, the phosphonate groups are largely responsible for the increase. This result is consistent with our hypothesis that the pendant phosphonate groups on the copolymer may help support mineralization of the ions deposited (e.g. hydroxyapatite) during differentiation.

Our data has presently focused on physiology of osteoblasts on polymer-coated silicon wafers which are essentially smooth surfaces. Since surface roughness is known to be influential in regulating osteoblast proliferation and differentiation on polymer surfaces[237-239] and metal surfaces,[220,240-242] similar experiments to the ones described on rough surfaces may reveal differences in osteoblast proliferation and differentiation.

## 4 Conclusion

The post-polymerization modification of PLLA-*co*-AG using olefin cross metathesis, and hydroboration-oxidation followed by the synthesis of ester using DCC coupling has proven to be an effective way to screen substrates for biological activity when tethered to biodegradable polymers such as PLLA. The synthetic ease with which the modification takes place coupled with the commercial availability and diversity of the functional side chains, make this modification widely applicable to the fields of tissue engineering and drug delivery. Furthermore, the initial experiments conducted on the physiological response to these functional copolymer surfaces appear to have potential in the design of *in vivo* biodegradable materials.

Regardless of the modification, the common objective throughout the described work is to design materials which will help regulate cell adhesion and influence the cell conformation, and consequently, the function of the biological system. We have

designed a protocol which will allow us to fulfill this objective. Post-polymerization modification has expanded the physiological utility of PLA in the area of tissue engineering.

# 5 Experimental Section.

## 5.1 General Considerations.

$^{1}H$ NMR spectra were recorded on Varian Gemini–300 and Inova–300 (299.9 MHz) and Varian Unity-500 (499.9 MHz) spectrometers and referenced to residual proton solvent signals. $^{13}C$ NMR spectra were recorded on Varian Gemini–300 and Inova–300 (75.4 MHz) and Varian Unity-500 (125.7 MHz) spectrometers and referenced to residual solvent signals. $^{31}P$ NMR spectra were recorded on a Varian Inova–300 (121.5 MHz) and referenced using $H_3PO_4$ as the external standard. $^{11}B$ NMR spectra were recorded on a Varian VXR–300 (160.6 MHz) and referenced using $BF_3.OEt_2$ as the external standard. $^{19}F$ NMR spectra were recorded on a Varian Inova–300 (289.4 MHz) and referenced using $CFCl_3$ as the external standard. Differential Scanning Calorimetry (DSC) analyses of the polymers were performed under a helium atmosphere at a heating rate of 10°C/min on a Perkin-Elmer DSC 7, with the temperature calibrated using an indium standard. The reported DSC curves are second heating scans, taken after an initial heating to erase thermal history, and a slow cooling to at 10°C/min to -50°C. Molecular weights of the polymers were determined by gel permeable chromatography (GPC) using a Beckman 100A instrument, equipped with a Waters 410 differential refractometer detector and a Waters 960 photodiode array detector. Measurements were obtained in THF with a PLgel 5 μ Mix column (Polymer Laboratories) at a flow rate of 1.0 mL/min at 35°C. Results were calibrated with monodisperse polystyrene standards. Polished silicon wafers purchased from WaferWorld™ were cleaned by immersion in a 70:30 volume ratio solution of concentrated $H_2SO_4$ (98% by mass) and $H_2O_2$ (30% by mass) and rinsed in deionized water. Polymers were dissolved in toluene (1% w/w),

filtered two times through 0.2 μm PTFE filters and spin-coated onto polished silicon wafers (1″ diameter) at a spin rate of 2500 rpm for 40 s. Ellipsometric measurements were obtained with a rotating analyzer ellipsometer (model M-44, J.A. Woollam) using WVASE32 software. The angle of incidence was 75° for all measurements. For the calculation of the film thickness, a film refractive index of 1.50 was used.

**Contact Angle Measurements.** After spin-coating the polymers onto silicon wafers, the wafers were held under vacuum at 40°C for 12 hours to ensure all the solvent was removed from the wafers. The polymer-coated wafers were kept at room temperature for 1 hour under a constant purge of nitrogen. Samples were heated under a nitrogen atmosphere at a rate of 10°C/min to 160°C (15°C above the melting point of the all polymer samples) and held for 1 minute. The samples were immediately removed from the oven and placed on a clean surface at room temperature. Advancing and receding contact angles were measured by dispensing a droplet of Milli-Q grade water (18 MΩ cm) at a rate of 3 μL/s to a total volume of 30 μL on the surface of polymer-coated silicon wafers. Contact angles were measured by capturing the image as a movie with a Sanyo® B/W CCD camera (model VC8 3512). The angles were measured using the FTA200 software.

**Cell Culture.** MC3T3-E1 osteoblasts (OBS) were plated on silicon discs (WaferWorld™) at a concentration of 4,400 cells/cm$^2$. These were either cultured for 2 days for the proliferation studies or 14 days for the differentiation studies, where at this stage OBS exhibit maximal levels of alkaline phosphatase and mineralization). Cells were fed every two days with α-MEM containing 2mM β-glycerolphosphate (Sigma, St. Louis, MO) and 25μg/ml ascorbic acid (Sigma).

**Cell Growth and Shape.** After plating for 48 hours, osteoblasts were incubated with 10 μM BrdU (5-Bromo-2'Deoxyuridine) (Sigma, St. Louis, MO) for two hours. Subsequently, cells were fixed with 70% ethanol. The cell culture plates were then spun at 1500 rpm for 5 minutes to ensure all cells remained at the bottom of the plate, followed by quick rinse with 1Xphosphate buffered solution (1XPBS). Cells were permealized with 4 N HCl in 1XPBS. Subsequently washed gently with 1 mL of 1XPBS until the PBS in the wells reached a pH=7. Osteoblasts were further incubated in 20% anti-BrdU (BD Biosciences, San Jose, CA) antibody solution, in 1XPBS, 0.5% BSA, 0.1% Tween-20, for 45 minutes at 37°C under humid conditions. Brdu antibody was removed and cells further introduced to propidium iodide stain at 200 μg/ml PBS (BD Biosciences, San Jose, CA) immediately after which nuclei of the cells were visualized by fluorescence microscopy and recorded with a digital camera. BrdU stains the nuclei at S phase of cell cycle, i.e. when cells are dividing, and therefore, used to determine cell growth. Propidium iodide stains all nuclei.

**Actin and Hoechst Stain.** Osteoblasts were fixed with 3.7% formaldehyde for 10 minutes at room temperature, 2 days after seeding, and subsequently permealized for 5minutes with 0.1% Triton X-100 in 1XPBS. Cells were blocked with 1% bovine serum albumin for 30 minutes and subsequently incubated for 20 minutes with rhodamine-pahlloidin (Molecular Probes Inc. Euegene, OR) and further incubated with at 10 μM stain in deionized $H_2O$, for 30 minutes. Actin localization and Hoechst stained (Molecular Probes Inc. Eugene, OR) nuclei were visualized by fluorescence microscopy and recorded with a digital camera.

**RNA Analysis.** RNA was extracted, on day 14, using TRI Reagent RNA isolation reagent (Molecular Research Center, Inc., Cincinnati, OH). Integrity of the RNA was verified by formaldehyde-agarose gel electrophoresis. Two-step quantitative RT-PCR was performed to verify gene expression. First strand cDNA was synthesized by reverse transcription of 2 μg RNA, using the Superscript II Kit and oligo d(T12-18) primers (Invitrogen Life Technologies, Carlsbad, CA). 1 μl of cDNA was amplified by Real Time PCR, by using the SYBR Green Core Reagents (PE Biosystems, Warrington, UK) and Taq DNA polymerase (Invitrogen Life Technologies, Carlsbad, CA) with a final volume of 25 μl. Genes associated with osteoblast differentiation, alkaline phosphatase, osteocalcin, and runx2, were analyzed using cyclophilin as the internal control. Real time PCR was carried out and analyzed for 40 cycles, using iCycler software (Biorad, Hecules, CA). Gel electrophoresis and melting curves were used to verify the integrity of a single PCR product (amplicon).

**Copolymer Degradation.** In a typical degradation, 0.20 g of polymer were suspended in 15 mL of ethanol and $Sn(Oct)_2$ (0.20 g, 0.49 mmol). The mixture was refluxed for 48 hours or until complete degradation as determined by $^1H$ NMR. The solution was then directly analyzed by GC/MS for the ethyl esters of L-lactic acid, 2-hydroxypent-4-enoic acid, and 2,7-dihydroxyl-oct-4-enoic-1,8-diacid (cross-link degradation product).

**Solvents.** Toluene, tetrahydrofuran, diethyl ether, and pentane were pre-dried over sodium and distilled from sodium/benzophenone ketyl. Dichloromethane was distilled from calcium hydride ($CaH_2$). All other reagents were used as received unless otherwise noted.

## 5.2 Synthesis

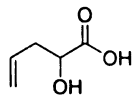

**2-Hydroxypent-4-enoic acid (2-HPA).**[243] Glyoxylic acid monohydrate (4.80 g, 0.053 mol) and freshly distilled allyl bromide (9.44 g, 0.078 mol) were added to a stirring suspension of zinc powder (7.12 g, 0.109 mol), and $BiCl_3$ (24.6 g, 0.078 mol) in 60 mL tetrahydrofuran. The reaction was initially kept at 0°C and allowed to warm to room temperature while stirring under $N_2$ for 16 h. After 16 h, the reaction is quenched with 40 mL of 1 M HCl, and the product is extracted with diethyl ether (3x80 mL). The organic phases were decanted from the solid, combined, and washed with saturated $NaCl_{(aq)}$ until the ether solution became colorless (5x20 mL). The ether layer was then dried over $MgSO_4$, and the solvent removed to give a colorless oil which crystallized under vacuum. The α-hydroxy acid was then recrystallized from $Et_2O$/Hexanes. Yield: 93%. $^1$H NMR (300 MHz, $CDCl_3$, δ): 5.65-5.85 (m, 1H, -$CHCH_2C\boldsymbol{H}$=$CH_2$), 5.0-5.2 (m, 2H, -$CHCH_2CH$=$C\boldsymbol{H_2}$), 4.27 (dd, 1H, $HO_2CC\boldsymbol{H}(OH)CH_2CH$=$CH_2$), 2.35-2.65 (m, 2H, -$CHC\boldsymbol{H_2}CH$=$CH_2$). $^{13}$C NMR (75.0 MHz, $CDCl_3$, δ): 177.3, 132.2, 118.8, 69.7, 38.2.

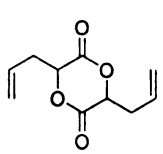

**3,6-Diallylglycolide (DAG).** 2-HPA (3.0 g, 0.025 mmol), and a catalytic amount (30 mg) of *p*-toluenesulfonic acid (pTsOH) were dissolved in 400 mL of toluene. The mixture was refluxed for 3 days and the water removed by Dean-Stark trap. After 3 days the mixture was cooled, washed 3 times with 10 mL saturated aqueous $NaHCO_3$ and the resultant oil distilled over ZnO under high vacuum at 80°C/0.01 mmHg. Gas

chromatography data indicates a statistical mixture of S/S, R/S, and R/R isomers of the diallylglycolide. Yield: 40%. $^1$H NMR (500MHz, $CDCl_3$, δ): 5.8 (m, 1H, -$CHCH_2C\boldsymbol{H}$=$CH_2$), 5.1-5.3 (m, 2H, -$CHCH_2CH$=$C\boldsymbol{H}_2$), 5.00 (dd, 1H, -$C\boldsymbol{H}CH_2CH$=$CH_2$, $J$ = 5.1 Hz), 4.91 (dd, 2H, *-$C\boldsymbol{H}CH_2CH$=$CH_2$, $J$ = 4.6 Hz), 2.60-2.90 (m, 4H, -$CHC\boldsymbol{H}_2CH$=$CH_2$). $^{13}$C NMR (125 MHz, $CDCl_3$, δ): *166.1, 164.8, *130.6, 129.8, 121.2, *120.0, 75.9, *75.1, 36.4, *34.1. LRMS (EI, *m/z*): 197 ($MH^+$), 98, 81, 54, 41. Anal. Calcd for $C_{10}H_{12}O_4$: C, 61.21; H, 6.18. Found: C, 61.29; H, 6.17. *Indicates RR/SS isomer. (Note: Using a combination of L-lactic acid and 2-HPA in the desired ratio under identical reaction conditions and workup results in a statistical mixture of L-lactide, 3-allyl-6-methylglycolide, and 3,6-diallylglycolide and appropriate stereoisomers.)

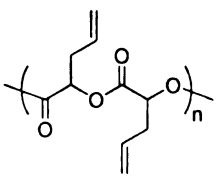

**Polymer Synthesis. Poly(diallylglycolide) (PDAG).** In a glovebox, diallylglycolide (0.163 g, 0.832 mmol) was combined in a Schlenk flask with tin(II)-2-ethylhexanoate (0.005 mmol) as the catalyst. The reaction tube was placed in an oil bath at 80°C and stirred for 72 h. The reaction mixture was pumped dry, dissolved in the minimal amount of $CH_2Cl_2$ and precipitated from cold methanol two times. Yield: 90%. $^1$H NMR (500 MHz, $CDCl_3$, δ): 5.8 (m, 1H, -$CHCH_2C\boldsymbol{H}$=$CH_2$), 5.0-5.2 (m, 3H, -$C\boldsymbol{H}CH_2CH$=$C\boldsymbol{H}_2$), 2.5-2.8 (m, 2H, -$C\boldsymbol{H}_2CH$=$CH_2$). $^{13}$C NMR (125 MHz, $CDCl_3$, δ): 168.1, 131.6, 119.1, 72.0, 35.2.

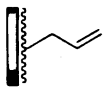

**Poly(L-lactide-*co*-diallylglycolide) (PLLA-*co*-AG).** In a typical synthesis of PLLA-*co*-AG, freshly sublimed L-lactide (2.88 g, 20 mmol) and distilled diallylglycolide (DAG) were combined in a glass tube with tin(II)-2-ethylhexanoate (0.067 mmol) and 4-*tert*-butylbenzylalcohol (BBA) (0.067 mmol) as the catalyst and initiator, respectively. The reaction tube was flame-sealed under vacuum and placed in an oil bath at 145°C. After 15 minutes, the sample was removed from the oil bath, cooled, and monitored for conversion. Crude $^1$H NMR revealed nearly complete conversion (> 90%). Polymers were dissolved in a minimal amount of $CH_2Cl_2$, and precipitated from cold methanol two times. Yield: 90%. $^1$H NMR (500 MHz, $CDCl_3$, δ): 5.8 (m, 1H, -CHCH$_2$C***H***=CH$_2$), 5.05-5.25 (q, *-C***H**(CH$_3$), -C***H***CH$_2$CH=C***H***$_2$), 2.5-2.8 (m, 2H, -C***H***$_2$CH=CH$_2$), 1.4-1.7 (d, *-CH(C***H**$_3$)). $^{13}$C NMR (125 MHz, $CDCl_3$, δ): *169.6, 168.4, 131.4, 119.1, 71.9, *69.0, 35.2, *16.6. *PLLA.

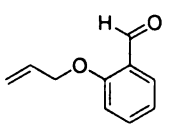


**2-(2-Propenyloxy)benzaldehyde.**[244] In a 500 mL round bottom flask, salicylaldehdye (14.6 g, 0.152 mol) and allyl bromide (23.0 g, 0.191 mol) were dissolved in 200 mL of acetone. Anhydrous potassium fluoride (35.4, 0.61 mol) was then added and the mixture refluxed for 72 h. After 72 h., the reaction mixture was filtered, then the solvent removed by rotary evaporation. The resultant oil was distilled twice at 75°C/0.1 mmHg to give pale yellow oil. Yield: 77%. $^1$H NMR (300 MHz, $CDCl_3$, δ): 10.5 (s, 1H, -C(O)***H***), 7.77 (dd, 1H, -***H***$_{Ar}$), 7.47 (m, 1H, -***H***$_{Ar}$), 6.9-7.0 (m, 2H, -***H***$_{Ar}$), 6.02 (m, 1H, -C***H***=CH$_2$), 5.24-5.44 (m, 2H, -CH=C***H***$_2$), 4.59 (q, 2H, -OC***H***$_2$CH=CH$_2$). $^{13}$C NMR

(75 MHz, $CDCl_3$, δ): 189.5, 160.7, 135.7, 132.2, 128.1, 124.8, 120.6, 117.8, 112.7, 68.9. LRMS (EI, *m/z*): 163 ($MH^+$), 161, 121.

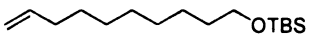


**9-Decenyl-1-oxy-*tert*-butyldimethylsilane.**[245] In an 250 mL Erlenmeyer flask, 9-decen-1-ol (2.0 g, 12.8 mmol) was dissolved in 25 mL $CH_2Cl_2$. To this solution was added Chloro-*tert*-butyldimethylsilane (2.12 g, 14.1 mmol) in 15 mL $CH_2Cl_2$. The reaction was stirred for 8 hours at room temperature under a nitrogen atmosphere. After 8 hours, the solvent is removed under rotary evaporation. The product was extracted with $Et_2O$, filtered and dried *in vacuo*. The oil was purified by flash column chromatography through silica gel using hexanes/EtOAc (96/4) as the eluent. The product was obtained as an oil. Yield: 95%. $^1H$ NMR (300 MHz, $CDCl_3$, δ): 5.79 (m, 1H, -C***H***=$CH_2$), 4.90-5.00 (m, 2H, -CH=C***H***$_2$), 3.58 (t, 2H, -OC***H***$_2C_9H_{17}$), 2.01 (q, 2H, -C***H***$_2$CH=$CH_2$), 1.49 (m, 2H, -$OCH_2$C***H***$_2C_8H_{15}$), 1.2-1.4 (m, 10H, -$(CH_2)_2$(C***H***$_2)_5CH_2$CH=$CH_2$), 0.874 (s, 6H, SiC(C***H***$_3)_3$), 0.027 (s, 6H, Si(C***H***$_3)_2$). $^{13}C$ NMR (75 MHz, $CDCl_3$, δ): 139.2, 114.1, 63.3, 33.8, 32.9, 29.5, 29.4, 29.1, 28.9, 26.0, 25.8, 18.4, -5.6. LRMS (EI, *m/z*): 271 ($MH^+$), 255, 214.

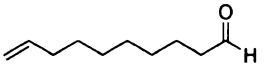


**9-Decen-1-al.**[246] In a round bottom flask, oxalyl chloride (13.35 mL, 0.0384 mol) was dissolved in $CH_2Cl_2$, and cooled to -78°C. DMSO (5.00 mL, 0.0704 mol) is slowly added neat via syringe and then stirred for 15 min. 9-decen-1-ol (5.0 g, 0.032 mol) in 10 mL of $CH_2Cl_2$ is added slowly, after which the reaction becomes cloudy. After stirring for 15 minutes, $NEt_3$ (22.6 g, 0.224 mol) is added via syringe and stirred for 10 minutes. The cold bath is removed and stirred to room temperature. The solvent is then removed

by rotary evaporation to give a yellow oil, which is first purified by flash chromatography through silica gel using hexanes as the eluent. The hexanes are removed by rotary evaporation. The oil is further purified by column chromatography using hexanes/EtOAc (80/20). Yield: 90%. $^1$H NMR (300 MHz, $CDCl_3$, δ): 9.57 (t, 1H, -C(O)***H***), 5.61 (m, 1H, -C***H***=$CH_2$), 4.68-4.86 (m, 2H, -CH=C***H***$_2$), 2.23 (m, 2H, -C***H***$_2$C(O)H), 1.85 (m, 2H, -C***H***$_2$CH=$CH_2$), 1.43 (m, 2H, -C***H***$_2$$CH_2$C(O)H), 1.05-1.25 (m, 8H, -(C***H***)$_4$$CH_2$CH=$CH_2$). $^{13}$C NMR (75 MHz, $CDCl_3$, δ): 202.8, 138.9, 114.1, 43.78, 33.64, 29.09, 28.98, 28.77, 28.69, 21.92. LRMS (EI, *m/z*): 155 ($MH^+$), 135, 121, 95, 81.

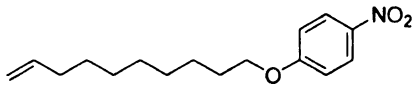


**9-decenyl-1-oxy-(4-*p*-nitrobenzene).** In a 500 mL round bottom flask, p-nitrophenol (2.0 g, 14.4 mmol), 9-decene-1-tosylate[247] (4.9 g, 15.8 mmol), $K_2CO_3$ (2.09 g, 15.12 mmol), and a catalytic amount of KI were refluxed for 2 days in 300 mL of dry acetone. After 2 days, the reaction is filtered and washed with $CH_2Cl_2$. The filtrate was concentrated, washed with saturated $NaHCO_3$, and extracted with $CH_2Cl_2$. The organic phases were then stirred with anhydrous $Na_2SO_4$, filtered, and the solvent removed to give an orange oil. The oil was purified by flash column chromatography through silica gel using Hexanes/EtOAc (97/3) as the eluent. The resultant yellow oil crystallized upon standing. Yield: 86%. $^1$H NMR (300 MHz, $CDCl_3$, δ): 8.13 (d, 2H, -***H***$_{Ar}$), 6.89 (d, 2H, -***H***$_{Ar}$), 5.76 (m, 1H, -C***H***=$CH_2$), 4.85-5.00 (m, 2H, -CH=C***H***$_2$), 4.00 (t, 2H, -OC***H***$_2$$C_9H_{17}$), 2.00 (q, 2H, -C***H***$_2$CH=$CH_2$), 1.78 (m, 2H, -$OCH_2$C***H***$_2$$C_8H_{15}$), 1.2-1.5 (m, 10H, -$(CH_2)_2$(C***H***$_2$)$_5$$CH_2$CH=$CH_2$). $^{13}$C NMR (75 MHz, $CDCl_3$, δ): 164.0, 141.0, 138.8, 125.6, 114.1, 113.9, 68.6, 33.5, 29.1, 29.0, 28.8, 28.7, 28.6, 25.6. LRMS (EI, *m/z*): 278 ($MH^+$),

232, 123. Anal. Calcd for $C_{16}H_{23}O_3N$: C, 69.27; H, 8.37; N, 5.05 Found: C, 69.23; H, 8.29; N, 5.13.

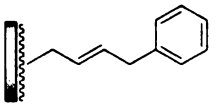

**PLLA-*g*-AB (AB = Allylbenzene).** In a small round-bottom flask, PLLA-*co*-AG was dissolved in $CH_2Cl_2$ (0.01 M) with approximately 5 equivalents of the olefin substrate. Grubbs' first or second generation ruthenium catalyst was added to the solution. An excess of olefin was introduced by a slow syringe pump addition (0.10 $mLh^{-1}$). Reaction was carried out for 24 h, quenched with ethyl vinyl ether and precipitated multiple times from hexanes and methanol. Yield: 90%. $^1H$ NMR (300 MHz, $CDCl_3$, δ): 7.5-7.1 (br, 5H, -$CH_2C_6\boldsymbol{H}_5$), 5.6-5.3 (br, 2H, -C***H***=C***H***-), 5.3-5.0 (m, *-C***H**($CH_3$), -C***H***($CH_2CH$=$CHC_7H_7$)), 3.33 (m, 2H, -C***H***$_2C_6H_5$), 2.8-2.5 (m, 2H, -C***H***$_2$CH=$CHC_7H_7$), 1.8-1.4 (m, *-CH(C***H**$_3$)). * PLLA.

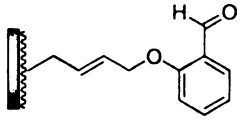


**PLLA-*g*-PB (PB = 2-(2-propenyloxy)benzaldehyde).** Polymer-bound olefin cross metathesis reaction conditions were identical to PLLA-*g*-AB. After 24 h, the reaction was quenched with ethyl vinyl ether and precipitated multiple times from methanol. Yield: 63%. $^1H$ NMR (300 MHz, $CDCl_3$, δ): 10.45 (s, 1H, -C(O)***H***), 7.80 (m, 1H, -***H***$_{Ar}$), 7.49 (m, 1H, -***H***$_{Ar}$), 7.1-6.9 (m, 2H, -***H***$_{Ar}$), 5.9-5.6 (m, 2H, -C***H***=C***H***), 5.3-5.0 (m, *-C***H**($CH_3$), -C***H***($CH_2CH$=$CHC_7H_7$)), 4.7-4.6 (m, 2H, -C***H***$_2OC_6H_4$(C(O)H)), 2.8-2.5 (m, 2H, -C***H***$_2$CH=$CHCH_2OC_6H_4$(C(O)H)), 1.8-1.4 (m, *-CH(C***H**$_3$)). * PLLA.

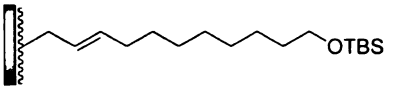


**PLLA-*g*-decenyloxy-TBS (Decenyloxy-TBS = 9-decen-1-oxy-*tert*-butyldimethylsilane).** Polymer-bound olefin cross metathesis reaction conditions were identical to PLLA-*g*-AB. After 24 h, the reaction was quenched with ethyl vinyl ether and precipitated from hexanes then precipitated from methanol. Yield: 26%. $^1$H NMR (300 MHz, $CDCl_3$, δ): 5.5-5.3 (br, 2H, -C***H***=C***H***$(CH_2)_8$OTBS), 5.3-5.0 (m, *-C***H**$(CH_3)$, -C***H***$(CH_2CH{=}CH(CH_2)_8$OTBS), 3.57 (t, 2H, -C***H***$_2$OTBS), 2.8-2.5 (m, 2H, -C***H***$_2CH{=}CH(CH_2)_8$OTBS), 1.96 (m, 2H, -CH=CHC***H***$_2C_7H_{14}$OTBS), 1.8-1.4 (m, *-CH(C***H**$_3$)), 1.26 (m, 12H, -(C***H***$_2)_6CH_2$OTBS), 0.868 (s, 9H, Si-C(C***H***$_3)_3$), 0.021 (s, 6H, Si(C***H***$_3)_2$. * PLLA.

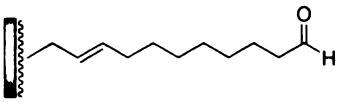


**PLLA-*g*-decenal.** Polymer-bound olefin cross metathesis reaction conditions were identical to PLLA-*g*-AB. After 24 h, the reaction was quenched with ethyl vinyl ether and precipitated from hexanes then precipitated from methanol. Yield: 48%. $^1$H NMR (300 MHz, $CDCl_3$, δ): 9.74 (m, 1H, -C(O)***H***), 5.5-5.3 (br, 2H, -C***H***=C***H***-$C_7H_{14}$C(O)H), 5.3-5.0 (m, *-C***H**$(CH_3)$, -C***H***$(CH_2CH{=}CH\ C_7H_{14}C(O)H)$), 2.9-2.5 (m, 2H, -C***H***$_2CH{=}CH$-), 2.39 (t, 2H, -C***H***$_2$C(O)H), 1.96 (m, 2H, -CH=CHC***H***$_2C_6H_{12}$C(O)H), 1.8-1.4 (m, *-CH(C***H**$_3$)). 1.26 (m, 10H, -(C***H***$_2)_5CH_2$C(O)H). * PLLA.

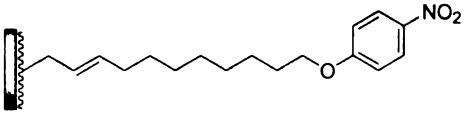


**PLLA-*g*-decenyloxy- NB (Decenyloxy- NB = 9-decenyl-1-oxy-(4-nitrobenzene).** The polymer-bound olefin cross metathesis reaction conditions were

identical to PLLA-*g*-AB. After 24 h, the reaction was quenched with ethyl vinyl ether and precipitated from hexanes then precipitated from methanol. Yield: 79%. $^1$H NMR (300 MHz, $CDCl_3$, δ): 8.17 (d, 2H, -$\boldsymbol{H}_{Ar}$), 6.92 (d, 2H, -$\boldsymbol{H}_{Ar}$), 5.6-5.2 (br, 2H, -C$\boldsymbol{H}$=C$\boldsymbol{H}$), 5.3-5.0 (m, *-C$\boldsymbol{H}$($CH_3$), -C$\boldsymbol{H}$($CH_2CH$=$CH(CH_2)_8OC_6H_4(NO_2)$), 4.02 (t, 2H, -$C\boldsymbol{H}_2OC_6H_4(NO_2)$), 2.8-2.5 (m, 2H, -$C\boldsymbol{H}_2CH$=$CH(CH_2)_8OC_6H_4(NO_2)$), 1.96 (m, 2H, -$CH$=$CHC\boldsymbol{H}_2C_7H_{14}OC_6H_4(NO_2)$), 1.79 (m, 2H, -$C\boldsymbol{H}_2C_6H_{12}OC_6H_4(NO_2)$), 1.7-1.4 (m, *-$CH(C\boldsymbol{H}_3)$), 1.30 (m, 10H, -$(C\boldsymbol{H}_2)_5CH_2OC_6H_4(NO_2)$). * PLLA.

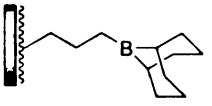


**Hydroboration of PLLA-*co*-AG.** The hydroborated copolymer was monitored using $^{11}$B NMR (160 MHz). In an NMR tube reaction, PLLA-*co*-AG (0.137 g, 2.59 $mmolg^{-1}$, 0.355 mmol) was dissolved in $CDCl_3$, after which 9-BBN (0.417 g, 0.342 mmol) was added. The reaction was gently warmed at 35°C for 2h. A broad resonance centered at 88 δ in the $^{11}$B NMR spectrum indicated a trialkylboron moiety and therefore, confirming the hydroboration step.

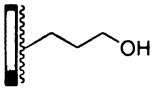


**PLLA-*g*-HP (Hydroboration-Oxidation of PLLA-*co*-AG).** In a round bottom flask, PLLA-*co*-AG (4.05 g, 1.19 $mmolg^{-1}$, 4.82 mmol) was dissolved in 100 mL of dry THF. 9-BBN (9.73 mL, 0.50 M, 4.87 mmol) was slowly added to the polymer solution *via* syringe and stirred at room temperature for 1.5 h. The reaction was then cooled to 0°C and a 1 M aqueous solution of sodium acetate (9.64 mL, 9.64 mmol) and a 30% solution of $H_2O_2$ (1.09 g, 9.64 mmol) were added. The mixture was and stirred for 13 h. The reaction was quenched with 2 M HCl (9.64 mmol) and the polymer solution dried by

rotary evaporation. The polymer was then redissolved in $CH_2Cl_2$ and further extracted from water and dried over $Na_2SO_4$. The polymer filtrate was concentrated and precipitated from methanol two times. The polymer was filtered and dried under vacuum. Avg. Yield (4 times): 60%. $^1$H NMR (300 MHz, $CDCl_3$, δ): 5.25-5.00 (q, *-C***H**$(CH_3)$, -C***H***$CH_2CH_2CH_2OH$), 3.66 (m, 2H, -$(CH_2)_2$C***H***$_2$OH), 2.04 (m, 2H, -C***H***$_2(CH_2)_2OH$), 1.68 (m, 2H, -$CH_2$C***H***$_2CH_2OH$), 1.6-1.4 (d, *-CH(C***H**$_3$)). $^{13}$C NMR (75 MHz, $CDCl_3$, δ): *169.6, 72.5, *69.0, 61.8, 27.7, 27.4, *16.6. * PLLA.

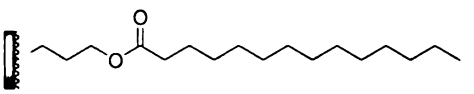

**PLLA-*g*-MyPr (MyPr = Myristic acid propyl ester).** A small round bottom flask containing PLLA-*g*-HP (0.352 g, 0.950 mmolg$^{-1}$, 0.333 mmol), myristic acid (0.114 g, 0.50 mmol), and DMAP (8.0 mg, 0.066 mmol) was stirred in 10 mL of $CH_2Cl_2$ until completely dissolved. 1,3-Dicyclohexylcarbodiimide (DCC) (0.50 mL, 1.0 M, 0.50 mmol) was then added *via* syringe and the reaction mixture was stirred under $N_2$ at room temperature. (Note: After 15 minutes, the colorless, homogeneous solution became cloudy, indicative of the esterification). After 12 h, the reaction mixture was filtered to remove the insoluble dicyclohexyl urea byproduct, further concentrated, and filtered a second time to fully remove the urea. The filtrate was then concentrated to dryness, redissolved in the minimal amount of $CH_2Cl_2$, precipitated and centrifuged from methanol two times. The polymer was filtered and dried under vacuum. Avg. Yield (2 times): 89%. $^1$H NMR (300 MHz, $CDCl_3$, δ): 5.2-5.0 (q, *-C***H**$(CH_3)$, -C***H***$(CH_2)_3CO_2C_{13}H_{27}$), 4.06 (m, 2H, -C***H***$_2CO_2C_{13}H_{27}$), 2.24 (td, 2H, -$CO_2$C***H***$_2C_{12}H_{25}$), 1.95 (m, 2H, -C***H***$_2(CH_2)_2CO_2C_{13}H_{27}$), 1.75 (m, 2H, -$CH_2$C***H***$_2CH_2CO_2C_{13}H_{27}$), 1.6-1.5 (m, 2H, -$CO_2CH_2$C***H***$_2C_{11}H_{23}$), 1.56 (d, *-CH(C***H**$_3$)), 1.23 (m, 20H, -(C***H***$_2)_{10}CH_3$), 0.855

(t, 3H, -$(CH_2)_{12}CH_3$). $^{13}C$ NMR (75 MHz, $CDCl_3$, δ): 173.7, *169.6, 72.1, *69.0, 63.2, 34.2, 33.9, 31.9, 29.6, 29.5, 29.4, 29.3, 29.2, 27.7, 24.9, 24.8, 24.2, 22.7, *16.6, 14.1. * PLLA.

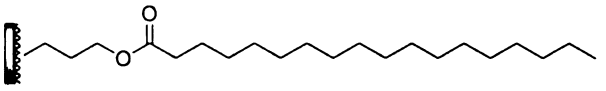

**PLLA-*g*-StPr (StPr = Stearic acid propyl ester).** The polymer-bound DCC coupling procedure was identical to PLLA-*g*-MyPr. Avg. Yield (3 times): 88%. $^1H$ NMR (300 MHz, $CDCl_3$, δ): 5.2-5.0 (q, *-C***H**$(CH_3)$, -C**H**$(CH_2)_3CO_2C_{17}H_{35}$), 4.06 (m, 2H, -C**H**$_2CO_2C_{17}H_{35}$), 2.27 (td, 2H, -$CO_2$C**H**$_2C_{16}H_{33}$), 1.95 (m, 2H, -C**H**$_2(CH_2)_2CO_2C_{17}H_{35}$), 1.75 (m, 2H, -$CH_2$C**H**$_2CH_2CO_2C_{18}H_{37}$), 1.6-1.5 (d, *-CH(C**H**$_3$), -$CO_2CH_2$C**H**$_2C_{15}H_{31}$), 1.23 (m, 28H, -(C**H**$_2)_{14}CH_3$), 0.856 (t, 3H, -$(CH_2)_{16}$C**H**$_3$). $^{13}C$ NMR (75 MHz, $CDCl_3$, δ): 173.7, *169.6, 72.2, *69.0, 63.2, 34.2, 33.9, 31.9, 29.7, 29.5, 29.3, 29.2, 29.1, 27.6, 24.9, 24.7, 24.2, 22.7, *16.6, 14.1. * PLLA.

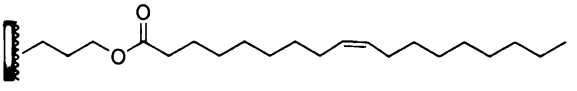

**PLLA-*g*-OlPr (OlPr = Oleic acid propyl ester).** The polymer-bound DCC coupling procedure was identical to PLLA-*g*-MyPr. Avg. Yield (2 times): 89%. $^1H$ NMR (300 MHz, $CDCl_3$, δ): 5.32 (m, 2H, -C**H**=C**H**), 5.2-5.0 (q, *-C**H**$(CH_3)$, -C**H**$(CH_2)_3CO_2C_{17}H_{33}$), 4.06 (m, 2H, -C**H**$_2CO_2C_{17}H_{33}$), 2.27 (td, 2H, -$CO_2$C**H**$_2C_{16}H_{31}$), 1.98 (m, 6H, -C**H**$_2CH_2CH_2CO_2C_{17}H_{33}$, -(C**H**$_2$)(CH=CH)(C**H**$_2$)), 1.75 (m, 2H, -$CH_2$C**H**$_2CH_2CO_2C_{17}H_{33}$), 1.6-1.5 (d, *-CH(C**H**$_3$), -$CO_2CH_2$C**H**$_2C_{15}H_{29}$), 1.27-1.24 (m, 20H, -(C**H**$_2)_4(CH_2)$(CH=CH)$(CH_2)$(C**H**$_2)_6CH_3$), 0.855 (t, 3H, -$(CH_2)_6$C**H**$_3$). $^{13}C$ NMR (75 MHz, $CDCl_3$, δ): 173.7, *169.5, 129.9, 129.7, 72.2, *69.0, 63.2, 34.2, 33.8, 31.8,

29.7, 29.6, 29.5, 29.3, 29.2, 29.1, 27.6, 27.2, 27.1, 24.9, 24.7, 24.2, 22.6, *16.6, 14.1. * PLLA.

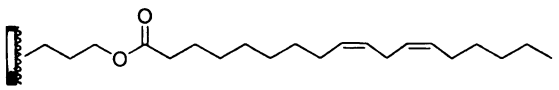

**PLLA-*g*-LnPr (LnPr = Linoleic acid propyl ester).** The polymer-bound DCC coupling procedure was similar to PLLA-*g*-MyPr. This polymer can be oxidized, and therefore should be carried out and worked up in an inert atmosphere where exposure to oxygen is minimal. Avg. Yield (3 times): 81%. $^{1}$H NMR (300 MHz, $CDCl_3$, δ): 5.35 (m, 4H, -C***H***=C***H***-($CH_2$)-C***H***=C***H***), 5.2-5.0 (q, *-C***H**($CH_3$), -C***H***($(CH_2)_3CO_2C_{17}H_{31}$), 4.06 (m, 2H, -C***H***$_2CO_2C_{17}H_{31}$), 2.75 (t, 2H, =CH-(C***H***$_2$)-CH), 2.4-2.2 (m, 2H, -$CO_2$C***H***$_2C_{16}H_{29}$), 2.02 (m, 6H, -C***H***$_2CH_2CH_2CO_2C_{17}H_{31}$, -C***H***$_2(C_5H_6)$C***H***$_2$), 1.76 (m, 2H, -$CH_2$C***H***$_2CH_2CO_2C_{17}H_{31}$), 1.6-1.5 (d, *-CH(C***H***$_3$), -$CO_2CH_2$C***H***$_2C_{15}H_{27}$), 1.29 (m, 14H, -(C***H***$_2)_4(CH_2)(C_5H_6)(CH_2)$(C***H***$_2)_3CH_3$), 0.866 (t, 3H, -$(CH_2)_6$C***H***$_3$). $^{13}$C NMR (75 MHz, $CDCl_3$, δ): 173.7, *169.6, 130.2, 130.0, 128.0, 127.9, 72.2, *69.0, 63.2, 34.2, 32.5, 31.5, 29.6, 29.3, 29.5, 29.3, 29.2, 29.1, 27.6, 27.2, 25.6, 24.8, 24.2, 22.5, *16.6, 14.0. * PLLA.

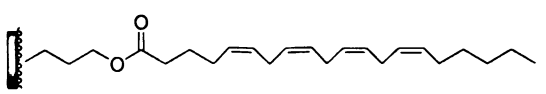

**PLLA-*g*-ArPr (ArPr = Arachidonic acid propyl ester).** The polymer-bound DCC coupling procedure was similar to PLLA-*g*-LnPr. This polymer can be oxidized, and therefore should be carried out and worked up in an inert atmosphere where exposure to oxygen is minimal. Avg. Yield (3 times): 84%. $^{1}$H NMR (300 MHz, $CDCl_3$, δ): 5.35 (m, 8H, -(C***H***=C***H***-$CH_2)_3$C***H***=C***H***), 5.2-5.0 (q, *-C***H**($CH_3$), -C***H***($(CH_2)_3CO_2C_{19}H_{31}$), 4.06 (m, 2H, -C***H***$_2CO_2C_{19}H_{31}$), 2.79 (m, 6H, -(CH=CH-C***H***$_2)_3$), 2.4-2.2 (m, 2H, -$CO_2$C***H***$_2C_{18}H_{29}$), 2.15-1.9 (m, 6H, -C***H***$_2CH_2CH_2CO_2C_{19}H_{31}$, -C***H***$_2$(CH=CH-

$CH_2)_3(CH{=}CH)C\boldsymbol{H}_2)$, 1.8-1.6 (m, 4H, $-CO_2CH_2C\boldsymbol{H}_2C_{17}H_{27}$, $-CH_2C\boldsymbol{H}_2CH_2CO_2C_{19}H_{31}$), 1.6-1.5 (d, *$-CH(C\boldsymbol{H}_3)$), 1.28 (m, 6H, $-(C\boldsymbol{H}_2)_3CH_3$), 0.865 (t, 3H, $-(CH_2)_4C\boldsymbol{H}_3$). $^{13}C$ NMR (75 MHz, $CDCl_3$, δ): 173.4, *169.6, 130.46, 128.85, 128.57, 128.22, 128.17, 128.12, 127.83, 127.52, 72.1, *69.0, 63.3, 33.58, 33.54, 33.25, 31.48, 29.29, 27.63, 27.19, 26.55, 26.44, 25.60, 24.76, 24.63, 24.20, 22.54, *16.6, 14.0. * PLLA.

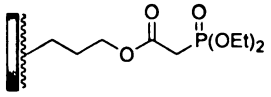


**PLLA-*g*-DPAPr (DPAPr = Diethylphosphonoacetic acid propyl ester).** In a small round bottom flask, PLLA-*g*-HP (0.500 g, 1.31 $mmolg^{-1}$, 0.655 mmol), diethyphosphonoacetic acid (0.141 g, 0.720 mmol) and DMAP (16 mg, 0.131 mmol) were stirred in 10 mL of $CH_2Cl_2$ until completely dissolved. 1,3-Dicyclohexylcarbodiimide (DCC) (0.720 mL, 1.0 M, 0.720 mmol) was then added *via* syringe and the reaction mixture is stirred under $N_2$ at room temperature. (Note: After 15 minutes, the colorless, homogeneous solution became cloudy, indicative of the esterification). After 12 h, the reaction mixture was filtered to remove the insoluble dicyclohexyl urea byproduct, further concentrated, and filtered a second time to fully remove the urea. The filtrate was then concentrated to dryness, redissolved in the minimal amount of $CH_2Cl_2$, precipitated and centrifuged from methanol two times. Avg. Yield (3 times): 88%. $^1H$ NMR (300 MHz, $CDCl_3$, δ): 5.2-5.0 (m, *$-C\boldsymbol{H}(CH_3)$, $-C\boldsymbol{H}(CH_2)_3CO_2CH_2P(=O)(OEt)_2)$, 4.14 (m, 6H, $-C\boldsymbol{H}_2CO_2CH_2P(=O)(OC\boldsymbol{H}_2CH_3)_2)$, 2.94 (d, 2H, $-C\boldsymbol{H}_2P(=O)(OEt)_2$, $J_{P\text{-}H}$ = 22 Hz), 1.99 (m, 2H, $-C\boldsymbol{H}_2(CH_2)_2CO_2CH_2P(=O)(OEt)_2)$, 1.78 (m, 2H, $-CH_2C\boldsymbol{H}_2CH_2CO_2CH_2P(=O)(OEt)_2)$, 1.6-1.4 (d, *$-CH(C\boldsymbol{H}_3)$), 1.4-1.2 (t, 6H, $-P(=O)(OCH_2C\boldsymbol{H}_3)$. $^{13}C$ NMR (75 MHz, $CDCl_3$, δ): *169.5, 169.2, 165.7 ($J_{P\text{-}C}$ = 5.8

Hz), 72.0, 69.0, 64.5, 62.7 ($J_{P\text{-}C}$ = 6.3 Hz), 34.2 ($J_{P\text{-}C}$ = 134.6 Hz), 27.4, 24.0, *16.6, 16.3 ($J_{P\text{-}C}$ = 5.9 Hz). $^{31}$P NMR (121 MHz, $CDCl_3$, δ): 20.2. * PLLA.

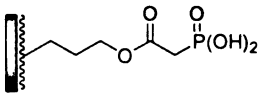


**PLLA-*g*-PAPr (Phosphonoacetic acid propyl ester).** In a small vial PLLA-*g*-DPAPr (0.355 g, 0.665 mmolg$^{-1}$, 0.236 mmol) was dissolved in 3 mL of $CH_2Cl_2$. Bromotrimethylsilane (0.361 g, 2.36 mmol) was added *via* syringe and stirred at room temperature for 8 hours. The solution was concentrated and precipitated from aqueous methanol/water (90/10 v/v) two times. The polymer was then filtered and dried. Avg. Yield (3 times): 71%. $^1$H NMR (300 MHz, $CDCl_3$, δ): 5.2-5.0 (m, *-C***H**($CH_3$), C***H***($CH_2$)$_3$$CO_2CH_2PO_3H_2$), 4.17 (m, 2H, ($CH_2$)$_2$C***H***$_2CO_2CH_2PO_3H_2$), 3.00 (d, 2H, C***H***$_2PO_3H_2$), 1.98 (m, 2H, -C***H***$_2$($CH_2$)$_2$$CO_2CH_2PO_3H_2$), 1.78 (m, 2H, -$CH_2$C***H***$_2CH_2CO_2CH_2P$(=O)(OEt)$_2$), 1.6-1.4 (d, *-CH(C***H***$_3$)). $^{13}$C NMR (75 MHz, $d_6$-DMSO, δ): *169.2, 166.9 ($J_{P\text{-}C}$ = 6.0 Hz), 72.0, *68.7, 63.6, 36.5 ($J_{P\text{-}C}$ = 127.8 Hz), 27.1, 23.6, *16.5. $^{31}$P NMR (121 MHz, $CDCl_3$, δ): 23.3.

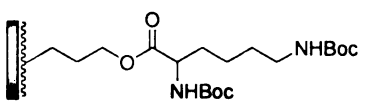


**PLLA-*g*-BocLysPr (BocLysPr = N,N′-Di-Boc-lysine propyl ester).** In a small round bottom flask, PLLA-*g*-HP (0.470 g, 1.31 mmolg$^{-1}$, 0.616 mmol), N,N′-di-Boc-lysine (0.256 g, 0.740 mmol) and DMAP (15 mg, 0.123 mmol) were stirred in 10 mL of $CH_2Cl_2$ until completely dissolved. 1,3-Dicyclohexylcarbodiimide (DCC) (0.740 mL, 1.0 M, 0.740 mmol) was then added *via* syringe and the reaction mixture is stirred under $N_2$ at room temperature. (Note: After 15 minutes, the colorless, homogeneous solution became cloudy, indicative of the esterification). After 12 h, the reaction mixture was

filtered to remove the insoluble dicyclohexyl urea byproduct, further concentrated, and filtered a second time to fully remove the urea. The filtrate was then concentrated to dryness, redissolved in the minimal amount of $CH_2Cl_2$, precipitated and centrifuged from methanol two times. Avg. Yield (3 times): 70%. $^1$H NMR (300 MHz, $CDCl_3$, δ): 5.2-5.0 (m, *-C***H**($CH_3$), -C***H***($(CH_2)_3CO_2$Lys(Boc)$_2$), 4.66 (m, 1H, -$CH_2$N***H***Boc), 4.23 (m, 1H, -$(CH_2)_3CO_2$C***H***(NHBoc)$(CH_2)_4$NHBoc), 4.12 (m, 2H, -$(CH_2)_2$C***H***$_2CO_2$Lys(Boc)$_2$), 3.07 (d, 2H, -C***H***$_2$NHBoc), 1.97 (m, 2H, -C***H***$_2(CH_2)_2CO_2$Lys(Boc)$_2$), 1.77 (m, 2H, -$CH_2$C***H***$_2CH_2CO_2$Lys(Boc)$_2$), 1.7-1.5 (d, *-CH(C***H**$_3$)), 1.41 (s, 18H, -C(C***H**$_3$)$_3$), 1.7-1.3 (s, 6H, -(C***H**$_2$)$_3CH_2$NHBoc). $^{13}$C NMR (75 MHz, $CDCl_3$, δ): 172.7, *169.6, 156.1, 155.5, 79.8, 79.0, 72.0, *69.0, 64.2, 53.3, 40.1, 32.3, 29.6, 28.4, 28.3, 27.5, 24.1, 22.5, 22.1, *16.6. * PLLA.

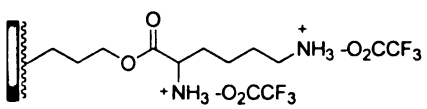


**PLLA-*g*-LysTFAPr (LysTFAPr = lysine bis(trifluoroacetate) propyl ester).** In a small round bottom flask, PLLA-*g*-BocLysPr (0.150 g, 1.31 mmolg$^{-1}$, 0.616 mmol) was dissolved in 4 mL of $CH_2Cl_2$. Trifluoroacetic acid (1.0 mL, 12.98 mmol) was added (20% v/v) and the solution stirred for 25 minutes, at which point the solution became slightly turbid. The solution was then directly precipitated into an aqueous solution containing a ten-fold excess of $NaHCO_3$ (Note: Precipitation into the basic solution must be performed slowly as $CO_2$ is evolved). The polymer was centrifuged from water 3 times to give the pure polymer as the ammonium salt. Avg. Yield (2 times): 95%. $^1$H NMR (300 MHz, $d_8$-thf, δ): 5.3-5.0 (m, *-C***H**($CH_3$), -C***H***($(CH_2)_3CO_2$Lys-$NH_3$(TFA)), 4.20 (m, 2H, -C***H***$_2CO_2$Lys-$NH_3$(TFA)), 3.81 (m, 1H, -$(CH_2)_3CO_2$C***H***($NH_3$(TFA))$(CH_2)_4NH_3$(TFA)), 2.98 (m, 2H, -

$CO_2CH(NH_3(TFA))(CH_2)_3C\boldsymbol{H}_2NH_3(TFA))$, 1.99 (m, 2H, $-C\boldsymbol{H}_2(CH_2)_2CO_2Lys-NH_3(TFA)$), 1.83 (m, 2H, $-CH_2C\boldsymbol{H}_2CH_2CO_2Lys-NH_3(TFA)$), 1.9-1.3 (m, *-$CH(C\boldsymbol{H}_3)$, 6H, $-(C\boldsymbol{H}_2)_3CH_2NH_3(TFA)$). $^{13}C$ NMR (75 MHz, $d_8$-thf, δ): *170.1, 162.3 ($J_{C-F}$ = 33.2 Hz), 118.0 ($J_{C-F}$ = 292 Hz), *69.7, 53.9, 39.8, 31.9, 28.5, 27.6, 22.7, 20.9, *16.9. $^{19}F$ NMR (289 MHz, $d_8$-thf, δ): -76.8. * PLLA.

## 6 References


(1) Mrksich, M. *Current Opinion in Chemical Biology* **2002**, *6*, 794-797.

(2) Sinclair, R. G. *J. Macromol. Sci.-Pure Appl. Chem.* **1996**, *A33*, 585-597.

(3) Drumright, R. E.; Gruber, P. R.; Henton, D. E. *Adv. Mater.* **2000**, *12*, 1841-1846.

(4) Datta, R.; Tsai, S. P. *Fuels and Chemicals from Biomass* **1997**, *666*, 224-236.

(5) Waris, T.; Pohjonen, T.; Tormala, P. *Eur. J. Plast. Surg.* **1994**, *17*, 236-238.

(6) Hofmann, G. O. *Arch. Orthop. Trauma Surg.* **1995**, *114*, 123-132.

(7) Tormala, P.; Rokkanen, P. *Ann. Chir. Gynaecol.* **2001**, *90*, 81-85.

(8) Bos, R. R. M.; Rozema, F. R.; Boering, G.; Nijenhuis, A. J.; Pennings, A. J.; Verwey, A. B.; Nieuwenhuis, P.; Jansen, H. W. B. *Biomaterials* **1991**, *12*, 32-36.

(9) Ogawa, Y. *J. Biomater. Sci.-Polym. Ed.* **1997**, *8*, 391-409.

(10) Davis, S. S.; Illum, L.; Stolnik, S. *Curr. Opin. Colloid Interface Sci.* **1996**, *1*, 660-666.

(11) Langer, R. *Accounts Chem. Res.* **2000**, *33*, 94-101.

(12) Uhrich, K. E.; Cannizzaro, S. M.; Langer, R. S.; Shakesheff, K. M. *Chem. Rev.* **1999**, *99*, 3181-3198.

(13) Hutmacher, D. W. *Biomaterials* **2000**, *21*, 2529-2543.

(14) Agrawal, C. M.; Athanasiou, K. A.; Heckman, J. D. In *Porous Materials For Tissue Engineering*, 1997; Vol. 250, pp 115-128.

(15) Chen, G. P.; Ushida, T.; Tateishi, T. *Macromol. Biosci.* **2002**, *2*, 67-77.

(16) Yang, S. F.; Leong, K. F.; Du, Z. H.; Chua, C. K. *Tissue Engineering* **2001**, *7*, 679-689.

(17) Yang, S. F.; Leong, K. F.; Du, Z. H.; Chua, C. K. *Tissue Engineering* **2002**, *8*, 1-11.

(18) Maquet, V.; Jerome, R. *Porous Materials for Tissue Engineering* **1997**, *250*, 15-42.

(19) Middleton, J. C.; Tipton, A. J. *Biomaterials* **2000**, *21*, 2335-2346.

(20) Shalaby, S. W.; Johnson, R. A. In *Biomedical Polymers: Designed to Degrade Systems*; Shalaby, S. W., Ed.; Hanson Publishers: New York, 1994, pp 1-34.

(21) Perrin, D. E.; English, J. P. In *Handbook of Biodegradable Polymers*; Domb, A. J., Kost, J., Wiseman, D. M., Eds.; Harwood Academic Publishers: New York, 1997, pp 3-27.

(22) Ostuni, E.; Yan, L.; Whitesides, G. M. *Colloid Surf. B-Biointerfaces* **1999**, *15*, 3-30.

(23) Mrksich, M.; Whitesides, G. M. In *Poly(Ethylene Glycol)*; AMER CHEMICAL SOC: Washington, 1997; Vol. 680, pp 361-373.

(24) Luk, Y. Y.; Kato, M.; Mrksich, M. *Langmuir* **2000**, *16*, 9604-9608.

(25) Houseman, B. T.; Mrksich, M. *Angewandte Chemie-International Edition* **1999**, *38*, 782-785.

(26) Roberts, C.; Chen, C. S.; Mrksich, M.; Martichonok, V.; Ingber, D. E.; Whitesides, G. M. *Journal of the American Chemical Society* **1998**, *120*, 6548-6555.

(27) Houseman, B. T.; Mrksich, M. *Biomaterials* **2001**, *22*, 943-955.

(28) Ostuni, E.; Grzybowski, B. A.; Mrksich, M.; Roberts, C. S.; Whitesides, G. M. *Langmuir* **2003**, *19*, 1861-1872.

(29) Pardo, L.; Wilson, W. C.; Boland, T. J. *Langmuir* **2003**, *19*, 1462-1466.

(30) Tan, J. L.; Tien, J.; Chen, C. S. *Langmuir* **2002**, *18*, 519-523.

(31) Blawas, A. S.; Reichert, W. M. *Biomaterials* **1998**, *19*, 595-609.

(32) Taguchi, T.; Kishida, A.; Sakamoto, N.; Akashi, M. *J. Biomed. Mater. Res.* **1998**, *41*, 386-391.

(33) Chen, G.; Ito, Y.; Imanishi, Y.; Magnani, A.; Lamponi, S.; Barbucci, R. *Bioconjugate Chemistry* **1997**, *8*, 730-734.

(34) Ozawa, N.; Yao, T. *J. Biomed. Mater. Res.* **2002**, *62*, 579-586.

(35) Liu, G. Y.; Amro, N. A. *Proc. Natl. Acad. Sci. U. S. A.* **2002**, *99*, 5165-5170.

(36) Gallant, N. D.; Capadona, J. R.; Frazier, A. B.; Collard, D. M.; Garcia, A. J. *Langmuir* **2002**, *18*, 5579-5584.

(37) Detrait, E.; Lhoest, J. B.; Knoops, B.; Bertrand, P.; de Aguilar, P. V. D. *J. Neurosci. Methods* **1998**, *84*, 193-204.

(38) Patel, N.; Padera, R.; Sanders, G. H. W.; Cannizzaro, S. M.; Davies, M. C.; Langer, R.; Roberts, C. J.; Tendler, S. J. B.; Williams, P. M.; Shakesheff, K. M. *Faseb Journal* **1998**, *12*, 1447-1454.

(39) Patel, N.; Bhandari, R.; Shakesheff, K. M.; Cannizzaro, S. M.; Davies, M. C.; Langer, R.; Roberts, C. J.; Tendler, S. J. B.; Williams, P. M. *Journal of Biomaterials Science-Polymer Edition* **2000**, *11*, 319-331.

(40) Ghosh, P.; Amirpour, M. L.; Lackowski, W. M.; Pishko, M. V.; Crooks, R. M. *Angewandte Chemie-International Edition* **1999**, *38*, 1592-1595.

(41) Chen, C. S.; Mrksich, M.; Huang, S.; Whitesides, G. M.; Ingber, D. E. *Science* **1997**, *276*, 1425-1428.

(42) Ingber, D. *Faseb J.* **1999**, *13*, S3-S15.

(43) Dike, L. E.; Chen, C. S.; Mrksich, M.; Tien, J.; Whitesides, G. M.; Ingber, D. E. *In Vitro Cell. Dev. Biol.-Anim.* **1999**, *35*, 441-448.

(44) Lee, K. Y.; Mooney, D. J. *Chemical Reviews* **2001**, *101*, 1869-1879.

(45) Woodfield, T. B. F.; Bezemer, J. M.; Pieper, J. S.; van Blitterswijk, C. A.; Riesle, J. *Crit. Rev. Eukaryot. Gene Expr.* **2002**, *12*, 209-236.

(46) Mooney, D. J.; Baldwin, D. F.; Suh, N. P.; Vacanti, L. P.; Langer, R. *Biomaterials* **1996**, *17*, 1417-1422.

(47) Harris, L. D.; Kim, B. S.; Mooney, D. J. *J. Biomed. Mater. Res.* **1998**, *42*, 396-402.

(48) Nam, Y. S.; Yoon, J. J.; Park, T. G. *Journal of Biomedical Materials Research* **2000**, *53*, 1-7.

(49) Yoon, J. J.; Park, T. G. *J. Biomed. Mater. Res.* **2001**, *55*, 401-408.

(50) Zhang, R. Y.; Ma, P. X. *J. Biomed. Mater. Res.* **1999**, *44*, 446-455.

(51) Zhang, R. Y.; Ma, P. X. *J. Biomed. Mater. Res.* **1999**, *45*, 285-293.

(52) Kiyotani, T.; Teramachi, M.; Takimoto, Y.; Nakamura, T.; Shimizu, Y.; Endo, K. *Brain Res.* **1996**, *740*, 66-74.

(53) Cooper, M. L.; Hansbrough, J. F.; Spielvogel, R. L.; Cohen, R.; Bartel, R. L.; Naughton, G. *Biomaterials* **1991**, *12*, 243-248.

(54) Saxena, A. K.; Marler, J.; Benvenuto, M.; Willital, G. H.; Vacanti, J. P. *Tissue Eng.* **1999**, *5*, 525-531.

(55) Kim, B. S.; Baez, C. E.; Atala, A. *World Journal of Urology* **2000**, *18*, 2-9.

(56) Brown, A. N.; Kim, B. S.; Alsberg, E.; Mooney, D. J. *Tissue Eng.* **2000**, *6*, 297-305.

(57) Mooney, D. T.; Mazzoni, C. L.; Breuer, C.; McNamara, K.; Hern, D.; Vacanti, J. P.; Langer, R. *Biomaterials* **1996**, *17*, 115-124.

(58) Dunn, M. G.; Bellincampi, L. D.; Tria, A. J.; Zawadsky, J. P. *J. Appl. Polym. Sci.* **1997**, *63*, 1423-1428.

(59) Chen, G. P.; Ushida, T.; Tateishi, T. *Chem. Lett.* **1999**, 561-562.

(60) Bessho, K.; Carnes, D. L.; Cavin, R.; Ong, J. L. *J. Biomed. Mater. Res.* **2002**, *61*, 61-65.

(61) Eid, K.; Chen, E.; Griffith, L.; Glowacki, J. *J. Biomed. Mater. Res.* **2001**, *57*, 224-231.

(62) Ko, I. K.; Iwata, H. In *Reparative Medicine: Growing Tissues and Organs*, 2002; Vol. 961, pp 288-291.

(63) Kim, T. H.; Browne, F.; Upton, J.; Vacanti, J. P.; Vacanti, C. A. *Tissue Eng.* **1997**, *3*, 303-308.

(64) Strayhorn, C. L.; Garrett, J. S.; Dunn, R. L.; Benedict, J. J.; Somerman, M. J. *J. Periodont.* **1999**, *70*, 1345-1354.

(65) Park, Y. J.; Ku, Y.; Chung, C. P.; Lee, S. J. *J. Control. Release* **1998**, *51*, 201-211.

(66) Sheridan, M. H.; Shea, L. D.; Peters, M. C.; Mooney, D. J. *J. Control. Release* **2000**, *64*, 91-102.

(67) Roether, J. A.; Gough, J. E.; Boccaccini, A. R.; Hench, L. L.; Maquet, V.; Jerome, R. *J. Mater. Sci.-Mater. Med.* **2002**, *13*, 1207-1214.

(68) Rich, J.; Jaakkola, T.; Tirri, T.; Narhi, T.; Yli-Urpo, A.; Seppala, J. *Biomaterials* **2002**, *23*, 2143-2150.

(69) Winn, S. R.; Schmitt, J. M.; Buck, D.; Hu, Y. H.; Grainger, D.; Hollinger, J. O. *J. Biomed. Mater. Res.* **1999**, *45*, 414-421.

(70) Peter, S. J.; Lu, L.; Kim, D. J.; Stamatas, G. N.; Miller, M. J.; Yaszemski, M. J.; Mikos, A. G. *J. Biomed. Mater. Res.* **2000**, *50*, 452-462.

(71) King, T. W.; Patrick, C. W. *J. Biomed. Mater. Res.* **2000**, *51*, 383-390.

(72) Murphy, W. L.; Peters, M. C.; Kohn, D. H.; Mooney, D. J. *Biomaterials* **2000**, *21*, 2521-2527.

(73) Edlund, U.; Albertsson, A. C. In *Degradable Aliphatic Polyesters*; SPRINGER-VERLAG BERLIN: Berlin, 2002; Vol. 157, pp 67-112.

(74) Langer, R. S.; Peppas, N. A. *Biomaterials* **1981**, *2*, 201-214.

(75) Jalil, R.; Nixon, J. R. *J. Microencapsul.* **1990**, *7*, 297-325.

(76) Sakellariou, P.; Rowe, R. C. *Prog. Polym. Sci.* **1995**, *20*, 889-942.

(77) Rege, P. R.; Shukla, D. J.; Block, L. H. *Int. J. Pharm.* **1999**, *181*, 49-60.

(78) Jameela, S. R.; Suma, N.; Jayakrishnan, A. *Journal of Biomaterials Science-Polymer Edition* **1997**, *8*, 457-466.

(79) Winckler, S.; Brug, E.; Meffert, R.; Teupe, C.; Ritzerfeld, W.; Tormala, P. *Langenbecks Archiv Fur Chirurgie* **1992**, *377*, 112-117.

(80) Gu, Z. W.; Ye, W. P.; Yang, J. Y.; Li, Y. X.; Chen, X. L.; Zhong, G. W.; Feng, X. D. *Journal of Controlled Release* **1992**, *22*, 3-14.

(81) Jain, R.; Shah, N. H.; Malick, A. W.; Rhodes, C. T. *Drug Development and Industrial Pharmacy* **1998**, *24*, 703-727.

(82) Park, Y. J.; Nam, K. H.; Ha, S. J.; Pai, C. M.; Chung, C. P.; Lee, S. J. *Journal of Controlled Release* **1997**, *43*, 151-160.

(83) Li, Y. X.; Volland, C.; Kissel, T. *Polymer* **1998**, *39*, 3087-3097.

(84) Hagan, S. A.; Coombes, A. G. A.; Garnett, M. C.; Dunn, S. E.; Davis, M. C.; Illum, L.; Davis, S. S.; Harding, S. E.; Purkiss, S.; Gellert, P. R. *Langmuir* **1996**, *12*, 2153-2161.

(85) Cleek, R. L.; Ting, K. C.; Eskin, S. G.; Mikos, A. G. *Journal of Controlled Release* **1997**, *48*, 259-268.

(86) Morlock, M.; Kissel, T.; Li, Y. X.; Koll, H.; Winter, G. *J. Control. Release* **1998**, *56*, 105-115.

(87) Li, X. H.; Yuan, M. L.; Xiong, C. D.; Deng, X. M.; Jia, W. X.; Zhang, Y. H. *Acta Polym. Sin.* **1999**, 156-161.

(88) Yeh, M. K. *Journal of Microencapsulation* **2000**, *17*, 743-756.

(89) Jameela, S. R.; Misra, A.; Jayakrishnan, A. *J. Biomater. Sci.-Polym. Ed.* **1994**, *6*, 621-632.

(90) Chandy, T.; Das, G. S.; Rao, G. H. R. *J. Microencapsul.* **2000**, *17*, 625-638.

(91) Blanco, M. D.; Gomez, C.; Olmo, R.; Muniz, E.; Teijon, J. M. *Int. J. Pharm.* **2000**, *202*, 29-39.

(92) Pradhan, R. S.; Vasavada, R. C. *J. Control. Release* **1994**, *30*, 143-154.

(93) Rosen, H. B.; Chang, J.; Wnek, G. E.; Linhardt, R. J.; Langer, R. *Biomaterials* **1983**, *4*, 131-133.

(94) Leong, K. W.; Brott, B. C.; Langer, R. *J. Biomed. Mater. Res.* **1985**, *19*, 941-955.

(95) Leong, K. W.; Damore, P.; Marletta, M.; Langer, R. *J. Biomed. Mater. Res.* **1986**, *20*, 51-64.

(96) Mathiowitz, E.; Langer, R. *J. Control. Release* **1987**, *5*, 13.

(97) Mathiowitz, E.; Amato, C.; Dor, P.; Langer, R. *Polymer* **1990**, *31*, 547-555.

(98) Wu, M. P.; Tamada, J. A.; Brem, H.; Langer, R. *J. Biomed. Mater. Res.* **1994**, *28*, 387-395.

(99) Domb, A. J.; Maniar, M. *Journal of Polymer Science Part a-Polymer Chemistry* **1993**, *31*, 1275-1285.

(100) Domb, A. J.; Nudelman, R. *Journal of Polymer Science Part a-Polymer Chemistry* **1995**, *33*, 717-725.

(101) Domb, A. J.; Bentolila, A.; Teomin, D. *Acta Polymerica* **1998**, *49*, 526-533.

(102) Teomim, D.; Nyska, A.; Domb, A. J. *Journal of Biomedical Materials Research* **1999**, *45*, 258-267.

(103) Teomim, D.; Domb, A. J. *Biomacromolecules* **2001**, *2*, 37-44.

(104) Maniar, M.; Domb, A.; Haffer, A.; Shah, J. *J. Control. Release* **1994**, *30*, 233-239.

(105) Dang, W. B.; Daviau, T.; Brem, H. *Pharm. Res.* **1996**, *13*, 683-691.

(106) Teomim, D.; Fishbien, I.; Golomb, G.; Orloff, L.; Mayberg, M.; Domb, A. J. *J. Control. Release* **1999**, *60*, 129-142.

(107) Ishaug, S. L.; Yaszemski, M. J.; Bizios, R.; Mikos, A. G. *J. Biomed. Mater. Res.* **1994**, *28*, 1445-1453.

(108) Mikos, A. G.; Bao, Y.; Cima, L. G.; Ingber, D. E.; Vacanti, J. P.; Langer, R. *J. Biomed. Mater. Res.* **1993**, *27*, 183-189.

(109) Otto, T. E.; Nulend, J. K.; Patka, P.; Burger, E. H.; Haarman, H. *J. Biomed. Mater. Res.* **1997**, *35*, 407-408.

(110) Gugala, Z.; Gogolewski, S. *J. Biomed. Mater. Res.* **2000**, *49*, 183-191.

(111) Lieb, E.; Tessmar, J.; Hacker, M.; Fischbach, C.; Rose, D.; Blunk, T.; Mikos, A. G.; Gopferich, A.; Schulz, M. B. *Tissue Eng.* **2003**, *9*, 71-84.

(112) Han, D. K.; Hubbell, J. A. *Macromolecules* **1997**, *30*, 6077-6083.

(113) Lu, L. C.; Nyalakonda, K.; Kam, L.; Bizios, R.; Gopferich, A.; Mikos, A. G. *Biomaterials* **2001**, *22*, 291-297.

(114) Lucke, A.; Tessmar, J.; Schnell, E.; Schmeer, G.; Gopferich, A. *Biomaterials* **2000**, *21*, 2361-2370.

(115) Gopferich, A.; Peter, S. J.; Lucke, A.; Lu, L. C.; Mikos, A. G. *J. Biomed. Mater. Res.* **1999**, *46*, 390-398.

(116) Li, S. M.; Rashkov, I.; Espartero, J. L.; Manolova, N.; Vert, M. *Macromolecules* **1996**, *29*, 57-62.

(117) Mohammadi-Rovshandeh, J.; Farnia, S. M. F.; Sarbolouki, M. N. *J. Appl. Polym. Sci.* **1998**, *68*, 1949-1954.

(118) Stevels, W. M.; Ankone, M. J. K.; Dijkstra, P. J.; Feijen, J. *Macromol. Chem. Phys.* **1995**, *196*, 3687-3694.

(119) Sawhney, A. S.; Pathak, C. P.; Vanrensburg, J. J.; Dunn, R. C.; Hubbell, J. A. *J. Biomed. Mater. Res.* **1994**, *28*, 831-838.

(120) Jarrett, P.; Lalor, C. B.; Chan, L.; Redmon, M. P.; Hickey, A. J. *Colloid Surf. B-Biointerfaces* **2000**, *17*, 11-21.

(121) Reeve, M. S.; McCarthy, S. P.; Gross, R. A. *Macromolecules* **1993**, *26*, 888-894.

(122) Zhang, S.; Hou, Z.; Gonsalves, K. E. *Journal of Polymer Science Part a-Polymer Chemistry* **1996**, *34*, 2737-2742.

(123) Jacobs, C.; Dubois, P.; Jerome, R.; Teyssie, P. *Macromolecules* **1991**, *24*, 3027-3034.

(124) Breitenbach, A.; Kissel, T. *Polymer* **1998**, *39*, 3261-3271.

(125) Li, Y. X.; Nothnagel, J.; Kissel, T. *Polymer* **1997**, *38*, 6197-6206.

(126) Klok, H. A.; Hwang, J. J.; Iyer, S. N.; Stupp, S. I. *Macromolecules* **2002**, *35*, 746-759.

(127) Hwang, J. J.; Iyer, S. N.; Li, L. S.; Claussen, R.; Harrington, D. A.; Stupp, S. I. *Proc. Natl. Acad. Sci. U. S. A.* **2002**, *99*, 9662-9667.

(128) Lee, W. K.; Losito, I.; Gardella, J. A.; Hicks, W. L. *Macromolecules* **2001**, *34*, 3000-3006.

(129) Kassab, R.; Fenet, B.; Fessi, H.; Parrot-Lopez, H. *Tetrahedron Letters* **2000**, *41*, 877-881.

(130) Lavik, E. B.; Hrkach, J. S.; Lotan, N.; Nazarov, R.; Langer, R. *J. Biomed. Mater. Res.* **2001**, *58*, 291-294.

(131) John, G.; Tsuda, S.; Morita, M. *Journal of Polymer Science Part a-Polymer Chemistry* **1997**, *35*, 1901-1907.

(132) Barrera, D. A.; Zylstra, E.; Lansbury, P. T.; Langer, R. *Macromolecules* **1995**, *28*, 425-432.

(133) Elisseeff, J.; Anseth, K.; Langer, R.; Hrkach, J. S. *Macromolecules* **1997**, *30*, 2182-2184.

(134) Kricheldorf, H. R.; Hauser, K. *Macromolecular Rapid Communications* **1999**, *20*, 319-324.

(135) Marchi-Artzner, V.; Lorz, B.; Gosse, C.; Jullien, L.; Merkel, R.; Kessler, H.; Sackmann, E. *Langmuir* **2003**, *19*, 835-841.

(136) Schaffner, P.; Dard, M. M. *Cell. Mol. Life Sci.* **2003**, *60*, 119-132.

(137) Boger, D. L.; Goldberg, J.; Silletti, S.; Kessler, T.; Cheresh, D. A. *J. Am. Chem. Soc.* **2001**, *123*, 1280-1288.

(138) Cook, A. D.; Hrkach, J. S.; Gao, N. N.; Johnson, I. M.; Pajvani, U. B.; Cannizzaro, S. M.; Langer, R. *J. Biomed. Mater. Res.* **1997**, *35*, 513-523.

(139) Jo, S.; Shin, H.; Mikos, A. G. *Biomacromolecules* **2001**, *2*, 255-261.

(140) Na, K.; Choi, H. K.; Akaike, T.; Park, K. H. *Bioscience Biotechnology and Biochemistry* **2001**, *65*, 1284-1289.

(141) Zheng, J.; Ito, Y.; Imanishi, Y. *Journal of Biomaterials Science-Polymer Edition* **1995**, *7*, 515-522.

(142) Quirk, R. A.; Chan, W. C.; Davies, M. C.; Tendler, S. J. B.; Shakesheff, K. M. *Biomaterials* **2001**, *22*, 865-872.

(143) Irvine, D. J.; Ruzette, A. V. G.; Mayes, A. M.; Griffith, L. G. *Biomacromolecules* **2001**, *2*, 545-556.

(144) Jin, S.; Gonsalves, K. E. *Macromolecules* **1998**, *31*, 1010-1015.

(145) Kumar, R.; Gao, W.; Gross, R. A. *Macromolecules* **2002**, *35*, 6835-6844.

(146) Yin, M.; Baker, G. L. *Macromolecules* **1999**, *32*, 7711-7718.

(147) Parrish, B.; Quansah, J. K.; Emrick, T. *J. Polym. Sci. Pol. Chem.* **2002**, *40*, 1983-1990.

(148) Penczek, S.; Duda, A. *Macromol. Symp.* **1996**, *107*, 1-15.

(149) Penczek, S.; Biela, T.; Duda, A. *Macromolecular Rapid Communications* **2000**, *21*, 941-950.

(150) Albertsson, A. C.; Eklund, M. *Journal of Polymer Science Part a-Polymer Chemistry* **1994**, *32*, 265-279.

(151) Wen, J.; Zhuo, R. X. *Polymer International* **1998**, *47*, 503-509.

(152) Kolstad, J. J. *Journal of Applied Polymer Science* **1996**, *62*, 1079-1091.

(153) Barrett, A. G. M.; Hamprecht, D.; James, R. A.; Ohkubo, M.; Procopiou, P. A.; Toledo, M. A.; White, A. J. P.; Williams, D. J. *J. Org. Chem.* **2001**, *66*, 2187-2196.

(154) Maleczka, R. E.; Terrell, L. R.; Geng, F.; Ward, J. S. *Org. Lett.* **2002**, *4*, 2841-2844.

(155) Fraser, C.; Grubbs, R. H. *Macromolecules* **1995**, *28*, 7248-7255.

(156) Delaude, L.; Jan, D.; Simal, F.; Demonceau, A.; Noels, A. F. *Macromol. Symp.* **2000**, *153*, 133-144.

(157) Schitter, R. M. E.; Jocham, D.; Stelzer, F.; Moszner, N.; Volkel, T. *J. Appl. Polym. Sci.* **2000**, *78*, 47-60.

(158) Schwendeman, J. E.; Church, A. C.; Wagener, K. B. *Adv. Synth. Catal.* **2002**, *344*, 597-613.

(159) Grubbs, R. H.; Miller, S. J.; Fu, G. C. *Accounts Chem. Res.* **1995**, *28*, 446-452.

(160) Trnka, T. M.; Grubbs, R. H. *Accounts Chem. Res.* **2001**, *34*, 18-29.

(161) Scholl, M.; Ding, S.; Lee, C. W.; Grubbs, R. H. *Org. Lett.* **1999**, *1*, 953-956.

(162) Crowe, W. E.; Goldberg, D. R. *J. Am. Chem. Soc.* **1995**, *117*, 5162-5163.

(163) Crowe, W. E.; Goldberg, D. R.; Zhang, Z. J. *Tetrahedron Letters* **1996**, *37*, 2117-2120.

(164) Gibson, S. E.; Gibson, V. C.; Keen, S. P. *Chemical Communications* **1997**, 1107-1108.

(165) Brummer, O.; Ruckert, A.; Blechert, S. *Chem.-Eur. J.* **1997**, *3*, 441-446.

(166) Smith, I., A. B. ; Kozmin, S. A.; Adams, C. M.; Paone, D. V. *J. Am. Chem. Soc.* **2000**, *122*, 4984-4985.

(167) Diver, S. T.; Schreiber, S. L. *J. Am. Chem. Soc.* **1997**, *119*, 5106-5109.

(168) Schuster, M.; Lucas, N.; Blechert, S. *Chemical Communications* **1997**, 823.

(169) Breed, P. G.; Ramsden, J. A., Brown, J. M. *Canadian Journal of Chemistry* **2001**, *79*, 1049-1057.

(170) Poche, D. S.; Malter, L. M.; Perrault, J. M. *Polym. Bull.* **1999**, *43*, 43-49.

(171) Grubbs, R. H.; Chang, S. *Tetrahedron* **1998**, *54*, 4413-4450.

(172) Furstner, A.; Langemann, K. *J. Am. Chem. Soc.* **1997**, *119*, 9130-9136.

(173) Brown, H. C. *Organic Synthesis Via Boranes*; J. Wiley & Sons: New York, 1975.

(174) Brown, H. C.; Subba Rao, B. C. *Journal of Organic Chemistry* **1956**, *78*, 5694-5695.

(175) Brown, H. C.; Subba Rao, B. C. *Journal of Organic Chemistry* **1957**, *22*, 1136-1137.

(176) Brown, H. C.; Subba Rao, B. C. *Journal of the American Chemical Society* **1957**, *22*, 1137-1138.

(177) Chung, T. C.; Janvikul, W.; Bernard, R.; Hu, R.; Li, C. L.; Liu, S. L.; Jiang, G. J. *Polymer* **1995**, *36*, 3565-3574.

(178) Bergbreiter, D. E.; Xu, G.-F.; Zapata, J., C. *Macromolecules* **1994**, *27*, 1597-1602.

(179) Chung, T. C.; Janvikul, W.; Bernard, R.; Jiang, G. J. *Macromolecules* **1994**, *27*, 26-31.

(180) Ruckenstein, E.; Zhang, H. M. *J. Polym. Sci. Pol. Chem.* **2000**, *38*, 1195-1202.

(181) Yang, J. Y.; Yu, J.; Pan, H. Z.; Gu, Z. W.; Cao, W. X.; Feng, X. D. *Chin. J. Polym. Sci.* **2001**, *19*, 509-516.

(182) Yang, J. Y.; Yu, J.; Li, M.; Gu, Z. W.; Feng, X. D. *Chin. J. Polym. Sci.* **2002**, *20*, 413-417.

(183) Stassin, F.; Halleux, O.; Dubois, P.; Detrembleur, C.; Lecomte, P.; Jerome, R. *Macromol. Symp.* **2000**, *153*, 27-39.

(184) Vandenberg, E. J.; Tian, D. *Macromolecules* **1999**, *32*, 3613-3619.

(185) Yang, J.; Bei, J. Z.; Wang, S. G. *Polym. Adv. Technol.* **2002**, *13*, 220-226.

(186) Wang, Y. D.; Ameer, G. A.; Sheppard, B. J.; Langer, R. *Nat. Biotechnol.* **2002**, *20*, 602-606.

(187) Tian, D.; Dubois, P.; Jerome, R. *Macromolecules* **1997**, *30*, 1947-1954.

(188) Tian, D.; Dubois, P.; Grandfils, C.; Jerome, R. *Macromolecules* **1997**, *30*, 406-409.

(189) Ouchi, T.; Miyazaki, H.; Arimura, H.; Tasaka, F.; Hamada, A.; Ohya, Y. *Journal of Polymer Science Part a-Polymer Chemistry* **2002**, *40*, 1218-1225.

(190) Zheng, G. D.; Stover, H. D. H. *Macromolecules* **2003**, *36*, 1808-1814.

(191) Chen, X. H.; McCarthy, S. P.; Gross, R. A. *Macromolecules* **1998**, *31*, 662-668.

(192) Shen, Y. Q.; Chen, X. H.; Gross, R. A. *Macromolecules* **1999**, *32*, 2799-2802.

(193) Chen, X. H.; Gross, R. A. *Macromolecules* **1999**, *32*, 308-314.

(194) Shen, Y. Q.; Chen, X. H.; Gross, R. A. *Macromolecules* **1999**, *32*, 3891-3897.

(195) Ihre, H.; Hult, A.; Frechet, J. M. J.; Gitsov, I. *Macromolecules* **1998**, *31*, 4061-4068.

(196) Grinstaff, M. W. *Chem.-Eur. J.* **2002**, *8*, 2838-2846.

(197) Carnahan, M. A.; Grinstaff, M. W. *J. Am. Chem. Soc.* **2001**, *123*, 2905-2906.

(198) Chinchilla, R.; Dodsworth, D. J.; Najera, C.; Soriano, J. M. *Tetrahedron Letters* **2001**, *42*, 4487-4489.

(199) Ball, H. L.; King, D. S.; Cohen, F. E.; Prusiner, S. B.; Baldwin, M. A. *J. Pept. Res.* **2001**, *58*, 357-374.

(200) Park, Y. J.; Lee, J. Y.; Chang, Y. S.; Jeong, J. M.; Chung, J. K.; Lee, M. C.; Park, K. B.; Lee, S. J. *Biomaterials* **2002**, *23*, 873-879.

(201) Padmaja, T.; Lele, B. S.; Deshpande, M. C.; Kulkarni, M. G. *J. Appl. Polym. Sci.* **2002**, *85*, 2108-2118.

(202) Schmack, G.; Gorenflo, V.; Steinbuchel, A. *Macromolecules* **1998**, *31*, 644-649.

(203) Steinbuchel, A.; Schmack, G. *J. Environ. Polym. Degrad.* **1995**, *3*, 243-258.

(204) Hanhoff, T.; Lucke, C.; Spener, F. *Molecular and Cellular Biochemistry* **2002**, *239*, 45-54.

(205) Tsujimoto, T.; Uyama, H.; Kobayashi, S. *Biomacromolecules* **2001**, *2*, 29-31.

(206) Tsujimoto, T.; Uyama, H.; Kobayashi, S. *Macromolecular Bioscience* **2002**, *2*, 329-335.

(207) Uyama, H.; Kuwabara, M.; Tsujimoto, T.; Kobayashi, S. *Biomacromolecules* **2003**, *4*, 211-215.

(208) Kellerhals, M. B.; Kessler, B.; Witholt, B.; Tchouboukov, A.; Brandl, H. *Macromolecules* **2000**, *33*, 4690-4698.

(209) Maurin, A. C.; Chavassieux, P. M.; Vericel, E.; Meunier, P. J. *Bone* **2002**, *31*, 260-266.

(210) Watkins, B. A.; Lippman, H. E.; Le Bouteiller, L.; Li, Y.; Seifert, M. F. *Progress in Lipid Research* **2001**, *40*, 125-148.

(211) Nederberg, F.; Connor, E. F.; Glausser, T.; Hedrick, J. L. *Chemical Communications* **2001**, 2066-2067.

(212) Hoogsteen, W.; Postema, A. R.; Pennings, A. J.; Tenbrinke, G.; Zugenmaier, P. *Macromolecules* **1990**, *23*, 634-642.

(213) Marega, C.; Marigo, A.; Dinoto, V.; Zannetti, R.; Martorana, A.; Paganetto, G. *Makromolekulare Chemie-Macromolecular Chemistry and Physics* **1992**, *193*, 1599-1606.

(214) Garlotta, D. *Journal of Polymers and the Environment* **2002**, *9*, 63-84.

(215) Blanksby, S. J.; Ellison, G. B. *Accounts Chem. Res.* **2003**, *36*, 255-263.

(216) Vogl, O. *J. Polym. Sci. Pol. Chem.* **2000**, *38*, 4327-4335.

(217) Jin, S.; Gonsalves, K. E. *J. Mater. Sci.-Mater. Med.* **1999**, *10*, 363-368.

(218) Yuan, X. Y.; Mak, A. F. T.; Li, J. L. *J. Biomed. Mater. Res.* **2001**, *57*, 140-150.

(219) Hao, J. Y.; Liu, Y.; Zhou, S. B.; Li, Z.; Deng, X. M. *Biomaterials* **2003**, *24*, 1531-1539.

(220) Viornery, C.; Guenther, H. L.; Aronsson, B. O.; Pechy, P.; Descouts, P.; Gratzel, M. *Journal of Biomedical Materials Research* **2002**, *62*, 149-155.

(221) Durucan, C.; Brown, P. W. *Advanced Engineering Materials* **2001**, *3*, 227-231.

(222) Mou, L.; Singh, G.; Nicholson, J. W. *Chemical Communications* **2000**, 345-346.

(223) Sibold, N.; Madec, P.-J.; Masson, S.; Pham, T.-N. *Polymer* **2002**, *43*, 7257-7267.

(224) Shakesheff, K. M.; Cannizzaro, S. M.; Langer, R. *Journal of Biomaterials Science-Polymer Edition* **1998**, *9*, 507-518.

(225) Mann, B. K.; Schmedlen, R. H.; West, J. L. *Biomaterials* **2001**, *22*, 439-444.

(226) Tielinen, L.; Manninen, M.; Puolakkainen, P.; Pihlajamaki, H.; Pohjonen, T.; Rautavuori, J.; Tormala, P. *Clin. Orthop. Rel. Res.* **1998**, 312-322.

(227) Vinsova, J. *Chemicke Listy* **2001**, *95*, 22-27.

(228) Jin, S.; Gonsalves, K. E. *Polymer* **1998**, *39*, 5155-5162.

(229) Ouchi, T.; Nozaki, T.; Okamoto, Y.; Shiratani, M.; Ohya, Y. *Macromolecular Chemistry and Physics* **1996**, *197*, 1823-1833.

(230) Wang, D.; Feng, X. D. *Macromolecules* **1997**, *30*, 5688-5692.

(231) Elisseeff, J.; Anseth, K.; Langer, R.; Hrkach, J. S. *Macromolecules* **1997**, *30*, 2182-2184.

(232) Deng, X. M.; Yao, J. R.; Yuan, M. L.; Li, X. H.; Xiong, C. D. *Macromol. Chem. Phys.* **2000**, *201*, 2371-2376.

(233) Hrkach, J. S.; Ou, J.; Lotan, N.; Langer, R. *Macromolecules* **1995**, *28*, 4736-4739.

(234) Hrkach, J. S.; Ou, J.; Lotan, N.; Langer, R. In *Hydrogels and Biodegradable Polymers for Bioapplications*; AMER CHEMICAL SOC: Washington, 1996; Vol. 627, pp 93-102.

(235) Thiebaud, S.; Aburto, J.; Alric, I.; Borredon, E.; Bikiaris, D.; Prinos, J.; Panayiotou, C. *Journal of Applied Polymer Science* **1997**, *65*, 705-721.

(236) Rafler, G.; Jobmann, M. *Pharm. Ind.* **1996**, *58*, 1147-1151.

(237) Chim, H.; Ong, J. L.; Schantz, J. T.; Hutmacher, D. W.; Agrawal, C. M. *J. Biomed. Mater. Res. Part A* **2003**, *65A*, 327-335.

(238) Cai, K. Y.; Yao, K. D.; Hou, X.; Wang, Y. Q.; Hou, Y. J.; Yang, Z. M.; Li, X. Q.; Xie, H. Q. *J. Biomed. Mater. Res.* **2002**, *62*, 283-291.

(239) Kay, S.; Thapa, A.; Haberstroh, K. M.; Webster, T. J. *Tissue Eng.* **2002**, *8*, 753-761.

(240) Schneider, G. B.; Perinpanayagam, H.; Clegg, M.; Zaharias, R.; Seabold, D.; Keller, J.; Stanford, C. *J. Dent. Res.* **2003**, *82*, 372-376.

(241) Kieswetter, K.; Schwartz, Z.; Hummert, T. W.; Cochran, D. L.; Simpson, J.; Dean, D. D.; Boyan, B. D. *J. Biomed. Mater. Res.* **1996**, *32*, 55-63.

(242) Martin, J. Y.; Schwartz, Z.; Hummert, T. W.; Schraub, D. M.; Simpson, J.; Lankford, J.; Dean, D. D.; Cochran, D. L.; Boyan, B. D. *J. Biomed. Mater. Res.* **1995**, *29*, 389-401.

(243) Wada, M.; Honna, M.; Y., K.; Miyoshi N. Bull. Chem. Soc. Jpn. 1997, 2265-2267. *Bull. Chem. Soc. Jpn.* **1997**, *70*, 2265-2267.

(244) Shimizu, T.; Hayashi, Y.; Kitora, Y.; Teramura, K. *Bulletin of the Chemical Society of Japan* **1982**, *55*, 2450-2455.

(245) Chatterjee, A. K.; Morgan, J. P.; Scholl, M.; Grubbs, R. H. *J. Am. Chem. Soc.* **2000**, *122*, 3783-3784.

(246) Botteghi, C.; Dei Negri, C.; Paganelli, S.; Marchetti, M. *Journal of Molecular Catalysis a-Chemical* **2001**, *175*, 17-25.

(247) Yoshida, Y.; Sakakura, Y.; Aso, N.; Okada, S.; Tanabe, Y. *Tetrahedron* **1999**, *55*, 2183-2192.